U.S. DEPARTMENT OF COMMERCE
National Technical Information Service

PB-271 515

Venturi Scrubber Performance Model

Air Pollution Technology, Inc, San Diego, Calif

Prepared for

Industrial Environmental Research Lab, Research Triangle Park, N C

Aug 77

PB 271 515

PA-600/2-77-172
ugust 1977

Environmental Protection Technology Series

UNITED STATES ENVIRONMENTAL PROTECTION AGENCY

NATIONAL TECHNICAL
INFORMATION SERVICE

RESEARCH REPORTING SERIES

Research reports of the Office of Research and Development, U.S. Environmental Protection Agency, have been grouped into nine series. These nine broad categories were established to facilitate further development and application of environmental technology. Elimination of traditional grouping was consciously planned to foster technology transfer and a maximum interface in related fields. The nine series are:

1. Environmental Health Effects Research
2. Environmental Protection Technology
3. Ecological Research
4. Environmental Monitoring
5. Socioeconomic Environmental Studies
6. Scientific and Technical Assessment Reports (STAR)
7. Interagency Energy-Environment Research and Development
8. "Special" Reports
9. Miscellaneous Reports

This report has been assigned to the ENVIRONMENTAL PROTECTION TECHNOLOGY series. This series describes research performed to develop and demonstrate instrumentation, equipment, and methodology to repair or prevent environmental degradation from point and non-point sources of pollution. This work provides the new or improved technology required for the control and treatment of pollution sources to meet environmental quality standards.

REVIEW NOTICE

This report has been reviewed by the participating Federal Agencies, and approved for publication. Approval does not signify that the contents necessarily reflect the views and policies of the Government, nor does mention of trade names or commercial products constitute endorsement or recommendation for use.

This document is available to the public through the National Technical Information Service, Springfield, Virginia 22161.

TECHNICAL REPORT DATA
(Please read Instructions on the reverse before completing)

1. REPORT NO. EPA-600/2-77-172	2.	3. RECIPIENT'S ACCESSION NO. PB-271 515
4. TITLE AND SUBTITLE Venturi Scrubber Performance Model		5. REPORT DATE August 1977 6. PERFORMING ORGANIZATION CODE
7. AUTHOR(S) Shui-Chow Yung, Seymour Calvert, and Harry F. Barbarika		8. PERFORMING ORGANIZATION REPORT NO.
9. PERFORMING ORGANIZATION NAME AND ADDRESS A. P. T., Inc. 4901 Morena Boulevard, Suite 402 San Diego, California 92117		10. PROGRAM ELEMENT NO. 1AB012; ROAP 21ADL-002 11. CONTRACT/GRANT NO. 68-02-1328, Task 13
12. SPONSORING AGENCY NAME AND ADDRESS EPA, Office of Research and Development Industrial Environmental Research Laboratory Research Triangle Park, NC 27711		13. TYPE OF REPORT AND PERIOD COVERED Task Final; 3-6/76 14. SPONSORING AGENCY CODE EPA/600/13

15. SUPPLEMENTARY NOTES IERL-RTP task officer for this report is Leslie E. Sparks, Mail Drop 61, 919/541-2925.

16. ABSTRACT The report gives results of a review and evaluation of available venturi scrubber design equations. Calvert's differential equation for particle collection and Boll's differential equation for pressure drop were selected for numerical solution, and the results are presented graphically. Particle collection and pressure drop of venturi scrubbers can be approximated by the collection occurring in the venturi throat and by the drop acceleration loss, respectively. Simplified equations were derived by applying Calvert's and Boll's equations to the venturi throat section. The new design equations are much simpler to use and compare favorably with available performance data.

17. KEY WORDS AND DOCUMENT ANALYSIS

a. DESCRIPTORS		b. IDENTIFIERS/OPEN ENDED TERMS	c. COSATI Field/Group	
Air Pollution	Dust	Air Pollution Control	13B	11G
Scrubbers	Flue Gases	Stationary Sources	07A	21B
Venturi Tubes	Entrainment	Particulate	14B	07D
Design	Separators	Venturi Scrubbers		
Performance				
Mathematical Models			12A	

18. DISTRIBUTION STATEMENT Unlimited	19. SECURITY CLASS (This Report) Unclassified	21. NO. OF PAGES 215
	20. SECURITY CLASS (This page) Unclassified	22. PRICE PC A10 A01

EPA Form 2220-1 (9-73)

i

EPA-600/2-77-172
August 1977

VENTURI SCRUBBER PERFORMANCE MODEL

by

Shui-Chow Yung, Seymour Calvert, and
Harry F. Barbarika

A.P.T., Inc.
4901 Morena Boulevard, Suite 402
San Diego, California 92117

Contract No. 68-02-1328
Task No. 13
ROAP No. 21ADL-002
Program Element No. 1AB012

EPA Task Officer: Leslie E. Sparks

Industrial Environmental Research Laboratory
Office of Energy, Minerals, and Industry
Research Triangle Park, N.C. 27711

Prepared for

U.S. ENVIRONMENTAL PROTECTION AGENCY
Office of Research and Development
Washington, D.C. 20460

ABSTRACT

A review and evaluation of the available venturi scrubber design equations are presented. Calvert's differential equation for particle collection and Boll's differential equation for pressure drop are selected for numerical solution and the results presented graphically.

The particle collection and pressure drop of venturi scrubbers can be approximated by the collection occurring in the venturi throat and by the drop acceleration loss respectively. Simplified equations were derived by applying Calvert's and Boll's equations to the venturi throat section. The new design equations are much simpler to use and compare well with available performance data.

This report was submitted in partial fulfillment of Contract Number 68-02-1328, Task Number 13 by Air Pollution Technology, Inc. under the sponsorship of the U.S. Environmental Protection Agency. This report covers the period March 1, 1976 to May 30, 1976, and work was completed as of June 30, 1976.

CONTENTS

Page

Abstract ii

Figures. iv

Tables ix

Abbreviations and Symbols x

Acknowledgement xv

1. Introduction 1
2. Summary and Conclusions 4
3. Literature Search 16
4. Comparison of Model with Experimental Data. . . . 41
5. Performance Model 61
6. Comparing Model Predictions with Performance Data 114
7. Design Analysis 128
8. Entrainment Separator 161

References 191

Appendix 195

FIGURES

Number		Page
1-1	Venturi Scrubber System	3
3-1	Target Efficiency Results of Various Investigators	20
3-2	Drag Coefficient of a Sphere	27
4-1	Dimensions of OAP Venturi Scrubber	43
4-2	Comparison of Predicted Pressure Drop with Experimental Data from Wen and Uchida	44
4-3	Comparison of Predicted Pressure Drop with Experimental Data from Wen and Uchida	45
4-4	Comparison between Behie and Beeckmans' Prediction and Experimental Data from Wen and Uchida	46
4-5	Comparison of Predicted Pressure Drop by Modified Calvert's Equation with Data from Wen and Uchida	51
4-6	Prototype Venturi Scrubber Used by Boll	52
4-7	Comparison of Boll's Pressure Drop Data with Theory	53
4-8	Dimension of Pease-Anthony Venturi Scrubber Used by Brink and Contant	55
4-9	Comparison of Brink and Contant Experimental Data with Theories	57
4-10	Dimensions of the Ekman and Johnstone Venturi	58
4-11	Comparison of Ekman and Johnstone's Pressure Drop Data with Theories	59
5-1	Chart for Obtaining u_d^* for a Circular Duct	72

FIGURES (continued)

Number — Page

5-2 Chart for Obtaining u_d^* for a Rectangular Duct 73

5-3 Chart for Obtaining p_d^* for a Circular Duct 74

5-4 Chart for Obtaining p_d^* for a Rectangular Duct 75

5-5 Chart for Obtaining Penetration for Circular Duct 76

5-6 Chart for Obtaining Penetration for Circular Duct 77

5-7 Chart for Obtaining Penetration for Circular Duct 78

5-8 Chart for Obtaining Penetration for Circular Duct 79

5-9 Chart for Obtaining Penetration for Circular Duct 80

5-10 Chart for Obtaining Penetration for Rectangular Duct 81

5-11 Chart for Obtaining Penetration for Rectangular Duct 82

5-12 Chart to Obtain Penetration for Rectangular Duct 83

5-13 Chart to Obtain Penetration for Rectangular Duct 84

5-14 Chart to Obtain Penetration for Rectangular Duct 85

5-15 Chart to Obtain Penetration for a Rectangular Duct 86

5-16 Chart to Obtain Penetration for a Rectangular Duct 87

5-17 Concept of a Hypothetical Section 88

FIGURES (continued)

Number Page

5-18 Chart for Obtaining L_H for a Circular Duct 90

5-19 Chart for Obtaining L_H for a Rectangular Duct 91

5-20 Ventrui Scrubber for Sample Calculation. . 93

5-21 Predicted Grade Efficiency Curve 98

5-22 Predicted Grade Efficiency Curve 110

6-1 Experimental and Predicted Performance of AAF Kinpactor 32 Venturi Scrubber 116

6-2 Experimental and Predicted Performance for AAF Kinpactor 32 Venturi Scrubber 117

6-3 Predicted and Experimental Penetration for Venturi Scrubber Used by Brink ano Contant 118

6-4 Predicted and Measured Penetration for Chemico Venturi Scrubber 121

6-5 Predicted and Experimental Grade Efficiency Curve for Chemico Venturi Scrubber 122

6-6 APS Electrostatic Scrubber 123

6-7 Experimental and Predicted APS Venturi Scrubber Performance 124

6-8 Predicted and Experimental Performance for Venturi Rod Scrubber 126

7-1 Venturi Scrubber Integrated Penetration, "Pt" versus "d_{p50}/d_{pg}", with "K_{pg}" as parameter, "σ_g=2.5" 134

7-2 Venturi Scrubber Integrated Penetration, Pt versus d_{p50}/d_{pg}, with K_{pg} as parameter, σ_g=2 135

7-3 Venturi Scrubber Integrated Penetration, Pt versus d_{p50}/d_{pg}, with K_{pg} as parameter, σ=7.5 136

FIGURES (continued)

Number Page

7-4 "Pt" versus "B" with "K_{pg}" as parameter, "σ_g=2.5" 138

7-5 "Pt" versus "B" with "K_{pg}" as parameter, "σ_g=5" 139

7-6 "Pt" versus "B" with "K_{pg}" as parameter, "σ_g=7.5" 140

7-7 d_{pa50}/d_{pg} versus "B" with "K_{pg}" as parameter 141

7-8 Effect of Throat Length on Penetration . . . 142

7-9 Effect of Throat Length on Performance . . . 144

7-10 Predicted Venturi Scrubber Performance, K_{p50} versus B 145

7-11 Effect of Gas Velocity aad Liquid to Gas Flow Rate Ratio on Performance Cut Diameter 147

7-12 "B" vs "K_{p50}" for venturi throat of infinite length 148

7-13 Predicted Venturi Performance, "d_{pa50}" versus Q_L/Q_G with "u_G" and " P" as Parameter. . 149

7-14 Aerodynamic Cut Diameter Versus Pressure Drop with Liquid to Gas Ratio as Parameter . 150

7-15 Impaction parameter vs aerodynamic cut diameter for a venturi design 154

7-16 Pressure drop vs aerodynamic cut diameter for venturi design example 157

7-17 Impaction parameter vs Q_L/Q_G for venturi design example 160

8-1 Cyclone with tangential gas inlet. 166

8-2 Generalized flooding and pressure drop correlation for packed beds (Perry, 1963). . 174

FIGURES (continued)

Number Page

8-3 Theoretical and experimental collection efficiencies of rectangular aerosol jets. . 176

8-4 Theoretical impaction efficiency as a function of inertial parameter for different targets 177

8-5 Friction factor, f, versus Reynolds number, $N_{Re,G}$ for wire mesh entrainment separator with entrainment load 182

8-6 Pressure drop due to presence of liquid in the knitted mesh with the crimps in the same direction 183

8-7 Pressure drop due to presence of liquid in the knitted mesh with the crimps in the alternate direction 183

8-8 Drag coefficient versus Reynolds number after Foust et al (1959), with sphericity ψ as the parameter 187

8-9 Drag coefficients for flow past inclined flat plates (data from A. Fage & F.C. Johansen, (1927) 187

TABLES

Number Page

2-1 Correlation for Particle Collection in Venturi Scrubber 5

2-2 Correlations for Pressure Drop in Venturi Scrubber 8

2-3 Entrainment Separator Design Equations . . 12

3-1 Empirical Equations for Average Liquid Drop Size and Their Applicable Ranges . . 25

3-2 Correlations for Pressure Drop in Venturi Scrubber 37

4-1 Wen and Uchida's Experimental Pressure Drop Data on O.A.P. Venturi Scrubber . . . 42

4-2 Wen and Uchida's Experimental Data and Predictions by Boll and by Behie and Beeckmans 48

B-1 Bed Porosity, ε, for Various Packing Materials 171

B-2 Experimental Values of J, Channel Width as Fraction of Packing Diameter 171

B-3 Packing Factors "F", for Dumped Pieces (m^2/m^3) 172

B-4 Packing Factors "F" for Grids and Stacked Pieces (m^2/m^3) 173

ABBREVIATIONS AND SYMBOLS

Latin

A = cross-sectional area, cm^2
A_o = cross-sectional area at the duct inlet, cm^2
A_p = total projected area of baffles per row in the direction of inlet air flow, cm^2
A_r = ratio of exit to inlet duct cross-sectional area, dimensionless
A_t = throat cross-sectional area, cm^2
a_s = specific area of mesh, cm^2/cm^3
B = dimensionless liquid-to-gas flow-rate ratio parameter, dimensionless

$$= \frac{1}{C_{Do}} \frac{Q_L}{Q_G} \frac{\rho_L}{\rho_G} \left(\frac{u_{Go}}{u_{Go} - u_{do}}\right)^{0.6}$$

B_D = dimensionless parameter

$$= \frac{4\ B\ D_p}{u_{Go}\ d_d}$$

b = duct breadth, cm
b' = spacing between two consecutive baffles in same row, cm
C' = Cunningham slip factor, dimensionless
C_D = drag coefficient, dimensionless
C_{Do} = initial drag coefficient, dimensionless
c = concentration of particles, g/cm^3
c_a = capillary number
c_d = number concentration of drops, #/cm^3
c_i = concentration of particles in the main stream of gas, g/cm^3
D_p = diffusivity of particle, cm^2/s
d = cyclone diameter, cm
d_c = collector or packing diameter, cm
d_d = liquid drop diameter, cm
d_{eq} = equivalent diameter, cm

Abbreviations and Symbols (continued)

d_m = mean drop diameter, cm
d_n = nozzle diameter, mm
d_o = initial inlet or outlet duct diameter, cm
d_p = particle diameter, cm or μm
d_{pa} = aerodynamic particle diameter, μmA
d_{pc} = cut diameter, μmA
d_{RC} = required cut diameter, μmA
d_t = venturi throat diameter, cm
E = collection efficiency, fraction
E_d = eddy diffusivity of liquid drops, cm²/s
E_p = eddy diffusivity of particles, cm²/s
F = drop flux, g/cm²·s
F = packing factor, m²/m³
F_f = foam density
f = empirical constant, dimensionless
f = friction factor, dimensionless
f_t = average friction factor of the venturi throat, dimensionless
$\bar{f}_c$ = average friction factor of the convergent section, dimensionless
$\bar{f}_d$ = average friction factor of the divergent section, dimensionless
g_c = conversion factor
H_d = fractional liquid hold-up, fraction
j = ratio of channel width to packing diameter, dimensionless
K_p = inertial parameter, dimensionless
K_{pt} = inertial parameter at venturi throat, dimensionless
K_{po} = initial inertial parameter, dimensionless
K_{pg} = inertial parameter for mass median particle diameter, dimensionless
k = Boltzman's constant

Abbreviations and Symbols (continued)

L = dimensionless length parameter

$$= \frac{3\,\ell\,C_{Do}\,\rho_G}{2\,d_d\,\rho_L}\left(\frac{u_{Go}-u_{do}}{u_{Go}}\right)^{0.5}$$

ℓ = length, cm

ℓ_t = venturi throat length, cm

ℓ_p = thickness of mesh pad, cm

M = liquid-to-gas mass flow-rate ratio, dimensionless

m_G = gas mass flow rate, g/s

m_L = liquid mass flow rate, g/s

N = number of jet stages in the tube bank, i.e., (number of rows) - 1

N_c = number of collection transfer units

n = cyclone vortex component, dimensionless

n = number of zigzag baffle rows

P = drop flight path length, cm

$Pt(d_p)$ = particle penetration for particles with diameter d_p, fraction

$\overline{Pt}$ = overall penetration, fraction

p = local pressure, dyne/cm²

p_w = component of "p" associated with wall friction, dyne/cm²

Q_d = source strength, #/cm³

Q_G = gas volumetric flow rate, cm³/s

Q_L = liquid volumetric flow rate, cm³/s

R = radius (for circular duct) or half-width (for rectangular duct) at the start of a given duct, cm

R_d = washing factor for divergent section, dimensionless

R_t = washing factor for venturi throat, dimensionless

S = dimensionless parameter characterizing slope of the given duct

$$\frac{2}{3}\,\frac{\tan\theta}{R}\,\frac{d_d}{C_{Do}}\,\frac{\rho_L}{\rho_G}\left(\frac{u_{Go}}{u_{Go}-u_{do}}\right)^{0.5}$$

Abbreviations and Symbols (continued)

s = specific surface of drops formed, cm²/cm³
T = gas temperature, °K
t = time, s
u_d = liquid drop velocity, cm/s
u_{do} = initial drop velocity, cm/s
u_G = gas velocity, cm/s
u_{Go} = initial gas velocity, cm/s
u_{Gt} = gas velocity at the venturi throat, cm/s
u_L = liquid velocity, cm/s
u_o = relative undisturbed upstream velocity, cm/s
u_p = particle velocity, cm/s
u_{tg} = tangential gas velocity, cm/s
u_{tc} = drop terminal centrifugal velocity, cm/s
$\bar{u}_G$ = dimensionless gas velocity in x direction
u_p = dimensionless particle velocity in x direction
$\bar{v}_g$ = dimensionless gas velocity in y direction
v_p = dimensionless particle velocity in y direction
W = width of baffle, cm
= weight of particles collected, g
X = dimensionless parameter
$= \dfrac{3\ \zeta_t\ C_{Do}\ \rho_G}{16\ d_d\ \rho_L} + 1$
x = coordinate perpendicular to gas flow, cm
Y = d_{pa}/d_{pg}
y = coordinate perpendicular to gas flow, cm
z = axial coordinate, cm

__Greek Symbols__

θ = half angle of divergence or convergence, degrees
ζ_t = head-loss ratio for throat, dimensionless
ζ_d = head loss ratio for divergent section, dimensionless
δ = distance from collector center, cm

Abbreviations and Symbols (continued)

ρ_G = gas density, g/cm^3
ρ_m = manometer fluid density, g/cm^3
ρ_L = liquid density, g/cm^3
ρ_p = particle density, g/cm^3
θ = divergence angle or baffle angle, degrees
θ_1 = convergence angle, degrees
θ_2 = divergence angle, degrees
η = single drop collection efficiency, fraction
μ_G = gas viscosity, poise
μ_L = liquid viscosity, poise
ν_G = kinematic viscosity of gas, cm^2/s
ϕ = rate of deposition, g/s
σ = surface tension, dyne/cm
ΔP = pressure drop, cm W.C.
ΔP_d = dry pressure drop, cm W.C.
ΔT = temperature change, °F

Superscript

$*$ = dimensionless parameter

Dimensionless numbers

N_{Red} = drop Reynolds number based on diameter
N_{Reo} = initial drop Reynolds number
N_{Sc} = particle Schmidt number
N'_{Sh} = particle Sherwood number

ACKNOWLEDGEMENT

A.P.T., Inc. wishes to express its appreciation for excellent technical coordination and for very helpful assistance in support of our technical effort to Dr. Leslie E. Sparks, EPA Project Officer.

CHAPTER 1
INTRODUCTION

Venturi scrubber is one type of gas atomized spray scrubber. It employs gradually converging, then diverging sections. The venturi throat is the section between tho converging and diverging sections. Usually liquid enters the venturi upstream of the throat through nozzles. Alternately, the liquid may flow along the converging section walls until reaching the throat. At the throat, the liquid is shattered into drops by the high velocity gas. Sometimes the liquid is introduced as pre-atomized drops at or before the throat through a pressure nozzle. The venturi may have a round, square, or rectangular cross section. For the rectangular duct, the breadth of the duct is usually invariant and only duct width diverges or converges.

Venturi scrubbers have been widely recognized as having a high collection efficiency for fine particles and have been successfully used for years to remove particles and mists from gas streams. Particle collection efficiency in a venturi scrubber generally increases with pressure drop. High pressure drop (100 cm W.C. or 40 in. W.C.) venturi scrubbers can efficiently collect submicron particles.

The venturi scrubber has several distinct advantages when compared with other scrubber types. The scrubber construction is simple, thus the initial capital investment is low. Through adjusting pressure drop by varying liquid flow or gas velocity, it can be made to collect even submicron fume with good efficiency. Due to the absence of moving parts, it can be used for the collection of sticky particles.

The venturi scrubber also has disadvantages: It requires high pressure drop for the collection of submicron particles which results in a high operating cost, and its applicability for mass transfer problems is limited due to the co-current nature of the gas-liquid flow. To prevent possible water pollution problems, it also requires water treatment facilities.

Figure 1-1 describes a commonly encountered venturi scrubber system. It consists of a venturi scrubber, an entrainment separator, liquid treatment facilities, and gas and liquid movers.

The atomized liquid drops or liquid entrainment must be separated from the gas stream before the gas is emitted into the atmosphere. There are a number of devices which are commonly used as entrainment separators which are added either within the venturi outlet duct or in another vessel. Zig-zag baffles, cyclone separators, and guide vanes causing rotation of the gas stream are frequently used for this purpose.

In the present study, only the design of venturi scrubber itself and its entrainment separator will be reviewed and evaluated.

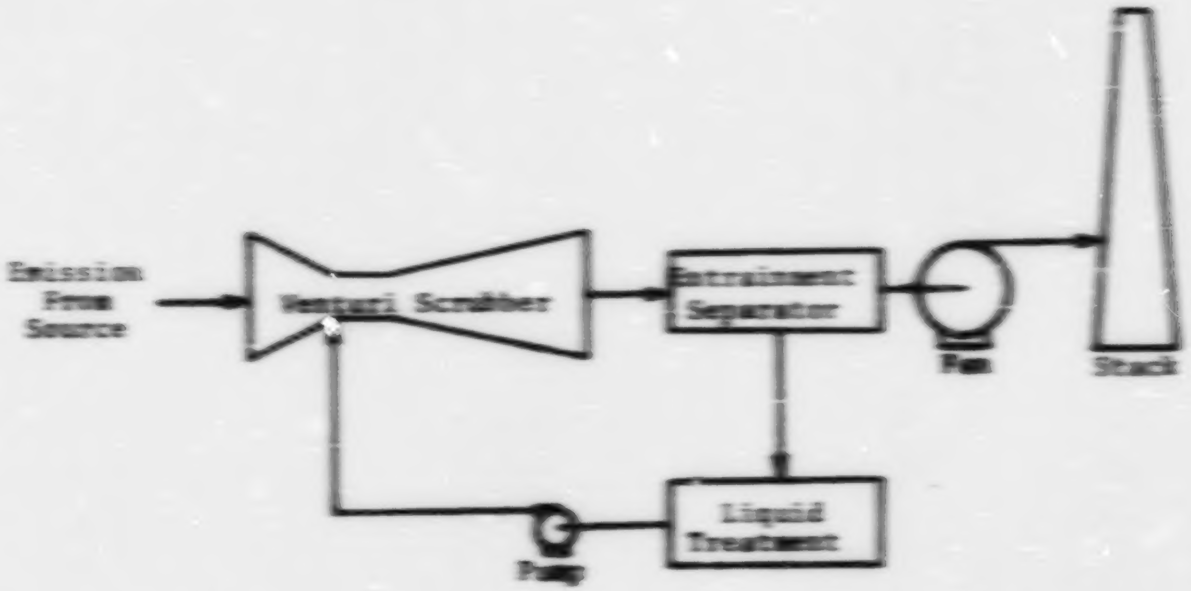
Emission
From
Source
Venturi Scrubber
Entrainment
Separator
Fan
Stack
Liquid
Treatment
Pump

Figure 1-1. Venturi scrubber system.

CHAPTER 2

SUMMARY AND CONCLUSIONS

Venturi scrubbers are used extensively for the collection of small particles. The major impediment to their practical use is that they have high pressure drops which result in high operating cost. With a better understanding of the fundamentals of the operation of this typu of scrubber, the pressure drop could be lowered without affecting particle collection.

The objectives of the study reported here were to (1) review and evaluate all available venturi scrubber performance models and design models (2) recommend the best model and (3) prepare a design manual based on this model.

LITERATURE SEARCH

Particle Collection Efficiency

The particle collection efficiency of a venturi scrubber is influenced by many parameters, such as particle size and size distribution, gas velocity, liquid-to-gas ratio, etc. There are several mathematical models available for the prediction of particle collection efficiency in a venturi scrubber. All models are based on particle impaction on liquid drops. Table 2-1 summaries all models.

Pressure Drop

Pressure drop in a venturi consists of two parts, namely acceleration loss and wall-friction loss. Most of the losses are due to acceleration and these may be calculated from hydrodynamics. Wall-friction loss depends on scrubber geometry and usually is determined experimentally. Table 222 lists several available correlations for the prediction of pressure drop in a venturi

TABLE 2-1. CORRELATION FOR PARTICLE COLLECTION IN VENTURI SCRUBBER

Investigator	Correlation
Ekman & Johnstone (1951)	$Pt(d_p) = \exp\left[-\frac{3\,\eta\,P\,s}{490{,}000}\right]$
Calvert (1968)	$-\frac{dc}{c} = \frac{u_r}{u_G}\,\frac{Q_L}{(u_G-u_r)A}\left(\frac{3}{4r_d}\right)\eta\;dz$
Calvert (1970)	$Pt(d_p) = \exp\left[\frac{2\,Q_L\,u_G\,\rho_L\,d_d}{55\,Q_G\,\mu_G}\,F(K_{pt}, f)\right]$ $F(K_{pt}, f) = \frac{1}{K_{pt}}\left[1.4\ln\left(\frac{K_{pt}\,f + 0.7}{0.7}\right)\right.$ $\left.+\frac{0.49}{0.7 + K_{pt}\,f} - (K_{pt}\,f + 0.7)\right]$
Morishima et al. (1971)	$Pt(d_p) = \exp\left[-(R_t + R_d)\,\frac{Q_L}{Q_G}\right]$ $R_t = \frac{3\ell_t}{2d_d}\int_0^1 \eta\,\frac{u_G}{u_d}\left(1-\frac{u_d}{u_G}\right)dX$ $R_d = \frac{3\ell_G}{2d_d}\int_1^{X_{max}} \eta\,\frac{u_G}{u_d}\left(\frac{1}{X^2}-\frac{u_G}{u_d}\right)dX$
Drepp & Akbrut (1972)	$Pt(d_p) = \exp\left[-\frac{3}{2}\int_0^z\left(\frac{Q_L}{Q_G}\right)\frac{\eta}{d_c}\,\frac{\lvert u_p-u_d\rvert}{u_d}\;dz\right]$
Boll (1973)	$Pt(d_p) = \exp\left[-\int_0^t 1.5\left(\frac{m_L}{m_G}\right)\left(\frac{\rho_G}{\rho_L}\right)\frac{\eta\lvert u_G - u_d\rvert}{d_c}\,dt\right]$

continued

TABLE 2-1. (Continued)

Investigator	Correlation
Behie & Beeckmans (1973)	$Pt(d_p) = \exp\left[-1.5\int_0^{\ell} \frac{F\ \eta\ (u_G - u_d)}{\rho_L\ d_d\ u_G\ u_d}\ dz\right]$
Taheri & Sheih (1975)	$\frac{\partial c}{\partial t} = -u_G \frac{\partial c}{\partial z} + E_p \left[\frac{\partial^2 c}{\partial y^2} + \frac{\partial^2 c}{\partial z^2}\right] - \frac{\pi\ \eta}{4}\ d_d^2\ (u_G - u_d)\ c\ c_d$ $\frac{\partial c_d}{\partial t} = -u_d \frac{\partial c_d}{\partial z} + E_d \left[\frac{\partial^2 c_d}{\partial y^2} + \frac{\partial^2 c_d}{\partial z^2}\right] + Q_d$

where A = cross-sectional area, cm²
c = concentration of particulates, g/cm³
c_d = number concentration of drops, #/cm³
d_d = drop diameter, cm
E_d = eddy diffusivity of drops, cm²/s
E_p = eddy diffusivity of particle, cm²/s
F = drop flux, g/cm²·s
f = empirical constant
K_{pt} = inertial parameter at venturi throat, dimensionless
ℓ = length, cm
m_G = gas mass flow rate, g/s
m_L = liquid mass flow, g/s
P = drop flight path length, cm
$Pt(d_p)$ = penetration for particles with diameter, d_p, fraction
Q_d = source strength, #/cm³

continued

where Q_G = volumetric gas flow rate, cm^3/s
Q_L = volumetric liquid flow rate, cm^3/s
s = specific surface of drops, cm^2/cm^3 of gas
t = time, s
u_d = drop velocity, cm/s
u_G = gas velocity, cm/s
u_r = drop particle relative velocity cm/s
x = rectangular coordinate, perpendicular to the direction of flow
X = dimensionless distance
y = rectangular coordinate, perpendicular to the direction of flow
z = rectangular coordinate, in the direction of flow
ρ_L = liquid density, g/cm
η = single drop collection efficiency, fraction

TABLE 2-2. CORRELATIONS FOR PRESSURE DROP IN VENTURI SCRUBBER

Investigator	Correlation
Matrosov (1953)	$\Delta P = \Delta P_d + 1.38 \times 10^{-3} u_{Gt}^{1.08} \left(\frac{Q_L}{Q_G}\right)^{0.63}$
Yoshida et al. (1960) (1965)	$\Delta P = \frac{\rho_G u_{Gt}^2}{2 g_c} \left(a + b \frac{Q_L}{Q_G}\right)$ $a = \frac{F_c}{2 \tan \frac{\theta_c}{2}} + 4 f_t \frac{s_t}{d_t} + \zeta\left(1 - 2 \frac{d_t^2}{d_0^2}\right)$ $b = (\zeta_t - 1) \frac{4 f_t s_t}{\rho_m d_t} + (\zeta_d - 1)\frac{\zeta}{\rho_m}\left(1 - \frac{d_t^2}{d_0^2}\right)$
Geiseke (1968)	$\Delta P = \frac{76}{g_c \delta t} \Big[m_G \Delta u_G + m_L \Delta u_L$ $+ \frac{\Delta m_L}{2} (u_{G1} + u_{G2} - u_{L1} - u_{L2}) \Big]$
Yamauchi et al. (1964)	$\Delta P = 0.3 (\Delta T)^{-0.28} \frac{\rho_G u_{Gt}^2}{2 g_c} \left(1 + \frac{Q_L}{Q_G}\right)$
Tohata et al. (1964)	$\Delta P = \frac{\rho_G u_{Gt}^2}{2 g_c} \Big\{ \left[1 - \left(\frac{A_t}{A_D}\right)^2\right]$ $\left[\frac{F_c}{8 \tan \theta_1} + \frac{F_d}{8 \tan \theta_2}\right] + f_t \frac{s_t}{d_t} + \zeta_1 + \zeta_2 \Big\}$

(continued)

TABLE 2-2. (Continued)

Investigator	Correlation
Volgin et al. (1968)	$\Delta P = 3.32 \times 10^{-6}\, u_{Gt}^2 \left(\frac{Q_L}{Q_G}\right)^{0.26} (\ell_t)^{1.43}$
Calvert (1968)	$\Delta P = 1.03 \times 10^{-3}\, u_{Gt}^2 \left(\frac{Q_L}{Q_G}\right)$
Gleason et al. (1971)	$\Delta P = 2.08 \times 10^{-5}\, u_{Gt}^2\, (0.264\, Q_L + 73.8)$
Boll (1973)	$-\frac{\Delta P}{\rho_G} = \frac{u_{G1}^2 - u_{G2}^2}{2\, g_c} + \frac{M}{g_c}\int_0^t u_G\left(\frac{d\, u_d}{dt}\right)dt + \frac{(M+1)}{2\, g_c}\int_0^t \frac{f\, u_G^2\, u_d}{d_{eq}}\, dt + \frac{1}{2\, g_c}\int_{x_1}^{x_2} \frac{f\, u_G^2}{d_{eq}}\, d$
Behie & Beeckman (1973)	$dp = -\left(\frac{6P}{\pi d_d^3\, \rho_d}\right)\left[\frac{1}{2}\, C_D\, \rho_G\, (u_G - u_d)^2\, \frac{\pi\, d_d^2}{4}\right] dt$
Hesketh (1974)	$\Delta P = 1.36 \times 10^{-4}\, u_{Gt}^2\, \rho_G\, A_t^{0.133} \left[0.56 + 935\left(\frac{Q_L}{Q_G}\right) + 1.29 \times 10^{-3}\left(\frac{Q_L}{Q_G}\right)^2\right]$

where A_t = throat cross-sectional area, cm^2
A_D = duct cross-sectional area, cm^2
d_d = liquid drop diameter, cm
d_{eq} = equivalent duct diameter, cm

(continued)

where d_t = throat diameter, cm
d_o = inlet or outlet duct diameter, cm
f = friction factor, dimensionless
f_t = average friction factor of the throat
$\bar{f}_c$ = average friction factor of convergent section, dimensionless
$\bar{f}_d$ = average friction factor of the divergent section, dimensionless
g_c = conversion factor
ℓ_t = throat length, cm
M = liquid-to-gas mass ratio
m_G = gas mass flow rate, g/s
m_L = liquid mass flow rate, g/s
Q_G = gas volumetric flow rate, cm^3/s
Q_L = liquid volumetric flow rate, cm^3/s
u_G = gas velocity, cm/s
u_{Gt} = gas velocity at the throat, cm/s
u_d = liquid drop velocity, cm/s
u_L = liquid velocity, cm/s
t = time, s
z = rectangular coordinate in the direction of flow, cm
ΔP = pressure drop, cm W.C.
ΔP_d = dry pressure drop, cm W.C.
ΔT = temperature change, $^{\circ}K$
ρ_G = gas density, g/cm^3
ρ_m = manometer fluid dnesity, g/cm^3
θ_1 = convergence angle, degree
θ_2 = divergence angle, degree
ζ = coefficient on divergent loss of gas flow, dimensionless
ζ_t = head-loss ratio for throat, dimensionless
ζ_d = head-loss ratio for divergent section, dimensionless

scrubber. Correlations by Matrozov (1953), Volgin et al. (1968), Gleason et al (1971) and Hesketh (1974) are experimental correlations. All others are theoretical equations.

Entrainment Separator

The entrainment separator is an integral part of the scrubber system. Generally, any device that can be used to collect particles can also be employed to knock out entrainment. However, due to economical reasons, only a few find practical usage. Calvert, et al. (1975) have evaluated several suitable entrainment separators experimentally. Table 2-3 lists several common entrainment separators and their design equations.

CONCLUSIONS

The principal objectives of this study were achieved. The following conclusions can be drawn.

(1) Collection by atomized liquid drops is the principal collection phenomena in a venturi scrubber. Even though each investigator presented a different equation for the prediction of particle collection in a venturi scrubber, most of these equations can be reduced to the same basic model, i.e.,

$$-\ln Pt\,(d_p) = \int_0^s \frac{3\, u_r\, Q_L\, \eta}{2\, u_G\, (u_G - u_r)\, d_d}\, ds \qquad (2\text{-}1)$$

where $Pt(d_p)$ = penetration for particles with diameter d_p, fraction

u_r = relative velocity between dust and drop, cm/s

u_G = gas velocity, cm/s

d_d = drop diameter, cm

η = single drop collection efficiency, fraction

Q_L = liquid volumetric flow rate, cm³/s

s = length, cm

TABLE 2-3. ENTRAINMENT SEPARATOR DESIGN EQUATIONS

Separator Type	Investigator	Design Equation
Gravity Settler		$E = \frac{u_t\,\text{[illegible]}}{\text{[illegible]}}$
Sieve Plate	Taheri & Calvert (1968)	$E = 1 - \exp\left(-40\, F^2 K_p\right)$
Mesh	Bradie & Dickson (1969)	$E = 1 - \exp\left(-\frac{2}{3}\frac{1}{\pi} a_2 L_2\, \eta\right)$
Packed Bed	Jackson & Calvert (1966)	$Pt = 1 - \exp\left[\frac{-\pi}{2(j + j^2)(\varepsilon - H_d)}\,\frac{Z}{d_c}\, K_p\right]$
Tube Bank	Calvert & Lundgren (1970)	$E = 1 - (1 - \eta_j)^N$
Cyclone	Leith & Licht (1971)	$\ln Pt = -2\left[\frac{\rho_d}{9\mu_G}\left(\frac{2d_d\, u_{tg}}{d_c}\right)^2 (n+1)\, t\right]^{\frac{1}{2n+2}}$ $n = 1 - \left[\frac{T}{283}\right]^{0.3}\left[1 - \frac{(0.393\, d_c)^{0.14}}{2.5}\right]$
Zig-zag Baffles	Calvert et al. (1974)	$\eta = 1 - \exp\left[-\frac{u_{tc}\, n w \theta}{57.3\, u_G\, b \tan\theta}\right]$

continued

TABLE 2-5. (continued)

Where a_s = specific area of mesh, cm²/cm³

b = settler width or baffle spacing within row, cm

d = cyclone diameter, cm

d_c = packing diameter, cm

F_f = foam density

H_d = fractional liquid hold-up in the bed

j = ratio of channel width to packing diameter

K_p = inertial parameter, dimensionless

ℓ = settler length, cm

t_s = thickness of mesh pad, cm

N = number of jet stages in the tube bank
= (number of rows) - 1

n = cyclone vortex or number of zig-zag rows

Q_G = volumetric gas flow rate, cm³/s

$Pt(d_d)$ = penetration for drops with diameter d_d, fraction

T = gas temperature, °K

t = residence time, s

u_G = gas velocity, cm/s

u_t = drop terminal settling velocity, cm/s

u_{tc} = centrifugal gas velocity, cm/s

u_{tg} = tangential velocity of gas, cm/s

w = width of baffle, cm

δ = bed length, cm

ρ_d = drop density, g/cm³

μ_G = gas viscosity, poise

θ = angle of inclination of the baffle to the flow path, degree

η = target efficiency of cylindrical wire, fraction

η_j = collection efficiency for a given drop diameter in one stage of rectangular jet impingement, fraction

ϵ = packed bed porosity

(2) A generalized method for applying equation 2-1 to predict particle collection in a venturi was developed.

(3) Particle collection predicted by equation 2-1 agrees satisfactorily with performance data.

(4) Most of the particle collection occurs in the venturi throat. The solution to equation 2-1 for the venturi throat, using the inertial collection efficiency correlation proposed by Calvert (1970) and assuming a zero initial drop velocity is,

$$\frac{\ln Pt(d_p)}{B} = \frac{1}{K_{po}(1-u^*_{de}) + 0.7}\left[4\ K_{po}(1-u^*_{de})^{1.5} + 4.2(1-u^*_{de})^{0.5}\right.$$

$$\left. - 5.02\ K_{po}^{0.5}\left(1-u^*_{de}+\frac{0.7}{K_{po}}\right)\tan^{-1}\left(\frac{(1-u^*_{de})K_{po}}{0.7}\right)^{0.5}\right]$$

$$- \frac{1}{K_{po} + 0.7}\left[4\ K_{po} + 4.2 - 5.02\ K_{po}^{0.5}\left(1 + \frac{0.7}{K_{po}}\right)\tan^{-1}\left(\frac{K_{po}}{0.7}\right)\right]$$

(2-2)

where

$u^*_{de} = \frac{u_{de}}{u_{Gt}}$ = dimensionless drop velocity (2-3)

$$u^*_{de} = 2\left\{1 - \left(\frac{L+B}{B}\right)^2 + \left(\frac{L+B}{B}\right)\left[\left(\frac{L+B}{B}\right)^2 - 1\right]^{0.5}\right\} \qquad (2\text{-}4)$$

$$B = \left(\frac{Q_L}{Q_G}\right)\left(\frac{\rho_L}{\rho_G}\right)\frac{1}{C_{Do}} \qquad (2\text{-}5)$$

$K_{po} = \frac{C'\ d_p^2\ \rho_p\ u_{Gt}}{9\ \mu_G\ d_d}$ = inertial parameter based on throat velocity, dimensionless

(2-6)

$$L = \frac{3\,\ell_t\,C_{Do}\,\rho_G}{2\,d_d\,\rho_L}$$ = dimensionless throat length (2-7)

and, C' = Cunningham slip factor, dimensionless
C_{Do} = initial drag coefficient, dimensionless
d_p = particle diameter, cm
ℓ_t = venturi throat length, cm
u_{de} = liquid drop velocity, cm/s
u_{Gt} = gas velocity at the venturi throat, cm/s
ρ_G = gas density, g/cm³
ρ_L = liquid density, g/cm³
ρ_p = particle density, g/cm³
μ_G = gas viscosity, poise

Equation 2-2 slightly underestimates the particle collection occurring in a venturi scrubber. For most industrial venturi scrubbers, particle collection can be predicted closely by neglecting the first term in the right hand side of equation (2-2).

(5) Pressure drop predictions by the modified Calvert's equation and by Boll's equation agree with experimentl data. The modified Calvert's equation has the following form,

$$\Delta P = 1.03 \times 10^{-3}\, u_{de}^{2}\, u_{Gt}^{2} \left(\frac{Q_L}{Q_G}\right) \qquad (2\text{-}8)$$

where ΔP = pressure drop, cm W.C.
Q_G = gas flow rate, cm³/s

(6) The use of a drag coefficient from the "Standard Curve" gives a better fit between model and experimental data than does Ingebo's correlation.

CHAPTER 3

LITERATURE SEARCH

The literature survey and background information discussed in this chapter summarize what could be distilled from a survey of the background information and represent what was known at the onset of this study.

COLLECTION MECHANISM

The basic approach to the study of collection of small particles is through the evaluation of unit mechanisms that can occur in the control device. The "Scrubber Handbook", Calvert, et al. (1972), discusses five basic unit mechanisms, namely:

(1) Collection by drops

(2) Collection by cylinders

(3) Collection of particles by bubbles

(4) Deposition from a moving aerosol in pipes and ducts

(5) Collection of particles by liquid jets. Of the five, collection by drops is the predominant mechanism occurring in the venturi scrubber.

Particle collection by liquid drops may arise through several mechanisms or phenomena, such as inertial collection, interception, diffusion, electrostatic collection, and gravitational collection. All investigators have concluded that inertial impaction in the principal mechanism of particle collection in a venturi scrubber for particles larger than 0.5 µm in diameter. For particles smaller than 0.1 µm in diameter, diffusional collection prevails.

Inertial Impaction

A drop moving through a gas will sweep out a cylindrical volume equal to the product of drop cross sectional area, relative velocity between gas and drop and time. However, not all of the particles in this gas volume will necessarily impinge upon and be collected by the drop.

As the gas stream approaches the drop, the fluid streamlines spread around it, while a particle suspended in the gas stream tends to move in a straight line due to its inertia. Therefore, as the gas flows around the drop, the particle keeps moving toward the drop. Due to the fluid drag some particles, especially the smaller ones, will be deflected from their path toward the drop and carried by the gas around the drop.

The trajectory of the particle determines the target efficiency of the drop. Target efficiency is defined as the ratio of the number of particles striking the drop to the number which would strike it if the streamlines were not diverted by the drop. If the particles bounce rather than stick on impaction, this definition of efficiency is incorrect. Thus an assumption is always made that all the particles adhere on striking.

Three factors determine the inertial impaction efficiency. The first is the velocity distribution of the gas flowing by the drop, which depends on the drop Reynolds number. The second factor is the trajectory of the particle. This depends on the mass of the particle, its air resistance, the size of the drop, and the flow rate of the gas stream. The third factor is the adhesion of the particles to the drop. Each of these factors is discussed below.

The drop Reynolds "N_{Red}" number is defined as,

$$N_{Red} = \frac{u_0 \rho_G d_d}{\mu_G} \qquad (5\text{-}1)$$

where "u_0" is the undisturbed upstream air velocity, with respect to the drop; "ρ_G" amd "μ_G" are respectively the air density and viscosity, and "d_d" is the drop diameter. At high values of "N_{Red}"(potential flow), the parting of the gas streamlines occurs close to the drop. Except near the drop surface, the flow pattern corresponds to that of an ideal gas. When the Reynolds number is low, flow is governed by viscosity (viscous flow) and the effect of the disturbance created by the drop is noticed at relatively large distances upstream. The sudden spreading of the streamlines at high Reynolds numbers enhances the influence of particle inertia and therefore causes a higher collection efficiency than at low "N_{Red}."

If all field forces are ignored and if it is assumed that the particles obey Stokes' law, then the equations of particles motion can be derived by equating the particle inertia force to the air drag on the particle. The equations in dimensionless form are:

$$K_p \frac{d\tilde{U}_p}{d\tilde{t}} = (\tilde{U}_G - \tilde{U}_p) \tag{3-2}$$

$$K_p \frac{d\tilde{V}_p}{d\tilde{t}} = (\tilde{V}_G - \tilde{V}_p) \tag{3-3}$$

where:

$$K_p = \frac{C' \rho_p d_p^2 u_0}{9 \mu_G d_d} \tag{3-4}$$

$$\tilde{U}_p = \frac{u_p}{u_0} \quad ; \quad \tilde{V}_p = \frac{v_p}{u_0} \qquad (3\text{-}5) ; (3\text{-}6)$$

$$\tilde{U}_G = \frac{u_G}{u_0} \quad ; \quad \tilde{V}_G = \frac{v_G}{u_0} \qquad (3\text{-}7) ; (3\text{-}8)$$

$$\tilde{t} = \frac{2 u_0 t}{d_d} \tag{3-9}$$

where K_p = inertial impaction parameter, dimensionless
ρ_p = particle density, g/cm³
d_p = particle diameter, cm
u_0 = undistrubed upstream gas velocity with respect to the drop, cm/s
μ_G = gas viscosity, poise
d_d = drop diameter, cm

C' = Cunningham correction factor
t = time, sec
u_p = particle velocity component in the X direction
v_p = particle velocity component in the Y direction
u_G = gas velocity component in the X direction
v_G = gas velocity component in the Y direction

The dimensionless inertial parameter, K_p, which characterized the motion of the particle, has a physical meaning. It is the ratio of the particle "stopping distance" to the radius of the collector. The particle stopping distance is that distance it would travel before coming to rest if injected into a still gas with velocity "u_G", when all forces on the particle except the drag force are zero.

The solutions to the equations of motion depend upon the velocity field assumed. Figure 3-1 shows theoretical and experimental target efficiencies for a single drop. As revealed by this figure, target efficiency depends on drop Reynolds number and inertial impaction parameter.

Walton and Woolcock's (1960) experimental data agree quite well with Langmuir and Blodgett's (1946) and Herne and Fonda's (1960) theoretical calculations for potential flow. That Walton and Woolcock's drop Reynolds numbers often fell substantially below the criterion for potential flow was apparently unimportant. For potential flow and for values of "K_p" greater than 0.2, the experimental values of inertial collection efficiency for spheres can be approximated by the correlation (Calvert, 1970):

$$\eta_p = \left(\frac{K_p}{K_p + 0.7} \right)^2 \qquad (3\text{-}10)$$

Diffusional Collection

Small particles, in the sub-micron size range, are

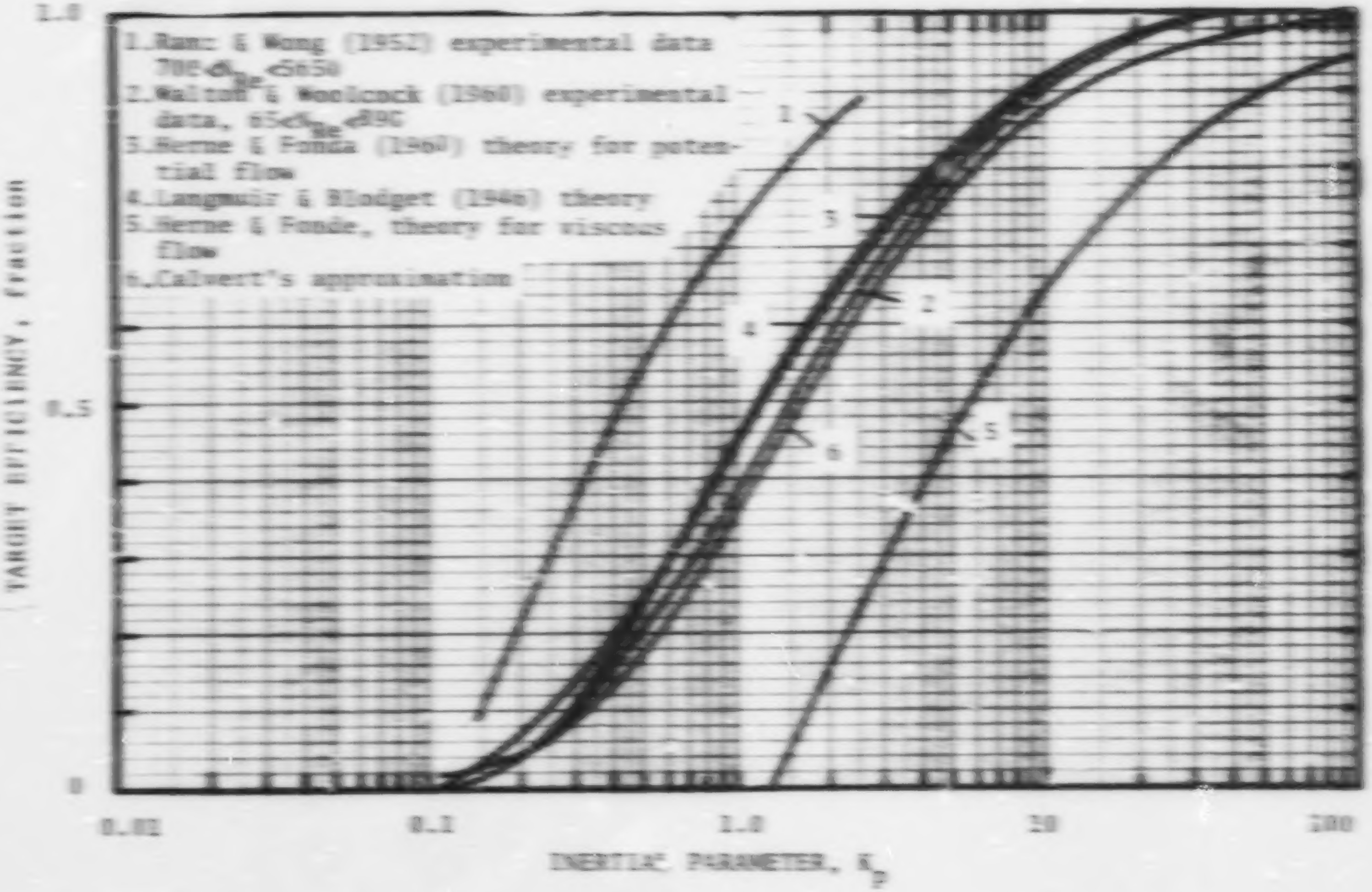

Figure 3-1. Target efficiency results of various investigators.

rarely collected by inertial impaction or interception because they follow the gas streamlines surrounding the collecting body, and their ratio of d_p/d_c is small. In a still gas, small particles move freely across gas streamlines due to random bombardment from gas molecules. Some of the particles hit the collector and are removed from the gas.

If one estimates that the aerosol concentration near the collector surface takes the form, Hidy and Brock (1970)

$$c = c_i \left(1 - \frac{r_c}{\delta} \right) \qquad (3\text{-}11)$$

where "r_c" is the collector radius, "δ" is the distance from the collector center and "c_i" is the concentration of particles in the main body of the gas stream, then the concentration gradient at the collector surface is:

$$\left. \frac{\partial c}{\partial \delta} \right|_{\delta = r_c} = \frac{c_i}{r_c} \qquad (3\text{-}12)$$

The rate of deposition, ϕ(g/s if c_i is g/cm³), on a spherical collector for a gas at rest is equal to:

$$\phi = 4 \pi D_p r_c c_i \qquad (3\text{-}13)$$

Particle diffusivities are several orders of magnitude smaller than diffusivities of gases, and are closer to the values obtained for diffusivities of solutes in liquids. The particle diffusivity may be calculated from an equation by Fuchs (1964)

$$D_p = \frac{k T C'}{3 \pi \mu_G d_p} \qquad (3\text{-}14)$$

where D_p = diffusivity of particle, cm²/s
k = Boltzmann constant = 1.38×10^{-16} erg/°K

T = temperature, °K
C' = Cunningham correction factor, dimensionless
μ_G = gas viscosity, poise
d_p = particle diameter, cm

For an aerosol flowing past a spherical collector, the rate of diffusion increases and becomes a function of the Reynolds and the Schmidt numbers. The Schmidt number "N_{Sc}" is a dimensionless group indicating the ratio of convective and diffusive transfer rates (at constant N_{Re}). The Schmidt number is defined as

$$N_{Sc} = \frac{\mu_G}{\rho_g D_p} \tag{3-15}$$

For low diffusivities, leading to high Schmidt numbers ($N_{Sc} > 10^3$), and low Reynolds numbers ($N_{Red} < 3$) Levich (1962) showed that:

$$\phi = 2 \pi D_p r_d c_i N_{Red}^{1/3} N_{Sc}^{1/3} \tag{3-16}$$

For large Reynolds numbers (600 - 2,000) and ($N_{Sc} > 10^3$, Akselrud (1953) showed that,

$$\phi = 1.6 \pi D_p r_d c_i N_{Red}^{1/2} N_{Sc}^{1/3} \tag{3-17}$$

For Reynolds number = 100 - 700 and Schmidt number = 10^3, Garner et al. (1958a and 1958b) showed that,

$$\phi = 1.9 \pi D_p r_d c_i N_{Red}^{1/2} N_{Sc}^{1/3} \tag{3-18}$$

Johnstone and Roberts (1949) presented an expression for estimation of single drop collection efficiency due to Brownian diffusion. Their expression is

$$\eta = \frac{4 D_p N'_{Sh}}{|u_G - u_d| d_d} \tag{3-19}$$

where η = single drop collection efficiency, dimensionless
D_p = particle diffusivity, cm²/s
d_d = drop diameter, cm
u_G = gas velocity, cm/s
u_d = drop velocity, cm/s
N'_{Sh} = particle transfer number analogous to the Nusselt number for heat transfer or the Sherwood number to mass transfer, dimensionless

By using the semi-theoretical equation of Frössling for "N'_{Sh}", i.e.,

$$N'_{Sh} = 2 + 0.552\, N_{Red}^{0.5}\, N_{Sc}^{1/3} \qquad (3\text{-}20)$$

equation 3-19 becomes

$$\eta = \frac{4\, D_p}{|u_G - u_d|\, d_d} \left(2 + 0.552\, N_{Red}^{0.5}\, N_{Sc}^{1/3} \right) \qquad (3\text{-}21)$$

where N_{Sc} = Schmidt number defined by equation 3-15
N_{Red} = drop Reynolds number

LIQUID DROP SIZE

As mentioned earlier, the principal collection mechanism occurring in a venturi scrubber is the collection of particles by liquid drops. The collection efficiency of a drop depends on its size. Thus, in order to model the particle collection by a venturi scrubber, we must have some knowledge about the atomized liquid drop size.

Hesketh et al. (1970), based on a study performed on a small venturi scrubber, claimed two types of atomization can occur.

Cloud-Type Atomization

This type of atomization can be achieved when nozzles larger than 1 mm I.D. are used and when gas velocity is above the critical gas velocity. The critical gas velocity is defined by the following equation

$$u_{G'} \text{ critical } (\text{cm/s}) = \left|\frac{47{,}203}{d\ (\text{mm I.D.})}\right|^{0.6} + 466.5 \qquad (3\text{-}22)$$

This type of atomization yields small drops and gives lower drop acceleration which results in better particle collection than drop type atomization.

Drop-Type Atomization

Several correlations are available for estimating the average liquid drop size in drop type atomization. These correlations are based on different mechanisms of atomization under various operating conditions. Each is applicable to a certain range of operation conditions and physical properties of fluids, such as viscosity, density, and surface tension. They are summarized in Table 3-1.

Most of the data taken in pneumatic atomization are for liquid injection, either parallel or opposite to the gas flow and with a small apparatus. Venturi scrubbers are quite large in comparison and normally have the liquid injection across the gas flow. While it is questionable that these correlations would apply to a venturi scrubber, they have been so applied.

The most widely quoted correlation is that of Nukiyama and Tanasawa, which gives the Sauter mean diameter, even though almost all investigators doubted its applicability to a full-size venturi scrubber. Boll (1973), after comparing the results of Nukiyama and Tanasawa with those of several subsequent investigators, stated that Nukiyama and Tanasawa correlation is subject to an uncertainty factor of two.

In a later study, Boll et al. (1974) measured the atomized drop size in a full-scale venturi scrubber by means of a transmissometer. They showed that the N-T equation gives values of mean drop size that are accurate within about 50% for L/G's and throat velocities of commercial

TABLE 3-1. EMPIRICAL EQUATIONS FOR AVERAGE LIQUID DROP SIZE AND THEIR APPLICABLE RANGES

Investigators	Equations	Applicable ranges		
		u_G, (cm/s)	m_G/m_L	μ_L (poise)
Nukiyama & Tanasawa (1938,1939,1940)	$d_s = \frac{5.85}{u_G}\left(\frac{\sigma}{\rho_L}\right)^{0.5} + 1.683\left(\frac{\mu_L}{(\sigma\,\rho_L)^{0.5}}\right)^{0.45}\left(\frac{Q_L}{Q_G}\right)^{1.5}$	10^4 -sonic velocity	1.8 -15	0.1-0.4
Nagele (1960)	$\frac{d_s}{d_n} = A(N_{Re})^B\left(\frac{\mu_L\,u_r}{\sigma}\right)^C$ (A,B,C are constants)	10^4 -sonic velocity	1.8 -15	-
Gretzinger & Marshall (1961)	$d_m = 0.26\left[\frac{m_L}{m_G}\ N_{ReG}\right]^{0.4}$	10^4 -sonic velocity	1 -15	0.01-0.3
Kim & Marshall (1971)	$d_m = 0.512\,\frac{\sigma^{0.41}\,\mu_L^{0.32}}{(u_G^2\,\rho_G)^{0.57}\,A^{0.36}\rho_L^{0.16}}$ $+ 1.89\left(\frac{\mu_L^2}{\rho_L\sigma}\right)^{0.17}\frac{\left(\frac{m_G}{m_L}\right)^m}{u_G^{0.54}}$ $m = -1$ for $\frac{m_G}{m_L} < 3$ $m = -0.5$ for $m_G/m_L > 3$	7.5×10^3- sonic velocity	0.06-40	0.01-0.5

where d_s = Sauter mean drop diameter, cm

d_m = mean drop diameter, cm

d_n = nozzle diameter, cm

u_G = relative velocity, cm/s

σ = surface tension, dyne/cm

Q = volumetric flow rate, cm^3/s

ρ_L = liquid density, g/cm^3

μ_L = liquid viscosity, poise

m_L = mass flow rate of liquid, g/s

m_G = mass flow rate of gas, g/s

A = flow area of atomizing air

u_r = relative velocity between gas and liquid, cm/s interest. For the particular venturi geometry they used, the N-T equation consistently over estimates mean drop diameter at high-gas velocities and under estimates it at low-gas velocities. They presented the following empirical equation to correlate their drop data.

$$d_d = \frac{6.75 \times 10^{\text{[illegible]}} + 5.28 \times 10^{\text{[illegible]}} \left(Q_L/Q_G\right)^{\text{[illegible]}}}{u_i^{\text{[illegible]}}} \qquad (3\text{-}23)$$

where d_d = Sauter mean drop diameter, μm
Q_L/Q_G = liquid-to-gas ratio, m^3/m^3
u_i = gas velocity at liquid injection point, cm/sec

DRAG COEFFICIENT

The inertial impaction parameter, "K_p" is also a function of the relative velocity between particle and drop. The atomized liquid drops will be accelerated by the gas. The effect of acceleration on the drag coefficient has been studied by Hughes et al. (1952), Ingebo (1955), Torobin et al. (1960), Crowe (1961), and others. Hughes et al. state that as a general rule, acceleration drag exists and that it is higher than the drag for steady motion. Ingebo's results disagree with this statement. He obtained acceleration drag coefficients lower than those predicted by the standard curve, (see Figure 3-2). According to Ingebo, the drag coefficients "C_D" for drops can be correlated fairly well with the Reynolds number according to the following empirical expression:

$$C_D = \frac{27}{N_{Red}^{0.84}} \qquad (3\text{-}24)$$

where C_D = drag coefficient
N_{Red} = drop Reynolds number

This expression is applicable for a Reynolds number range of 6 to 400 and spheres with a diameter range of 20 to 120

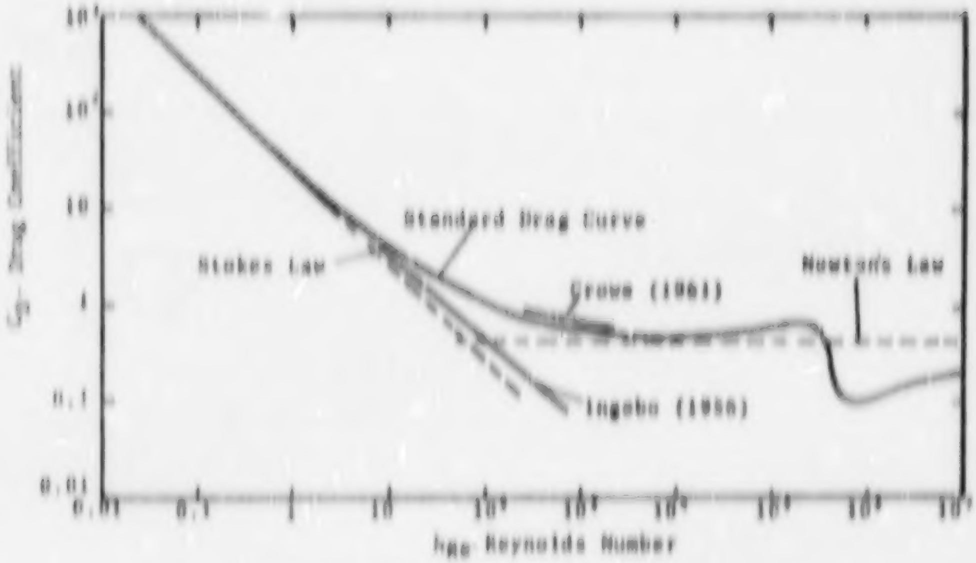

Figure 3-2, DRAG COEFFICIENT OF A SPHERE .

microns. Calvert (1968) used the Ingebo data and simplified the above equation to

$$C_D = \frac{55}{N_{Red}} \text{ for } 100 < N_{Red} < 500 \qquad (3\text{-}25)$$

However, this expression is applicable for a Reynolds number range between 100 and 500. While this range is more narrow than the range of the original correlation, it is the range that is of interest for venturi scrubbers. Calvert stated that this correlation is also a fairly good approximation for the Reynolds number up to 1,000.

The Ingebo correlation and the Standard curve have been used in the modeling of venturi scrubber by different investigators. However, Boll (1973) concluded that in the case of a venturi, the Standard curve of the drag coefficient is the better choise. He argued that Ingebo injected the particles or drops as a small concentrated stream into the center of a much larger duct. Thus, the high central concentration of slowly moving drops or particles would have much the same effect as a stationary porous body in the duct. Consequently, some of the gas must have flowed around the mass of drops rather than between them, reducing the actual gas velocity in the vicinity of the individual drops. This would have lowered the actual drop acceleration and reduced the apparent drag coefficient, accounting for the low C_D values.

Dickinson and Marshall (1968) approximated the Standard curve by the following correlation

$$C_D = 0.22 + \frac{24}{N_{Red}} \left(1 + 0.15\, N_{Red}^{0.6}\right) \qquad (3\text{-}26)$$

SCRUBBER COLLECTION EFFICIENCY

Calvert (1968 , 1970), by performing a material balance for dust over a differential scrubber volume with the assumption of constant liquid holdup, obtained a differential equation for the prediction of venturi scrubber performance. This equation is

$$-\frac{dc}{c} = \frac{3 \; |u_r| H_d \; \eta \; dz}{2 \; d_d \; u_G} \qquad (3\text{-}27)$$

where c = dust concentration, g/cm³

u_r = $u_p - u_d$ relative velocity between particle and liquid drop, cm/s

η = single drop collection efficiency, fraction

d_d = drop diameter, cm

u_G = gas velocity, cm/s

z = distance, cm

H_d = drop holdup or volume fraction of drops at any point

$= \frac{Q_L}{u_d A}$

Q_L = liquid flow rate, cm³/sec

u_d = drop velocity, cm/sec

A = cross-section area, cm²

By substituting the defining equation of "H_d" and "u_r" into equation 3-27, one obtains

$$-\frac{dc}{c} = \frac{1.5\,|u_p - u_d|}{u_d \; d_d}\left(\frac{Q_L}{Q_G}\right)\eta \; dz \qquad (3\text{-}28)$$

Another assumption in the derivation of this equation is that particle velocity is the same as gas velocity.

Calvert (1970) and Calvert et al. (1970) applied equation 3-28 to the venturi throat and obtained the following simplified equation for predicting particle penetration

$$Pt(d_p) = \exp\left[\frac{2\ Q_L\ u_{Gt}\rho_L\ d_d}{55\ Q_G\ \mu_G}\ F\left(K_{pt},\ f\right)\right] \tag{3-29}$$

where $Pt(d_p)$ = penetration of particles with diameter d_p, fraction
Q_L = liquid flow rate, cm³/s
Q_G = gas flow rate, cm³/s
d_d = average liquid drop diameter given by the empirical correlation of Nukiyama and Tanasawa, cm
u_{Gt} = velocity of the gas in the throat, cm/s
μ_G gas viscosity, poise
ρ_L = liquid density, g/cm³
K_{pt} = inertial parameter evaluated at the velocity of the gas in the throat.

"$F(K_{pt}, f)$" is a parameter defined by the following equation

$$F(K_{pt},\ f) = \frac{1}{K_{pt}}\left[1{,}4\ \ln\left(\frac{K_{pt}\ f + 0{,}7}{0{,}7}\right)\right. \tag{3-30}$$

$$\left. + \frac{0{,}49}{0{,}7 + K_{pt}\ f} - (K_{pt}\ f + 0{,}7)\right]$$

"f" is an empirical parameter. For hydrophobic aerosols a value of 0.25 is suggested by Calvert for this parameter. For hydrophilic particle materials it is usually equal to 0.5.

Boll (1973) took into account the particle collection, occurring in the venturi throat as well as in the divergent and convergent section of the venturi, and presented the following integral equation for the calculation of particle penetration

$$N_G = \int_0^t 1.5 \left(\frac{M \rho_G}{\rho_L}\right) \frac{|u_G - u_d|}{d_d} \eta \, dt \qquad (3\text{-}31)$$

where N_G = number of collection units
= $-\ln Pt(d_p)$
M = ratio of liquid-mass flow rate to gas-mass-flow rate
ρ_G = gas density, g/cm^3
ρ_L = liquid density, g/cm^3
η = target efficiency, fraction
t = time, s
d_d = liquid drop diameter given by Nukiyama and Tanasawa correlation, cm
u_G = gas velocity, cm/s
u_d = liquid drop velocity, cm/s

"$|u_G - u_d|$" is the relative velocity between gas and drops. This velocity depends on the geometry of the venturi scrubber. Boll assumed that the gas is incompressible. Thus, the gas velocity at any location in the scrubber is given by

$$u_G = \frac{m_G}{A \rho_G} \qquad (3\text{-}32)$$

where m_G = gas mass flow rate, g/s
A = cross-sectional area of the scrubber, cm^2

The drop velocity is equal to the time integral of drop acceleration

$$u_d = u_{di} + \int_0^t \left(\frac{d u_d}{dt}\right) dt$$

$$= u_{di} + \int_0^t \frac{3}{4} \frac{\rho_G}{\rho_L} \frac{(u_G - u_d)}{d_d} C_D \, dt \qquad (3\text{-}33)$$

where u_{di} = initial velocity of the drop, cm/s
C_D = drag coefficient

Boll used the Standard curve for C_D for solid spheres due to Lapple and Shepherd (1940).

Boll's equation, i.e., equation 3-31 can be reduced to Calvert's differential equation. Thus, these two equations are essentially the same.

Behie and Beeckmans (1973) also gave a differential equation for aerosol capture in the venturi scrubber. Their equation is

$$-d\ (\ln c) = \frac{3}{2}\frac{F\ \eta\ (u_G - u_d)}{\rho_L\ d_d\ u_G\ u_d}\ dz \qquad (3\text{-}34)$$

where c = dust concentration, g/cm³
F = drop mass flux, g/cm²-s
ρ_L = liquid density, g/cm³
η = target efficiency, fraction
u_G = gas velocity, cm/s
u_d = drop velocity, cm/s
d_d = drop diameter, cm
z = the distance from the origin in the direction of gas flow, cm

This equation is equivalent to Calvert's differential equation for particle collection in a venturi scrubber.

Calvert, Boll and Behie and Beeckmans all assumed that the particle velocity is the same as gas velocity. However, Dropp and Akbrut (1972), after evaluation of venturi performance data taken from several power plants, concluded that the model will over-predict the efficiency of a venturi scrubber for big particles if gas velocity is substituted for particle velocity. This is because while the fine particles move at practically the same velocity as the gas, the velocity of large particles differs markedly from the gas velocity. Big particles move at a lower velocity than the gas which results in a lower impaction parameter and lower efficiency. Dropp and Akbrut proposed the following equation to predict venturi scrubber performance.

$$Pt(d_p) = \exp\left[-\frac{3}{2}\int_0^{\ell}\frac{Q_L}{Q_G}\,\frac{\eta}{d_d}\,\frac{u_p - u_d}{u_d}\,ds\right] \qquad (3\text{-}35)$$

where $Pt(d_p)$ = penetration for particles with diameter d_p, fraction
Q_L = liquid-flow rate, cm³/s
Q_G = gas-flow rate, cm³/s
u_p = particle velocity, cm/s
u_d = drop velocity, cm/s

This equation has the same form as Calvert's differenvial equation except particle velocity is used in Dropp and Akbrut's equation.

Calvert derived his equation by considering particle collection by all liquid drops existing in a unit volume. Ekman and Johnstone (1951) employed another approach to arrive at an equation for the calculation of particle collection in a venturi scrubber. They looked upon a single liquid drop as a unit and followed the drop to determine its particle collection for its entire flying path length. Total particle collection of the venturi scrubber is then the sum of the collection of all liquid drops. Ekman and Johnstone's equation is,

$$Pt(d_p) = \exp\left|-\frac{3\,\eta\,Ps}{400{,}000}\right| \qquad (3\text{-}36)$$

where $Pt(d_p)$ = penetration for particles with diameter d_p, fraction
η = single drop impaction efficiency, fraction
P = length of effective path of liquid drop, cm
s = specific surface of drops formed in scrubber, cm²/cm³

Morishima et al. (1972) used the same approach as Ekman and Johnstone and considered the particle collection in the venturi throat and in the divergent section. They arrived at the following equation

$$Pt(d) = \exp\left[-(R_t + R_d)\frac{Q_L}{Q_G}\right] \qquad (5\text{-}37)$$

"R_t" and "R_d" are, respectively, the washing factor of gas in the venturi throat and in the divergent section. Washing factor is defined as the volume of gas swept clean by a liquid drop per unit volume of liquid drop. For venturi throat and divergent section, the defining equations for these two washing factors are,

$$R_t = \frac{3\ell_t}{2d_d}\int_0^1 \eta \frac{u_G}{u_d}\left(1 - \frac{u_d}{u_G}\right) dX \qquad (5\text{-}38)$$

$$R_d = \frac{3\ell_G}{2d_d}\int_1^{X_{max}} \eta \frac{u_G}{u_d}\left(\frac{1}{X^2} - \frac{u_G}{u_d}\right) dX \qquad (5\text{-}39)$$

where ℓ_t = venturi throat length, cm
X = dimensionless distance
$= \frac{x}{\ell_t}$
d_d = drop diameter from Nukiyama and Tanasawa correlation, cm
η = target efficiency

$\ell_G = \frac{d_t}{2\tan\frac{\theta}{2}}$, cm
d_t = venturi throat diameter
θ = divergence angle

All investigators cited earlier had assumed that the liquid drop distribution is uniform across the duct and there is no turbulent mixing between drops and particles. In reality, the drop concentration across the venturi throat is far from uniform (Taheri and Haines (1969), Boll (1973)). Taheri and Sheih (1975) took turbulent mixing and liquid drop distribution across the duct into account and obtained the following equations for predicting the transport and diffusion of the particles and water drops.

$$\frac{\partial c}{\partial t} = -u_G \frac{\partial c}{\partial z} + E_p \left| \frac{\partial^2 c}{\partial y^2} + \frac{\partial^2 c}{\partial x^2} \right| - \frac{\pi \eta}{4} d_d^2 (u_G - u_d)\, c\, c_d \tag{3-40}$$

$$\frac{\partial c_d}{\partial t} = -u_d \frac{\partial c_d}{\partial z} + E_d \left| \frac{\partial^2 c_d}{\partial y^2} + \frac{\partial^2 c_d}{\partial x^2} \right| + Q_d \tag{3-41}$$

where c = particle concentration, g/cm³
c_d = number concentration of liquid drop, #/cm³
u_G = gas velocity, cm/s
u_d = drop velocity, cm/s
E_p = eddy diffusivity of particle, cm²/s
E_d = eddy diffusivity of drop, cm²/s
x = rectangular coordinate, perpendicular to direction of the flow, cm
y = rectangular coordiante, perpendicular to the flow, cm
z = rectangular coordiante, in the direction of flow, cm
Q_d = source strength of drops, #/cm³

In all the above mentioned performance models, the liquid drops were assumed to have one size, namely the Sauter mean diameter calculated from Nukiyama and Tanasawa's empirical correlation. In reality, the liquid drop size varies widely. Morishima et al. (1967) performed a mathematical analysis to determine the influence of liquid drop size distribution on the particle impaction and diffusion collection efficiency. They found that as the range of size distribution widens, the impaction efficiency decreases.

PRESSURE DROP

Pressure drops for gas flowing through a venturi scrubber consists of the friction loss along the wall of the scrubber and the acceleration of liquid drops. Friction loss depends largely upon the geometry of the scrubber. Acceleration losses, which are frequently predominant in the venturi scrubber pressure drop, are fairly insensitive to scrubber geometry and in most cases can be predicted theoretically.

There are several correlations available, both theoretical and experimental correlations, for the prediction of pressure drop in a venturi scrubber. They are summarized in Table 3-3.

Correlations by Matrosov, Yamauchi et al., Volgin et al., Gleason et al., and Hesketh are experimental correlations. Matrosov's correlation and Volgin's correlation were obtained mainly on small-size venturi scrubbers. Yamauchi's correlation was based on experimental data taken from a venturi scrubber with high temperature gas flow (100°C - 900°C). Hesketh's correlation is an experimental correlation he obtained after he had evaluated data obtained from many fixed throat venturi scrubbers.

Equations proposed by Yoshida et al., Calvert, Tohata et al., Boll and Behie and Beeckmans are theoretical correlations. Calvert derived his equation by use of Newton's law to obtain the force required to change the momentum of liquid at a given rate. Wall friction and momentum recovery by the gas in the divergent section were neglected in the derivation. All other theoretical equations were derived from the equations of motion and momentum balance. Geiseke's equation also accounts for the mass transfer between liquid and gas. Boll's equation is similar to that of Geiseke's except Boll had

TABLE 3-2. CORRELATIONS FOR PRESSURE DROP IN VENTURI SCRUBBER

Investigator	Correlation
Matrozov (1953)	$\Delta P = \Delta P_d + 1.38 \times 10^{-3}\, u_{Gt}^{1.08} \left(\frac{Q_L}{Q_G}\right)^{0.63}$
Yoshida et al. (1960) (1965)	$\Delta P = \frac{\rho_G u_{Gt}^2}{2 g_c} \left\| a + b\left(\frac{Q_L}{Q_G}\right) \right\|$ $a = \frac{f_G}{2 \tan \frac{\theta_1}{2}} + 4 f_t \frac{\ell_t}{d_t} + \zeta\left(1 - 2\frac{d_t^2}{d_G^2}\right)$ $b = (\zeta_t - 1)\, \frac{4 f_t \ell_t}{\rho_m d_t} + (\zeta_d - 1)\frac{\xi}{\rho_m}\left(1 - \frac{d_t^2}{d_0^2}\right)$
Geiseke (1968)	$\Delta P = \frac{7G}{g_c g_c} \Big[m_G \Delta u_G + m_L \Delta u_L$ $+ \frac{\Delta m_L}{2} (u_{G_1} + u_{G_2} - u_{L_1} - u_{L_2}) \Big]$
Yamauchi et al. (1964)	$\Delta P = 0.3\, (\ell_T)^{-0.44} \frac{\rho_G u_{Gt}^2}{2 g_c} \left(1 + \frac{Q_L}{Q_G}\right)$
Tohata et al. (1964)	$\Delta P = \frac{\rho_G u_{Gt}^2}{2 g_c} \Big\{ \Big[1 - \left(\frac{A_t}{A_D}\right)^2\Big]$ $\Big[\frac{f}{8 \tan \theta_1} + \frac{f}{8 \tan \theta_2}\Big] + f_t \frac{\ell_t}{d_t} + \zeta_1 + \zeta_2 \Big\}$

(continued)

TABLE 3-2. (continued)

Investigator	Correlation
Volgin et al. (1968)	$\Delta P = 3.32 \times 10^{-6}\, u_{Gt}^2 \left(\frac{Q_L}{Q_G}\right)^{0.26} (A_t)^{0.133}$
Calvert (1968)	$\Delta P = 1.03 \times 10^{-3}\, u_{Gt}^2 \left(\frac{Q_L}{Q_G}\right)$
Gleason et al. (1971)	$\Delta P = 2.08 \times 10^{-5}\, u_{Gt}^2\, (0.264\, Q_L + 73.8)$
Boll (1973)	$-\frac{\Delta P}{\rho_G} = \frac{u_{G2}^2 - u_{G1}^2}{2\, g_c} + \frac{M}{g_c}\int_0^t u_G\left(\frac{d\, u_d}{dt}\right)dt + \frac{(M+1)}{2\, g_c}\int_0^t \frac{f\, u_G^2\, u_d}{d_{eq}}\, dt + \frac{1}{2\, g_c}\int_0^x \frac{f\, u_G^2}{d_{eq}}\, dx$
Behie & Beeckmans (1973)	$dp = -\left(\frac{6F}{\pi d_d^3\, \rho_d}\right)\left[\frac{1}{2}\, C_D\, \rho_G\, (u_G - u_d)^2\, \frac{\pi\, d_d^2}{4}\right] dt$
Hesketh (1974)	$\Delta P = 1.36 \times 10^{-4}\, u_{Gt}^2\, \rho_G\, A_t^{0.133} \left[0.56 + 935\left(\frac{Q_L}{Q_G}\right) + 1.29 \times 10^{-3}\left(\frac{Q_L}{Q_G}\right)^2\right]$

where A_t = throat cross-sectional area, cm²
A_G = duct cross-sectional area, cm²
d_d = liquid drop diameter, cm
d_{eq} = equivalent duct diameter, cm

(continued)

where d_t = throat diameter, cm
d_0 = inlet or outlet duct diameter, cm
f = friction factor, dimensionless
f_t = average friction factor of the throat, dimensionless
$\bar{f}_c$ = average friction factor of convergent section
$\bar{f}_d$ = average friction factor of the divergent section, dimensionless
g_c = conversion factor
ℓ_t = throat length, cm
M = liquid-to-gas mass ratio
m_G = gas mass flow rate, g/s
m_L = liquid mass flow rate, g/s
Q_G = gas volumetric flow rate, cm³/s
Q_L = liquid volumetric flow rate, cm³/s
u_G = gas velocity, cm/s
u_{Gt} = gas velocity at the throat, cm/s
u_d = liquid drop velocity, cm/s
u_L = liquid velocity, cm/s
t = time, s
x = rectangular coordinate in the direction of flow, cm
ΔP = pressure drop, cm W.C.
ΔP_d = dry pressure drop, cm W.C.
ΔT = temperature change, $^{\circ}$K
ρ_G = gas density, g/cm³
ρ_m = manometer fluid dnesity, g/cm³
θ_1 = convergence angle, degree
θ_2 = divergence angle, degree
ζ = coefficient on divergent loss of gas flow, dimensionless
ζ_t = head-loss ratio for throat, dimensionless
ζ_d = head-loss ratio for divergent section, dimensionless

neglected the mass transfer between phases. Equations by Tohata et al., Yoshida et al., and Boll contain terms attributed to wall friction. While Tohata et al. and Yoshida et al. had used different values for the friction factors in the covergent throat and divergent section, Boll suggested a single value for all sections. A value of 0.027 was suggested by Boll for the friction factor "f" because it gives a slightly better fit in the shape of the pressure drop curves he obtained experimentally.

CHAPTER 4

COMPARISON OF MODEL WITH EXPERIMENTAL DATA

There are numerous venturi scrubber performance data reported in literature. However, most of these data were found to be of a limited value for the testing of performance models. This is because some important information, such as scrubber geometry, water injection method, particle size distribution, etc. was generally not given. In the following sections, only those data which have been obtained under contolled conditions and for a well-defined scrubber system will be utilized to test the performance models.

COMPARISON OF PREDICTED PRESSURE DROP WITH EXPERIMENTAL DATA

Data by Wen and Uchida

Wen and Uchida (1972) obtained pressure drop data on a pilot scale O.A.P. venturi scrubber. Their pressure drop data are shown in Table 4-1. Figure 4-1 shows the dimensions of the scrubber.

Figures 4-2 through 4-4 compare pressure drop predictions by various models with Wen and Uchida's data. For the O.A.P. scrubber, the water injection nozzle is at the start of the convergent section. According to Wen and Uchida, the gas cools down quickly to scrubber outlet temperature once it is in contact with water (within 5 cm from the water injection point). Thus, in calculating the predicted pressure drop, the volumetric gas flow rate was adjusted for this temperature drop plus the volume increase due to vaporized water.

As can be seen from Figures 4-2 to 4-4, Calvert's equation consistently over estimates the pressure drop. Predictions by Volgin et al. and Hesketh are always lower than data.

TABLE 4-1. WEN AND UCHIDA'S EXPERIMENTAL PRESSURE DROP DATA ON G.A.P. VENTURI SCRUBBER

Run No.	Gas Temp. °C Inlet	Gas Temp. °C Outlet	Inlet gas Flow rate Am^3/min	Liquid Flow rate ℓ/min	Pressure Drop cm W.C.
1	154.4	46.1	29.4	37.9	22.2
2	160	43.3	30.8	37.9	21.8
3	160	46.1	29	37.9	19.8
4	157.2	43.3	34.8	37.9	30.5
5	148.9	37.8	34.2	37.9	29
6	154.4	43.3	28.5	56.8	22.9
7	135	43.3	28.6	37.9	21.6
8	154.4	43.3	30.3	37.9	21.3
9	160	46.1	29.8	56.8	24.1
10	148.9	46.1	25.5	37.9	21.8
11	148.9	46.1	25.5	37.9	19.8
12	148.9	37.8	31.2	37.9	29
13	148.9	43.3	25.5	56.8	22.9
14	121.1	43.3	25.5	77.9	21.6
15	148.9	46.1	25.5	37.9	21.3
16	148.9	46.1	25.5	56.8	23.4
17	148.9	37.8	31.2	37.9	31.5
18	121.1	35	25.5	37.9	25.9
19	148.9	40.6	25.5	37.9	21.8

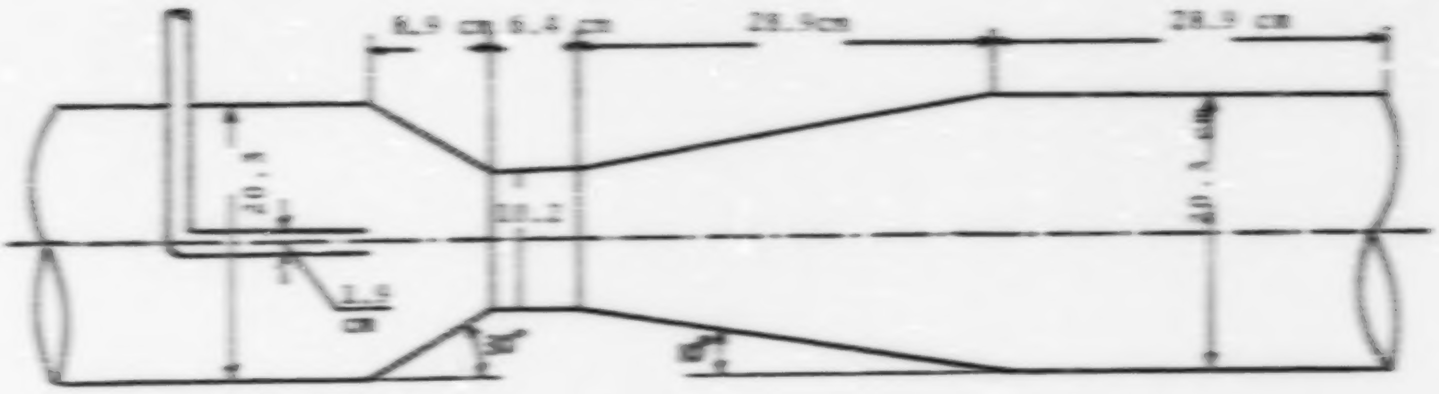
8.9 cm
6.4 cm
28.9cm
28.9 cm
40.6 cm
20.3
10.2
1.6
cm
30°
8°

Figure 4-1. Dimensions of GAP venturi scrubber.

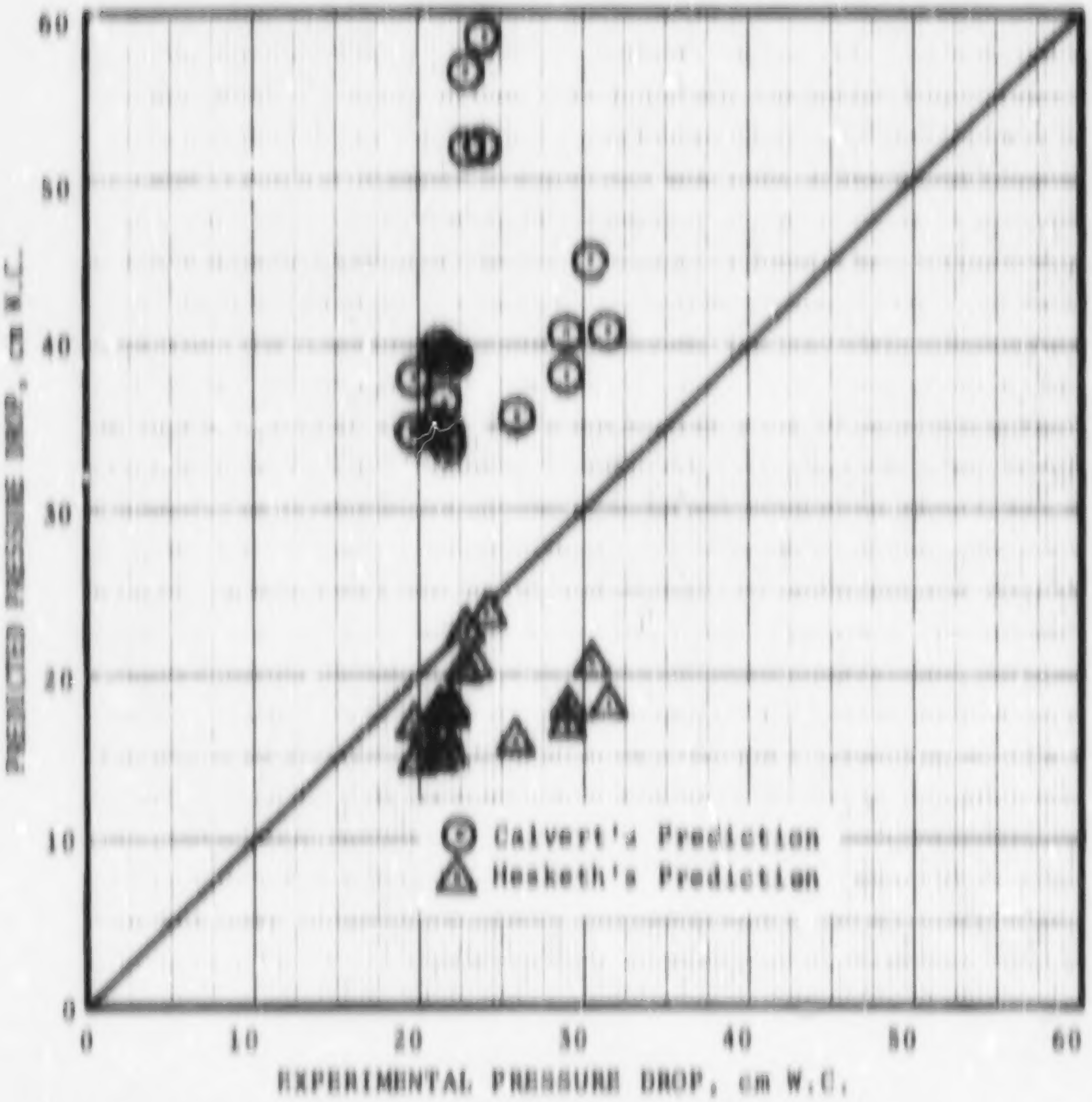

Figure 4-2. Comparison of predicted pressure drop with experimental data from Wen and Uchida.

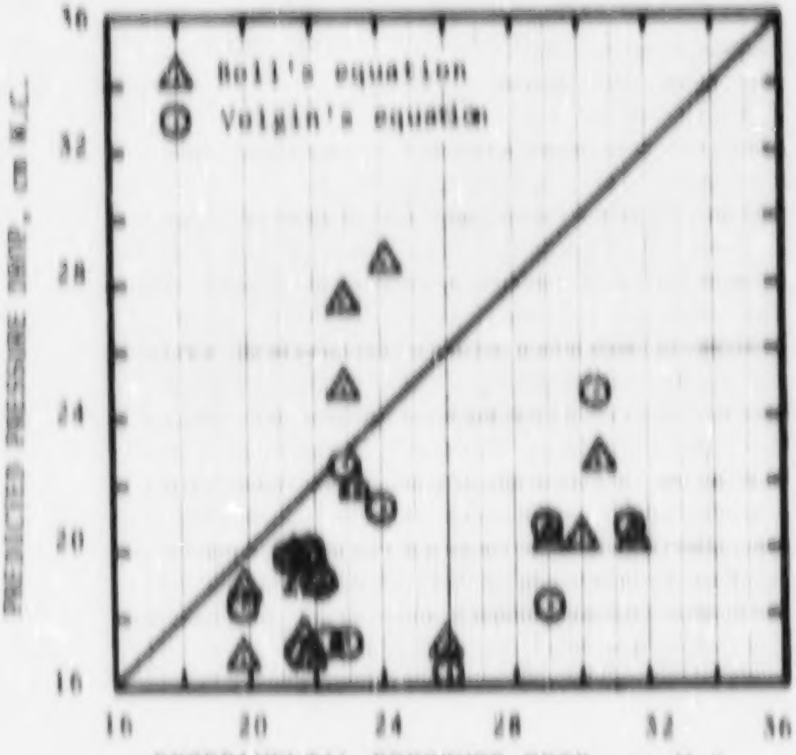

Figure 4-3. Comparison of predicted pressure drop with experimental data from Wen and Uchida.

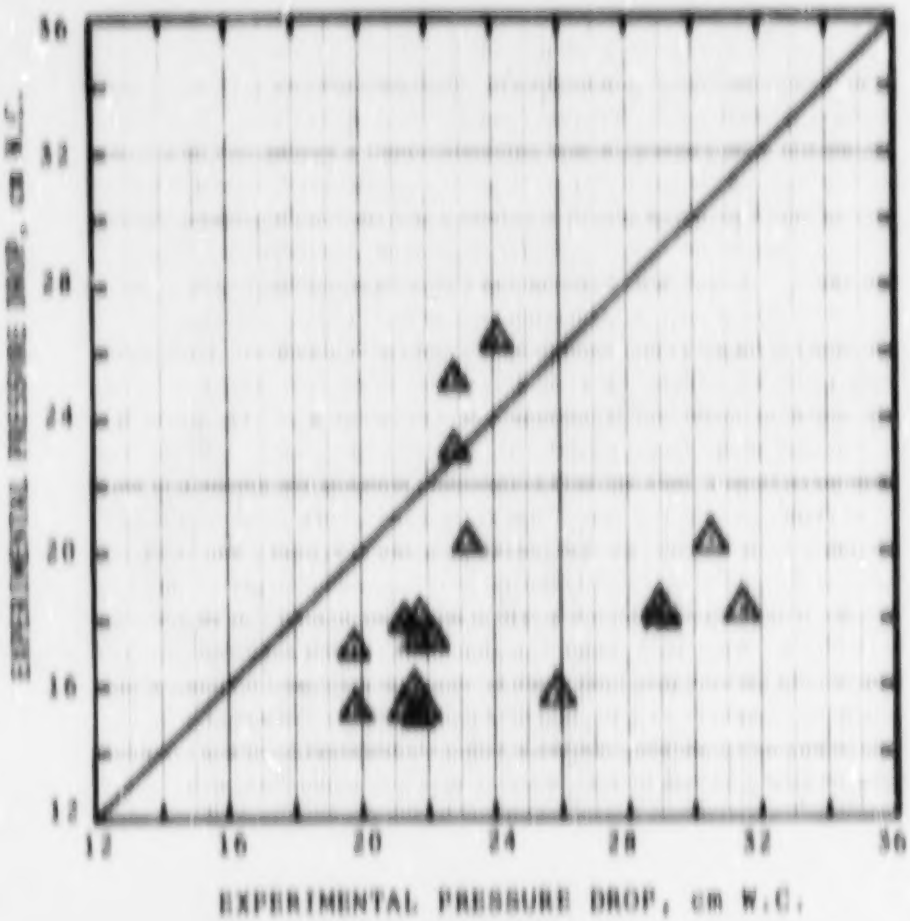

Figure 4-4. Comparison between Behie and Beeckmans' prediction and experimental data from Wen and Uchida.

Predictions by Boll and by Behie and Beeckmans are slightly better, but still have a tendency to under estimate pressure drop.

The only difference between models by Boll and by Behie and Beeckmans is that Behie and Beeckmans neglected wall-friction loss. In a venturi scrubber, most of the pressure drop is due to acceleration of liquid drops. Table 4-2 proves this statement. Table 4-2 lists Wen and Uchida's data along with predictions by Boll's equation and by Behie and Beeckman's equation. Behie and Beeckmans' equation always predicts a lower pressure drop than Boll's equation. The difference between the predictions by these two equations is equal to the wall friction. The last column in Table 4-2 shows the values of wall friction for all runs. For this particular scrubber geometry, the contribution of wall friction is less than ten per cent of the total loss.

Calvert's equation is based on the assumptions that all liquid drops accelerate to the gas velocity in the throat and that none of the drop momentum is converted to pressure in the diffuser. It is possible that in some scrubbers, liquid drops do not have sufficient residence time to accelerate to the gas velocity in the throat. In order to take this fact into account, a correction factor was developed and added to Calvert's equation. The new equation now reads

$$\Delta P = 1.0 \times 10^{-3}\ u_{Go}^{\text{[illegible]}}\ u_{Gt}^{2} \left(\frac{Q_L}{Q_G} \right) \qquad (4\text{-}1)$$

where ΔP = pressure, cm W.C.
u_{Gt} = gas velocity in the throat, cm/s
Q_L = liquid flow rate, cm³/s
Q_G = gas flow rate, cm³/s

TABLE 4-2. WEN AND UCHIDA'S EXPERIMENTAL DATA AND PREDICTIONS BY BOLL AND BY SEHIE AND BEECKMANS

Run No.	Experimental ΔP, cm W.C.	Prediction, cm W.C.		Wall Friction cm W.C.
		Boll	Sehie & Beeckmans	
1	22.2	19.2	17.4	1.8
2	21.8	19.9	18	1.9
3	19.8	18.9	17.1	1.8
4	30.5	22.7	20.4	2.3
5	29	20.4	18.1	2.3
6	22.9	27.5	25.3	2.2
7	21.6	19.1	17.4	1.7
8	21.3	19.8	17.9	1.9
9	24.1	28.7	26.4	2.3
10	21.8	16.8	15.3	1.5
11	19.9	16.8	15.3	1.5
12	29	20.4	18.4	2
13	22.9	24.9	23	1.9
14	21.6	17.4	15.9	1.5
15	21.3	16.8	15.3	1.5
16	23.4	21.9	20.4	1.5
17	31.5	20.3	18.3	2
18	25.9	17.2	15.7	1.5
19	21.8	16.7	15.2	1.5

where u^*_{de} = correction factor, dimensionless

and

$$u^*_{de} = \frac{u_{de}}{u_{Gt}} = 2 \left[1 - X^2 + (X^4 - X^2)^{0.5} \right] \qquad (4\text{-}2)$$

$$X = \frac{3 \ell C_{Do} \rho_G}{16 d_d \rho_L} + 1$$

u_{Gt} = gas velocity in the throat, cm/s

u_{de} = drop velocity at the exit of the throat, cm/s

ℓ = throat length or distance between liquid injection point and the exit of throat, cm

d_d = drop diameter from Nukiyama and Tanasawa correlation, cm

ρ_G = gas density, g/cm³

ρ_L = liquid density, g/cm³

C_{Do} = drag coefficient at the liquid injection point

"C_{Do}" is the drag coefficient obtained from Standard curve for spheres. Drop Reynolds number is defined as

$$N_{Re,d} = \frac{d_d \left(u_{Gt} - u_{do} \right)}{\nu} \qquad (4\text{-}3)$$

where $N_{Re,d}$ = drop Reynolds number

u_{do} = initial drop velocity, cm/s

ν = kinematic viscosity of gas, cm²/s

The physical meaning of "u^*_{de}" is the fraction of gas velocity to which the liquid drops have accelerated. If liquid drops are accelerated to gas throat velocity, "u^*_{de}" is equal to 1 and equation 4-1 reduces to Calvert's equation. Pressure drop prediction by equation 4-1 is lower than Wen and Uchida's data as shown in Figure 4-5.

Wall friction and pressure recovery in the diffuser were neglected in the correction factor to Calvert's equation, however, Boll's predictions are no better than the modified Calvert's equation.

Predictions based on the "standard" drag coefficient are better than those based on Ingebo's correlation, as shown in Figure 4-5. Because Ingebo's drag coefficients are low, drop velocity and pressure drop predictions are low.

Boll's Data

Boll (1973) derived an equation to predict the pressure drop in a venturi scrubber. He obtained some pressure drop data on a proto type venturi scrubber to confirm his equation. The cross-sectional dimensions of the venturi scrubber throat was 35.6 cm x 30.5 cm (14 x 12 inches). The throat length was 30.5 cm (12 in.). The convergence and divergence angles were 25° and 7°, respectively. Figure 4-6 is a sketch of the venturi scrubber used by Boll.

Figure 4-7 shows the comparison between Boll's data and theories by various investigators. The pressure drop was expressed in terms of the number of throat velocity heads, i.e.,

$$\text{Number of velocity heads lost} = \frac{-\Delta P}{\frac{1}{2g_c}\,\frac{\rho_G}{\rho_L}\,u_{Gt}^2}$$

where ΔP = pressure drop predicted by theory, cm W.C.

g_c = 980 cm/s^2

ρ_G = gas density, g/cm^3

ρ_L = water density, g/cm^3

u_{Gt} = gas velocity in the throat, cm/s

As can be seen, Calvert's equation predicts too high a pressure drop for liquid-to-gas ratio above 0.7 ℓ/m^3. Hesketh's equation gives too low a pressure drop. Volgin's equation gives a different slope.

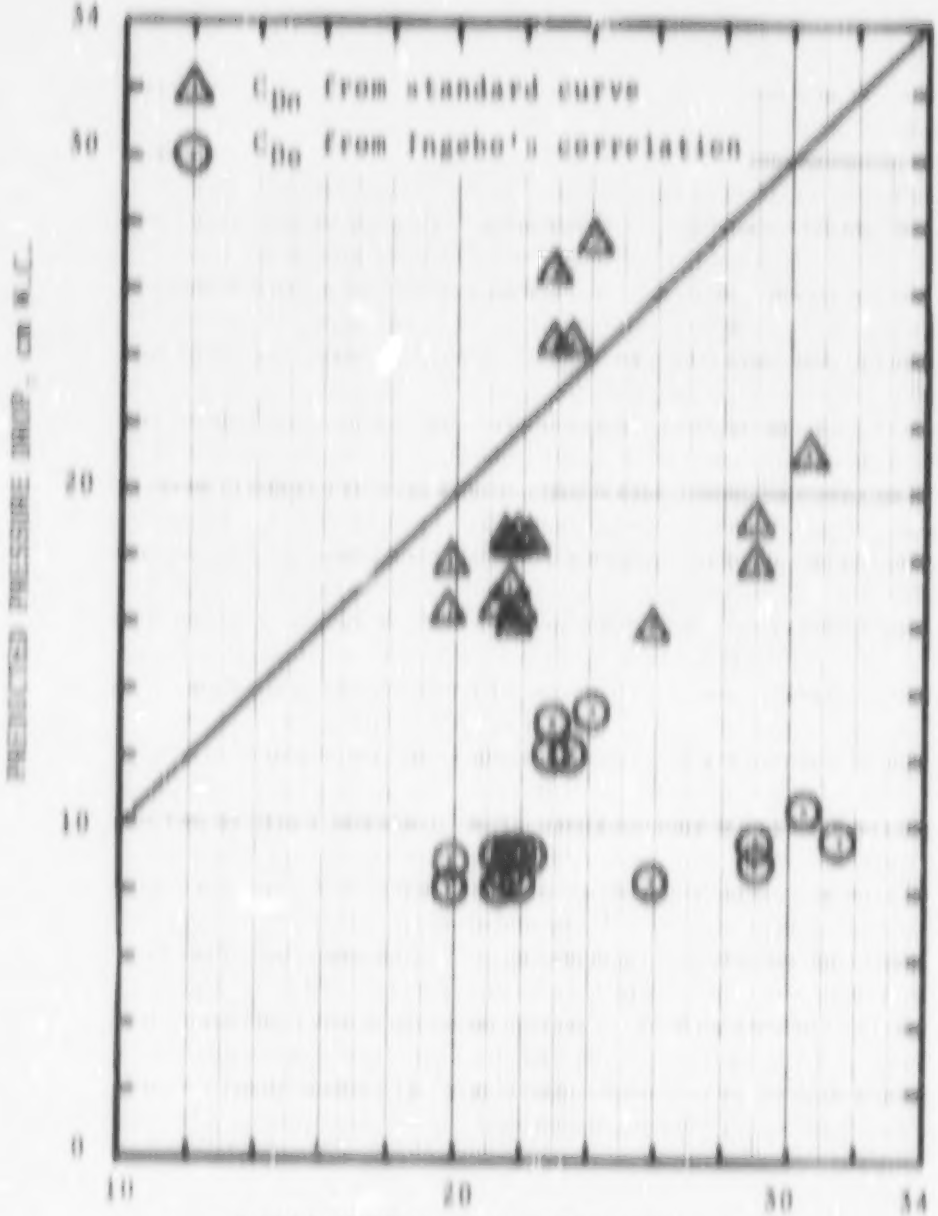

Figure 4-5. Comparison of predicted pressure drop by modified Calvert's equation with data from Wen and Uchida.

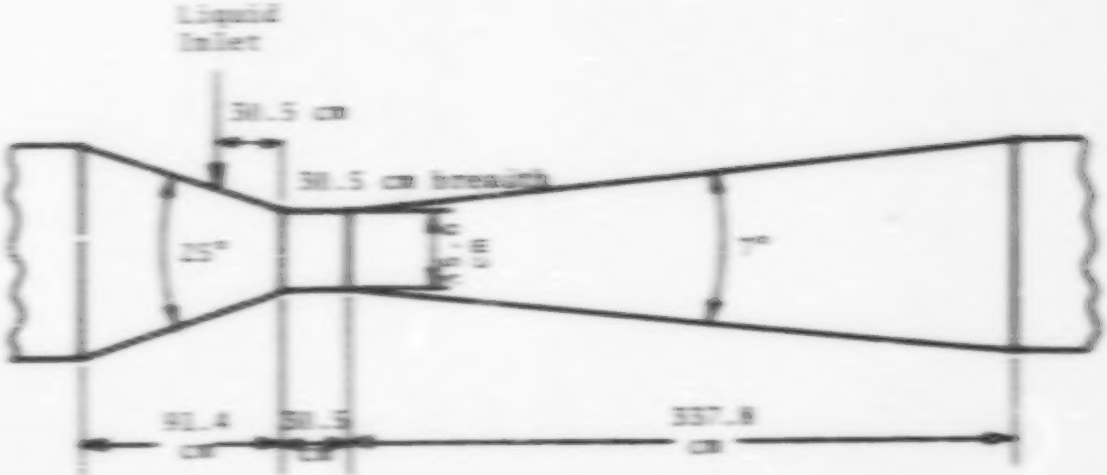
Liquid
Inlet
30.5 cm
30.5 cm breadth
25°
7°
91.4
cm
30.5
cm
337.8
cm

Figure 4-6. Prototype venturi scrubber used by Ball.

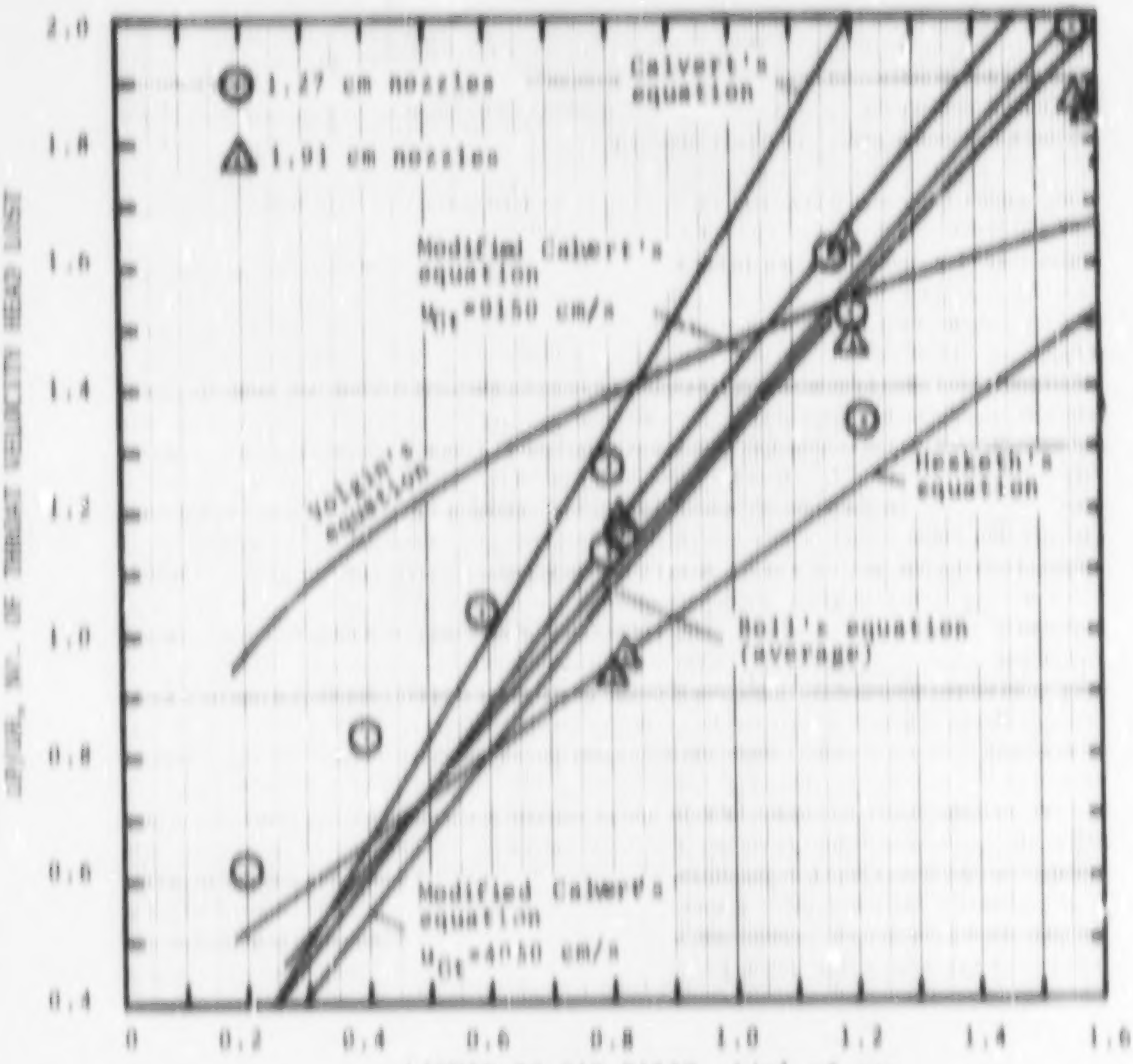

Figure 4-7. Comparison of Boll's pressure drop data with theory.

The range of gas velocity in throat covered by Boll was 45.8 m/s - 91.5 m/s (150 - 300 ft/s). The line representing the predictions by Boll's equation was an average curve for the predicted pressure drops. Even though Boll's equation slightly under estimates pressure drop at low values of liquid-to-gas ratio and slightly over estimates at high liquid-to-gas ratio, the agreement between his data and equation is considered to be satisfactory.

Predicted pressure drops by modified Calvert's equation for throat velocities of 40.5 m/s and 91.5 m/s are also shown in Figure 4-7. Since Boll operated his venturi scrubber in this throat velocity range, the area bounded by these two theoretical lines represents the range of expected pressure drops. The fact that Boll's theoretical curve, which is the average of predicted pressure drops, lies within this area signifies that the modified Calvert's equation and the more complicated Boll's equation predict pressure drop in equal accuracy.

Brink and Contant's Data

Brink and Contant (1958) perform a thorough study on an industrial-scale Pease-Anthony venturi scrubber. The scrubber had a rectangular cross section. Its throat measured 15.2 x 86.4 cm (6 x 34 inches) with a straight section 30.5 cm (12 inches) long. The angle of the convergent section was 25°; the divergent section had an angle of 2.2° for 152 cm (5 ft) following the vneturi throat and then an angle of 15°. Figure 4-8 is a sketch of the Pease-Anthony venturi scrubber.

Brink and Contant's pressure drop data are compared with theories by various investigators in Figure 4-9. Again, Calvert's equation consistently over predicts the pressure drop and Hesketh's equation consistently under estimates the pressure drop. Both Boll's equation and

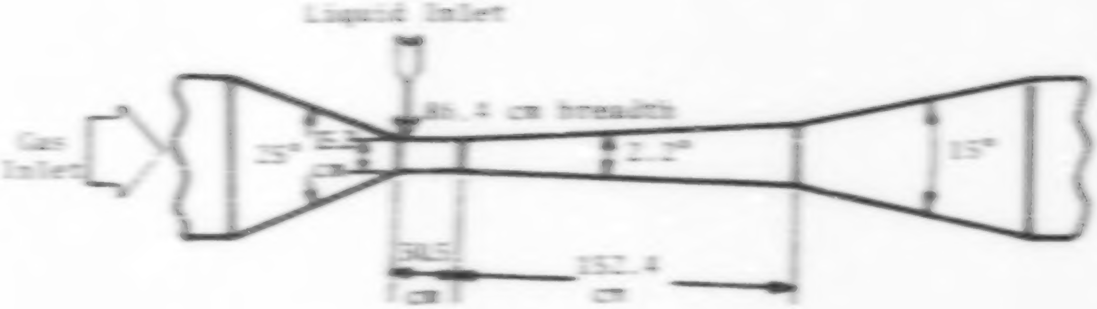
Liquid Inlet
86.4 cm breadth
Gas
Inlet
25°
15.2
cm
2.2°
15°
30.5
cm
152.4
cm

Figure 4-8. Dimension of Pease-Anthony venturi scrubber used by Brink and Contant.

the modified Calvert's equation compare favorably with experimental observations. As can be seen from Figure 4-9, Boll's equation is in better agreement with Brink and Contant's data for 90 spray jets and the modified Calvert's equation is in better agreement with 45 spray jet data. Overall, the modified Calvert's equation predicts slightly better than Boll's equation for this particular scrubber geometry.

Ekman and Johnstone Data

Ekman and Johnston (1951) have measured pressure drop across a laboratory-scale venturi scrubber. Figure 4-10 shows the venturi scrubber used by Ekman and Johnstone. The venturi throat was 3 cm (1-3/16") in diameter and 3.8 cm long. The convergent and divergent angles were 25° and 7°, respectively. Water was introduced in three ways: from a single 32 mm jet injected downstream along the axis of the throat radially outward from a brass pipe 32 mm in inside diameter with four 18.5 mm holes, and radially inward from a single 32 mm jet at the entrance of the throat. Ekman and Johnstone recorded a higher pressure drop for radial inward injection.

Figure 4-11 compares Ekman and Johnstone's experimental data with theoretical predictions. As can be seen, only Boll's equation and the modified Calvert's equation are in agreement with data.

Conclusions

Based on this evaluation, we can conclude that both Boll's equation and the modified Calvert's equation are adequate for the prediction of pressure drop in a venturi scrubber. Since the modified Calvert's equation is simpler, we will choose it as the venturi scrubber design equation. However, the method for applying Boll's equation to predict pressure drop will also be given.

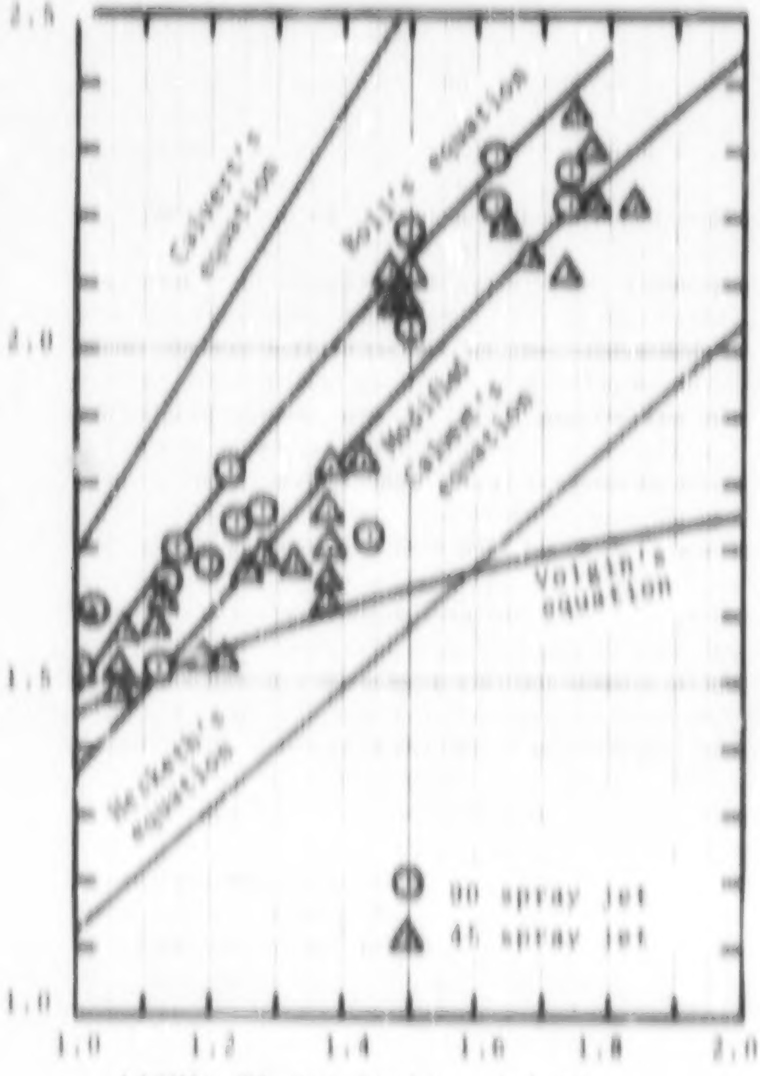

Figure 4.9. Comparison of Brink and Contant experimental data with theories.

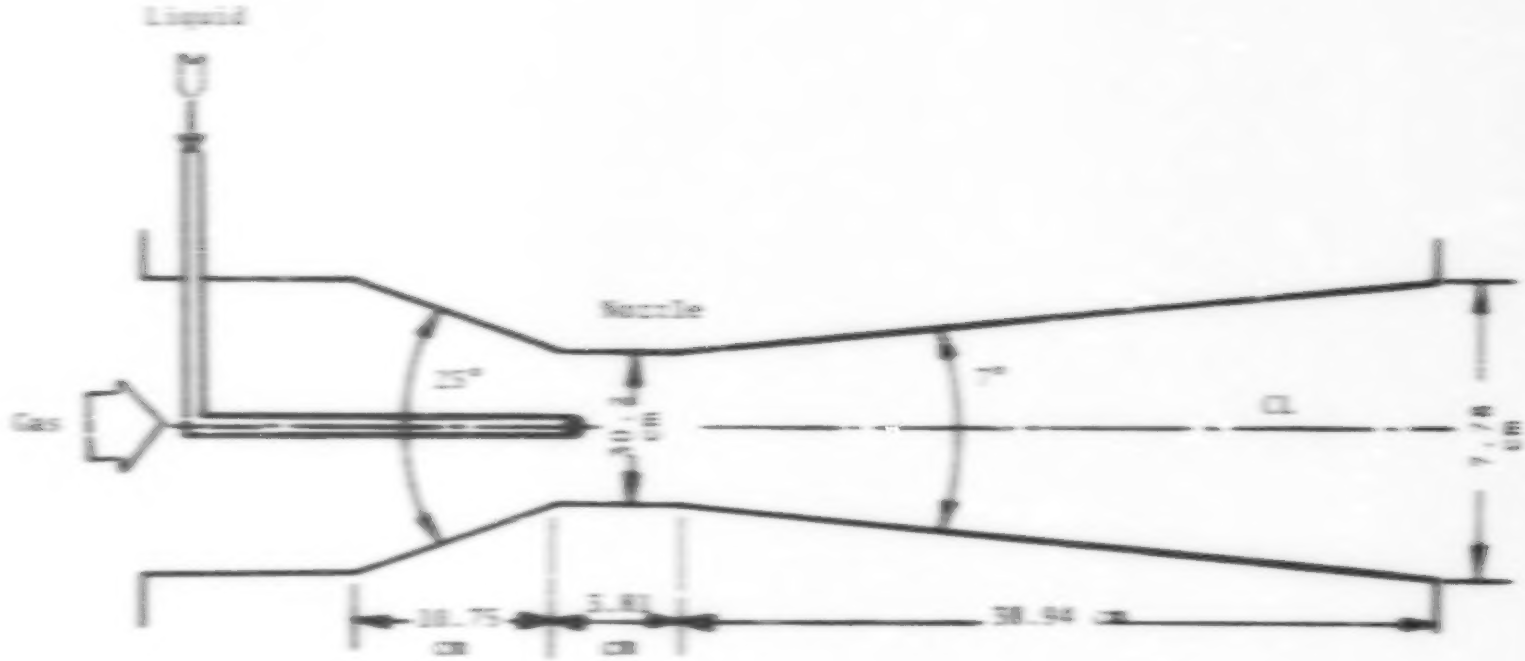
Liquid
Gas
Nozzle
25°
7°
CL
2.04 cm
7.78 cm
10.75 cm
3.81 cm
38.94 cm

Figure 4-10. Dimensions of the Ekman and Johnstone venturi.

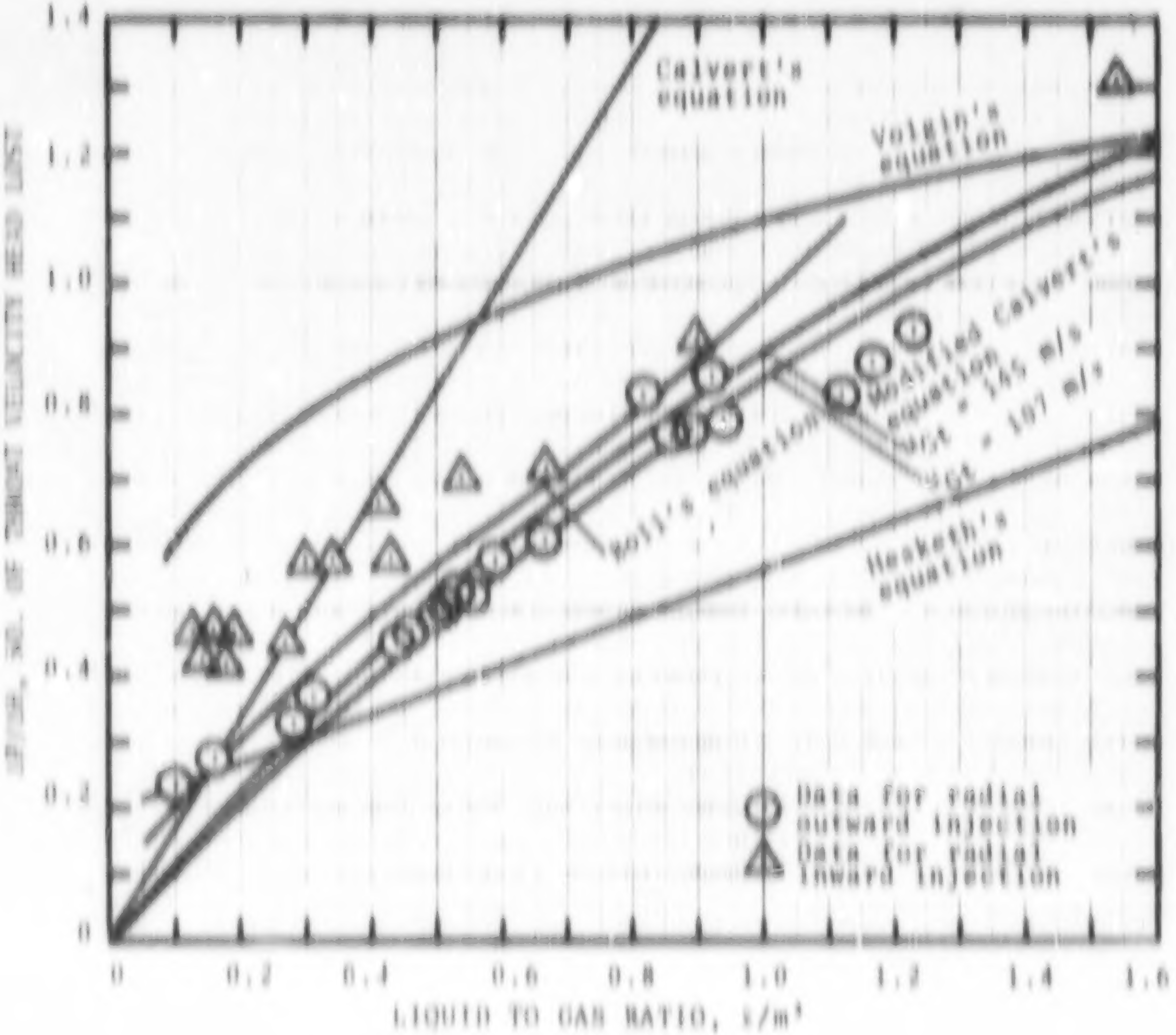

Figure 4-11. Comparison of Ekman and Johnstone's pressure drop data with theories.

PARTICLE COLLECTION

Most authors (except Taheri and Sheih) cited in the last chapter use the same basic model for the prediction of particle collection in a venturi scrubber, i.e.,

$$-\frac{dc}{c} = \frac{u_r}{u_G}\,\frac{Q_L}{(u_G - u_r)A}\left(\frac{3}{4r_d}\right)\eta\,dz \qquad (4\text{-}4)$$

where c = dust concentration
u_r = relative velocity between dust and drop, cm/s
u_G = gas or dust velocity, cm/s
A = duct cross-sectional area, cm²
r_d = drop radius, cm
= single drop collection efficiency, fraction
Q_L = liquid volumetric flow rate, cm³/s
z = axial distance, cm

Boll (1973) and Behie and Beeckmans (1973) had demonstrated the success of this equation in predicting venturi scrubber performance by comparing theoretical predictions with experimental data. Thus, we will choose this equation as the particle collection design equation for venturi scrubber.

No general solution for this equation was found in the literature. In order to calculate the particle collection efficiency, one must integrate this equation numerically, taking into account the scrubber geometry. It is inconvenient to use this equation to predict venturi scrubber performance.

A generalized method for predicting venturi scrubber performance by equation (4-4) was developed in this study. This method is similar to that used by Hollands and Goel (1975) to obtain pressure drop in venturi scrubber. Detailed derivation of the generalized method will be presented in the next chapter.

CHAPTER 5

PERFORMANCE MODEL

In this chapter, we will present the generalized method for predicting venturi scrubber performance by using both Boll's pressure drop equation and Calvert's modified pressure drop equation combined with Calvert's differential equation for particle collection. The method was developed by Hollands and Goel (1975). However, they only covered Boll's pressure drop equation. Their method was extended to Calvert's differential equation for particle collection.

MATHEMATICAL MODELING

The basic equations governing the particle collection and pressure drop in a venturi scrubber were developed by Calvert (1968, 1970) and Boll (1974); rewritten here after some rearrangement they are:

$$-\frac{dc}{c} = \frac{u_r}{u_G}\;\frac{Q_L}{(u_G - u_r)A}\left(\frac{3}{4r_d}\right)\eta\;dz \qquad (5\text{-}1)$$

$$\frac{du_d}{dz} = \frac{3}{4}\;\frac{\rho_G}{\rho_L}\;\frac{(u_G - u_d)^2}{d_d\;u_d}\;C_D \qquad (5\text{-}2)$$

$$\frac{dp}{dz} = \rho_G u_G\,\frac{du_G}{dz} - \frac{3}{4}\,\frac{\rho_G}{\rho_L}\,\frac{C_D}{d_d}\,\frac{(u_G - u_d)^2}{u_d}\;\frac{m_L}{A} - \frac{(m_L + m_G)}{m_G}\;\frac{f\rho_G u_G^2}{2d_h} \qquad (5\text{-}3)$$

B.C. at $z=0$, $c=c_0$; $u_d=u_{d0}$; $u_G=u_{G0}$; $p=p_0$

where A = duct cross-sectional area, cm²
c = dust concentration, g/cm³
C_D = drag coefficient, dimensionless
d_d = drop diameter, cm
d_h = hydraulic diameter of the duct, cm
f = friction factor, dimensionless

m_G = gas mass flow rate, g/s
m_L = liquid mass flow rate, g/s
p = pressure
Q_L = liquid volumetric flow rate, cm³/s
r_d = drop radius, cm
u_d = drop velocity, cm/s
u_G = gas velocity, cm/s
u_r = relative velocity between gas and liquid drop, cm/s
z = rectangular coordinate in the direction of flow
ρ_L = liquid density, g/cm³
ρ_G = gas density, g/cm³
η = single drop collection efficiency, dimensionless

Several assumptions were made in the derivation of these equations. They are:

(1) The flow is one-dimensional, incompressible and isothermal.

(2) Liquid drops are uniformly spread across the duct and the drop diameter is invariant with axial distance.

(3) Drops are of uniform diameter.

We will introduce several additional assumptions:

(4) There is no wall loss of liquid drops.

(5) At any cross section of the scrubber, liquid fraction is small. Therefore, at any location, the gas velocity can be calculated by the following equation:

$$u_G = \frac{m_G}{\rho_G A} \tag{5-4}$$

where m_G = gas mass flow rate, g/s
A = duct cross-sectional area, cm²
ρ_G = gas density, g/cm³

Duct cross-sectional area depends on location and can be be determined from the following general formula:

$$A = A_0 \left(1 + \frac{z \tan \beta}{R} \right)^j \qquad (5\text{-}5)$$

j = 1 for rectangular duct
j = 2 for circular duct

where A_0 = cross-sectional area of the duct at the start of a section, cm²
R = radius (for circular duct) or half width (for rectangular duct) at the start of a given section, cm
β = half angle of divergence or convergence, degree

"β" is positive when duct is diverging and is negative when duct is converging.

Equation (5-5) assumes that for rectangular duct, duct breadth remains unchanged; only duct width is converging or diverging.

(6) The drag coefficient is governed by the following relationship as suggested by Hollands and Goel (1975):

$$C_D = (\text{constant})\, N_{Re}^{-0.5}$$

$$= C_{Do} \left(\frac{u_{Go} - u_{do}}{|u_G - u_d|} \right)^{0.5} \qquad (5\text{-}6)$$

where C_{Do} = drag coefficient applying at $z=0$, dimensionless
u_{Go} = gas velocity at $z=0$, cm/s
u_{do} = drop velocity at $z=0$, cm/s

"C_{Do}" is determined from the "standard curve" using a Reynolds number calculated on the basis of the relative velocity applying at the beginning of the duct, i.e.,

$$N_{Re,o} = \frac{|u_{Go} - u_{do}|\, d_d}{\nu} \qquad (5\text{-}7)$$

where $N_{Re,o}$ = drop Reynolds number at the beginning of the duct, dimensionless

d_d = drop diameter, cm

ν_G = kinematic viscosity of gas, cm²/s

The equation for the standard curve, due to Dickinson and Marshall (1968), is:

$$C_{Do} = 0.22 + \frac{24}{N_{Re,o}}\left(1 + 0.15\, N_{Re,o}^{0.6}\right) \qquad (5\text{-}8)$$

(7) Liquid drop diameter is that predicted by Nukiyama and Tanasawa correlation.

(8) Particles are flowing at the same velocity as gas, then Equation (5-1) can be reduced to:

$$-\frac{dc}{c} = \frac{1.5\ |u_G - u_d|}{u_d\ d_d}\left(\frac{Q_L}{Q_G}\right) \eta\ dz \qquad (5\text{-}9)$$

(9) Particle collection is primarily due to inertial impaction. We will use the simplified equation by Calvert (1970) to estimate the single drop target efficiency.

$$\eta = \left(\frac{K_p}{K_p + 0.7}\right)^2 \qquad (5\text{-}10)$$

where
$$K_p = \frac{C'\ \rho_p\ d_p^2\ \ |u_G - u_d|}{9\ \mu_G\ d_d} \qquad (5\text{-}11)$$

If one defines total pressure as:

$$P_T = p + \tfrac{1}{2}\rho_G\ u_G^2 \qquad (5\text{-}12)$$

Equation (5-5) can be written as:

$$\frac{dp_T}{dz} = -\frac{3}{4}\frac{\rho_G}{\rho_L}\left(\frac{C_D}{d_d}\right)\frac{u_G-u_d\,|u_G-u_d|}{u_d}\left(\frac{m_L}{A}\right) - \frac{(M+1)\,f\,\rho_G u_G^2}{2d_h} \qquad (5\text{-}13)$$

where $M = m_L/m_G$

= liquid to gas mass flow rate ratio

The hydraulic diameter "d_h" is given for a circular duct by:

$$d_h = 2\,(R + z\tan\theta) \qquad (5\text{-}14)$$

and for a rectangular duct by:

$$d_h = \frac{2b\,(R + z\tan\theta)}{b + R + z\tan\theta} \qquad (5\text{-}15)$$

where R = radius (for circular duct) and half-width (for rectangular duct) at the start of a given section, cm

b = duct breadth for a rectangular duct, cm

Equations (5-2), (5-9) and (5-13) are the governing equations for venturi scrubber performance. These equations are now non-dimensionalized, using "u_{Go}" as the characteristic velocity scale, "$\frac{1}{2}\rho_G u_{Go}^2$" as the characteristic pressure scale, and $\frac{4}{3}\frac{d_d}{C_{Do}}\frac{\rho_d}{\rho_G}\left(\frac{u_{Go}}{u_{Go}-u_{do}}\right)^{0.5}$ as the characteristic length scale for the equations below (in the case of d_h, R_o, and b, duct length "ℓ" is used as characteristic length scale), i.e.,

$$u_d^* = \frac{u_d}{u_{Go}} \qquad (5\text{-}16)$$

$$z^* = \frac{z}{\left[\frac{4}{3}\frac{d_d}{C_{Do}}\frac{\rho_L}{\rho_G}\left|\frac{u_{Go}}{u_{Go}-u_{do}}\right|^2\right]^{0.5}} \qquad (5\text{-}17)$$

$$p_T^* = \frac{p_T}{\frac{1}{2}\rho_G u_{Go}^2} \qquad (5\text{-}18)$$

By using these definitions, we obtain

$$u_G - u_d = \frac{u_{Go}}{\left(1 + \frac{z\tan\beta}{R}\right)^2} - \frac{u_{Go}u_d}{u_{Go}}$$

$$= u_{Go}\left\{\left[\frac{1}{1 + \frac{\tan\beta}{R}\left(\frac{4}{3}\frac{d_d}{C_{Do}}\frac{\rho_L}{\rho_G}\left(\frac{u_{Go}}{u_{Go}-u_{do}}\right)^2\right)^{0.5} z^*}\right]^2 - u_d^*\right\} \qquad (5\text{-}19)$$

$$\text{Let } S = \frac{2\tan\beta}{3R}\frac{d_d}{C_{Do}}\frac{\rho_L}{\rho_G}\left(\frac{u_{Go}}{u_{Go}-u_{do}}\right)^{0.5} \qquad (5\text{-}19b)$$

"S" is the dimensionless parameter characterizing the slope of a given duct and it has the following characteristics

$S < 0$ for convergent section
$S = 0$ for venturi throat
$S > 0$ for divergent section.

By substituting equation (5-19b) into equation (5-19), we have:

$$u_G - u_d = u_{Go}\left[(1 + Sz^*)^{-2} - u_d^*\right]$$

From equation (5-10) we have:

$$\eta = \left(\frac{K_p}{K_p + 0.7}\right)^2 = \left[\frac{\frac{C'}{9}\frac{\rho_p}{\mu_G}\frac{d_p^2}{d_d}\,|u_G - u_d|}{\frac{C'}{9}\frac{\rho_p}{\mu_G}\frac{d_p^2}{d_d}\,|u_G - u_d| + 0.7}\right]^2$$

$$= \left[\frac{|(1 + 8z^*)^{-1/2} - u_d^*|}{|(1 + 8z^*)^{-1/2} - u_d^*| + \frac{0.7}{K_{po}}}\right]^2 \qquad (5\text{-}20)$$

where $K_{po} = \frac{C'}{9}\frac{\rho_p}{\mu_G}\frac{d_p^2\,u_{Go}}{d_d}$

By substituting equations (5-17), (5-19), and (5-20) into equation (5-9), we have:

$$\frac{dc}{c} = -\frac{1.58}{d_d \tan\theta}\left(\frac{Q_L}{Q_G}\right)\frac{B}{u_d^*}\left[\frac{|(1 + 8z^*)^{-1/2} - u_d^*|}{|(1 + 8z^*)^{-1/2} - u_d^*| + \frac{0.7}{K_{po}}}\right]^2 dz^* \qquad (5\text{-}21)$$

Let $B = \frac{Q_L}{Q_G}\,\frac{\rho_d}{\rho_G}\,\frac{1}{C_{Do}}\left(\frac{u_{Go}}{u_{Go} - u_{do}}\right)^{0.5}$ (5-22)

then we obtain

$$\frac{\ln P_t}{B} = -\int_0^L \frac{|(1 + 8z^*)^{-1/2} - u_d^*|^2}{u_d^*\left[|(1 + 8z^*)^{-1/2} - u_d^*| + \frac{0.7}{K_{po}}\right]^2} dz^* \qquad (5\text{-}23)$$

where L = dimensionless duct length

$$= \frac{3\, C_{Do}\, \ell\, \rho_G}{2\, d_d\, \rho_d} \left[\frac{u_{Go} - u_{do}}{u_{Go}} \right]^{0.5}$$

ℓ = duct length, cm

Equation (5-23) is the general equation to predict particle collection by inertial impaction in a venturi scrubber. By following the same procedures as the derivation of equation (5-23), the following equations are obtained for drop velocity and pressure drop:

$$\frac{du_d^*}{dz^*} = \frac{\left|(1 + Bz^*)^{-1} - u_d^*\right| \left|(1 + Bz^*)^{-1} - u_d^*\right|^{0.5}}{\ell\, u_d^*} \qquad (5\text{-}24)$$

$$\frac{dp_f^*}{dz^*} = \frac{M\left|(1 + Bz^*)^{-1} - u_d^*\right| \left|(1 + Bz^*)^{-1} - u_d^*\right|^{0.5}}{u_d^*}$$

$$+ \frac{(M + 1)\, f\, (1 + Bz^*)^{-2}}{d_h^*\, L} \qquad (5\text{-}25)$$

B.C. at $z^*=0$, $u_d^*=u_{do}^*$, $p_f^*=0$

$$\left.\begin{aligned} d_h^* &= 2R^*\,(1 + Bz^*) \quad \text{Circular duct} \\ d_h^* &= \frac{2\, b^*\, R^*(1 + Bz^*)}{b^* + R^*(1 + Bz^*)} \quad \text{Rectangular duct} \end{aligned}\right\} \quad (5\text{-}26)$$

f = friction factor, dimensionless

$b^* = b/\ell$ = dimensionless duct breadth,

$R^* = R/\ell$ = dimensionless radius

The first term on the right hand side of equation (5-25) represents the pressure change associated with the acceleration of liquid drops; the second term is the wall friction loss. From this equation, it seems that the contributions of the liquid acceleration loss and the wall friction loss to the total pressure loss are additive. Therefore, one may write:

$$p_T^* = p_d^* + p_w^* \qquad (5\text{-}27)$$

where p_T^* = total pressure, dyne/cm²
p_d = component of p_T^* associated with liquid flow, dyne/cm²
p_w^* = wall friction component of p_T^*, dyne/cm²

By this definition, we have:

$$\frac{dp_d^*}{dz^*} = \frac{M(1 + Sz^*)^{-1} \left|(1 + Sz^*)^{-1} - u_d^*\right| \left|(1 + Sz^*)^{-1} - u_d^*\right|^{0.5}}{u_d^*} \qquad (5\text{-}28)$$

and

$$\frac{dp_w^*}{dz^*} = \frac{(M + 1)\, f\, (1 + Sz^*)^{-2}}{d_h^*\, L} \qquad (5\text{-}29)$$

with boundary conditions

$$\text{at } z^* = 0,\ p_d^* = 0,\ p_w^* = 0 \qquad (5\text{-}30)$$

Equations (5-23), (5-24), (5-28), and (5-29) are the final forms of the governing equations.

For each section of the venturi scrubber, its pressure drop and particle penetration can be calculated from equations (5-23), (5-24), (5-28), and (5-29). Since pressure drops are additive, the overall pressure drop for the venturi scrubber is,

$$\Delta P_T = \sum_i (\Delta P)_i \qquad (5\text{-}31)$$

where ΔP_T = overall pressure drop, dyne/cm^2
$(\Delta P)_i$ = pressure drop of a section of the venturi scrubber, dyne/cm^2

The venturi scrubber is a scrubber with a convergent section, a throat section, and a divergent section connected in series. Particles that are collected in one section cannot be collected in another section. Therefore, if the particle penetration for each section is known, the overall penetration for the venturi scrubber will be,

$$Pt(d_p) = \prod_i \left| Pt(d_p) \right|_i \qquad (5\text{-}32)$$

where $Pt(d_p)$ = overall penetration for particles with diameter "d_p", fraction
$\left|Pt(d_p)\right|_i$ = penetration of a section, fraction

SOLUTION

The analytical solution to equation (5-29) is,

$$F_w^* = \frac{(M+1)f}{d_{ho}^*} F_w \qquad (5\text{-}33)$$

where $F_w = \left| \dfrac{1 - A_r^{-2}}{4(A_r^{0.5} - 1)} \right|$ for circular duct (5-34)

$F_w = \dfrac{1}{A_r^2} \left| 1 + \dfrac{B^*(A_r - 1)(1 + b^* + B^*)}{2(b^* + B^*)} \right|$ for rectangular duct and A_r = the ratio of exit to inlet cross-sectional area = $(1+SL)^2$

d^*_{ho} = dimensionless hydraulic diameter at duct inlet, cm

f = friction factor, dimensionless

A value of $f=0.027$ was suggested by Boll because it seemed to give a slightly better fit in the shape of the pressure drop curves than other values of "f".

Equations (5-23), (5-24), and (5-28) are solved by numerical integration on a digital computer. Figures 5-1 through 5-16 show the results of a numerical integration for the range of L, S, and K_{po} of interest and for $u^*_{do}=0$. These figures along with equation (5-32) may also be used to determine penetration for $u^*_{do}\neq 0$. The method is discussed in the following paragraphs.

The drop velocity at the beginning of the divergent section differs from zero. We will use the divergent section to illustrate the method of applying Figures 5-1 through 5-16 to determine the particle collection efficiency of a section where at its inlet the liquid drop velocity is not zero.

Refer to Figure 5-17 in order to find the penetration of the divergent section ABCD, we project it in the upstream direction with the same divergence angle "θ", i.e., add an imaginery section FEBA to the upstream of ABCD as depicted in Figure 5-17 by the dashed lines. The result is two venturi divergent sections connected in series. The outlet of the imaginary added on section is the inlet of the real section. By equation (5-32) the particle penetration for the real divergent section ABCD is equal to,

$$Pt_{ABCD} = \frac{Pt_{FECD}}{Pt_{FEBA}} \qquad (5\text{-}35)$$

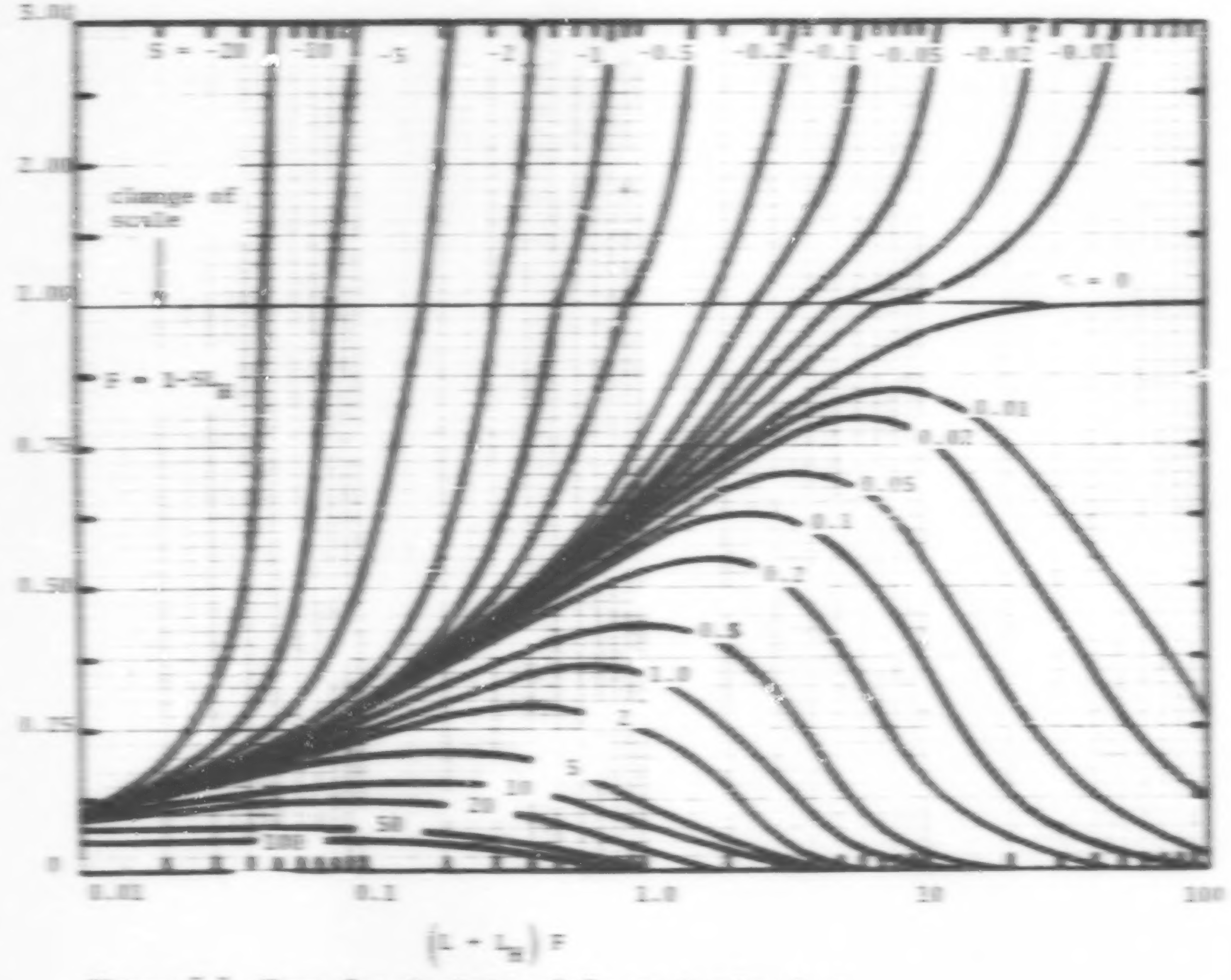

Figure 5-1. Chart for obtaining η_d^* for a circular duct.

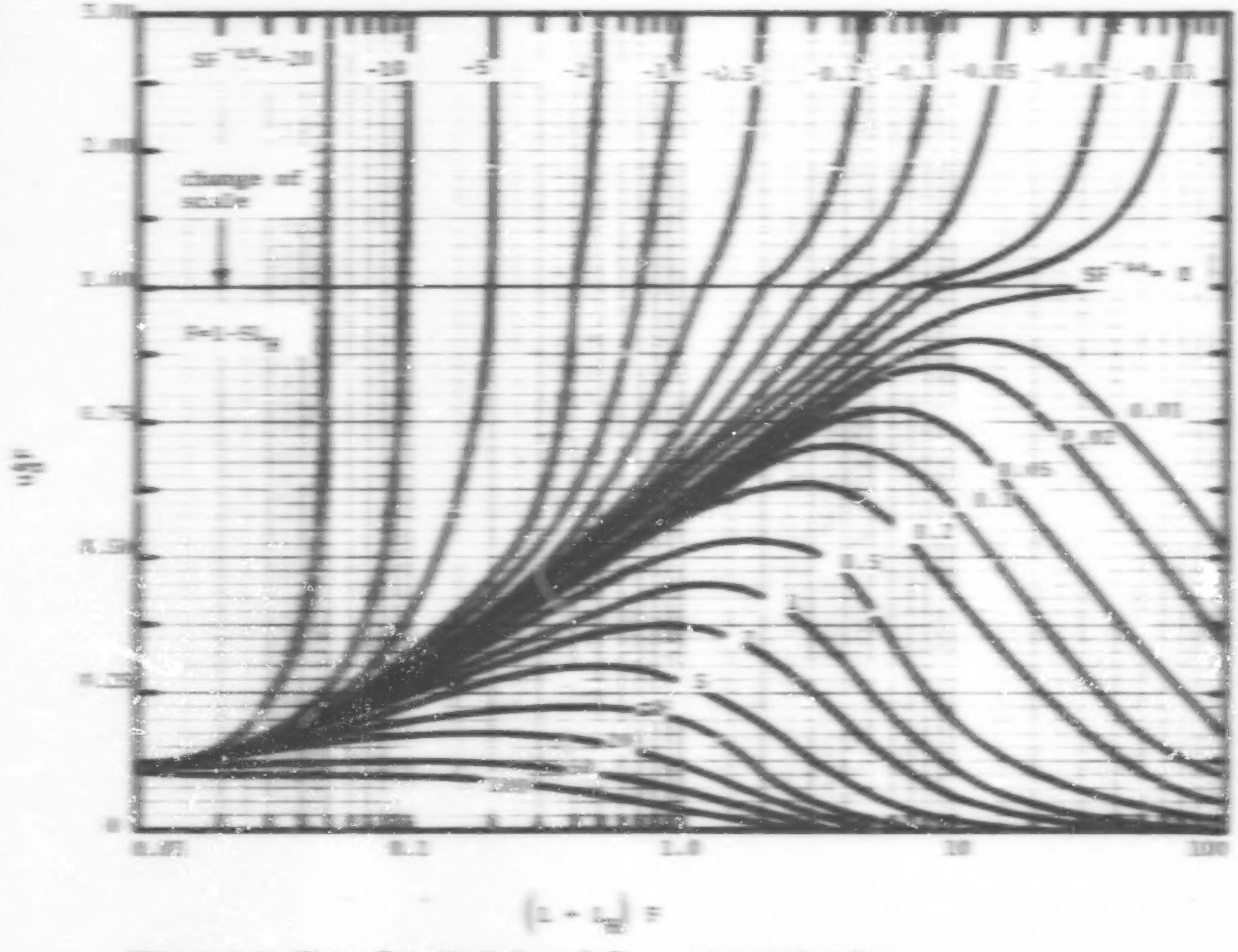

Figure 5-1. Chart for obtaining α_g^* for a rectangular duct.

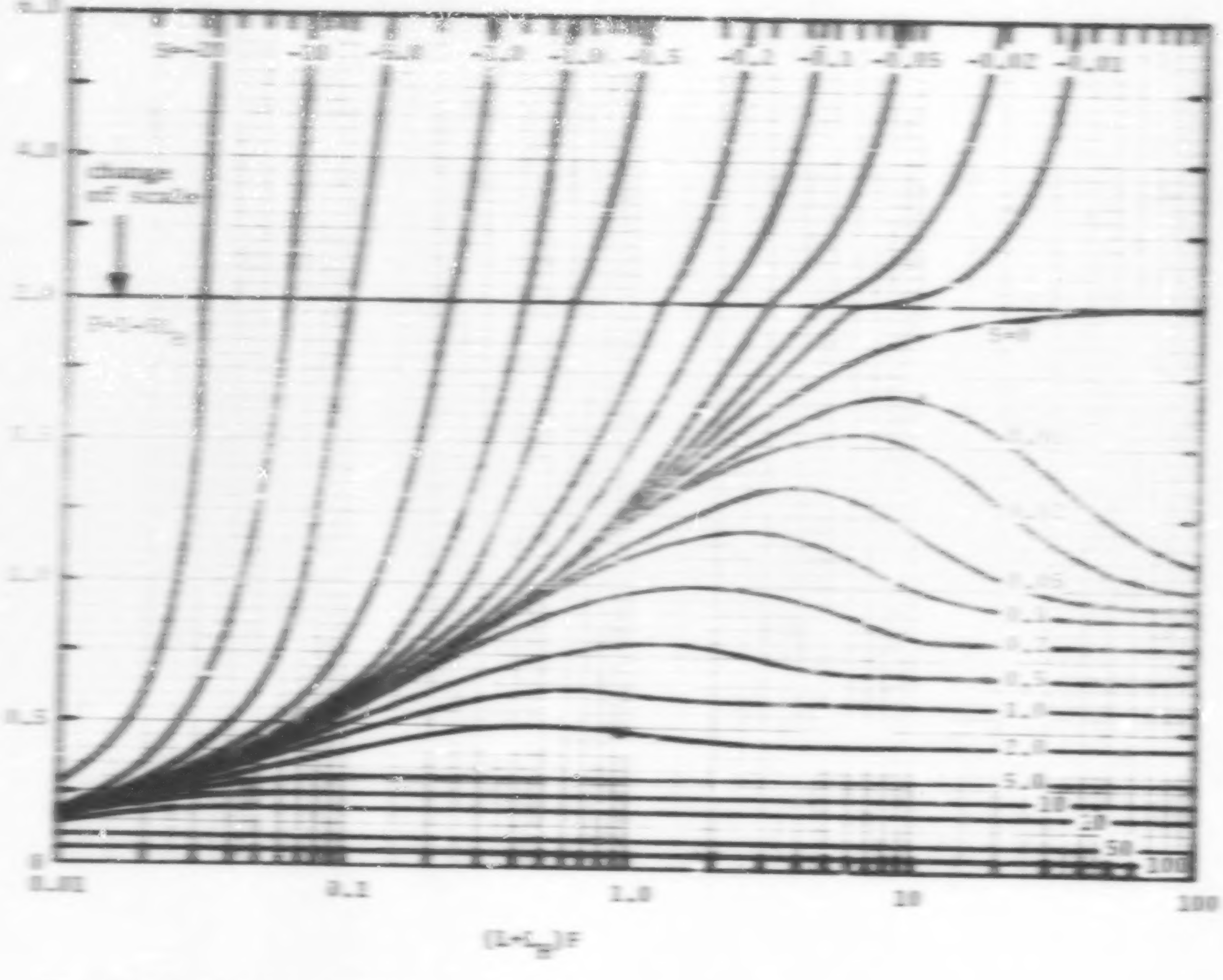

Figure 5-1. Chart for obtaining P_d^* for a circular duct.

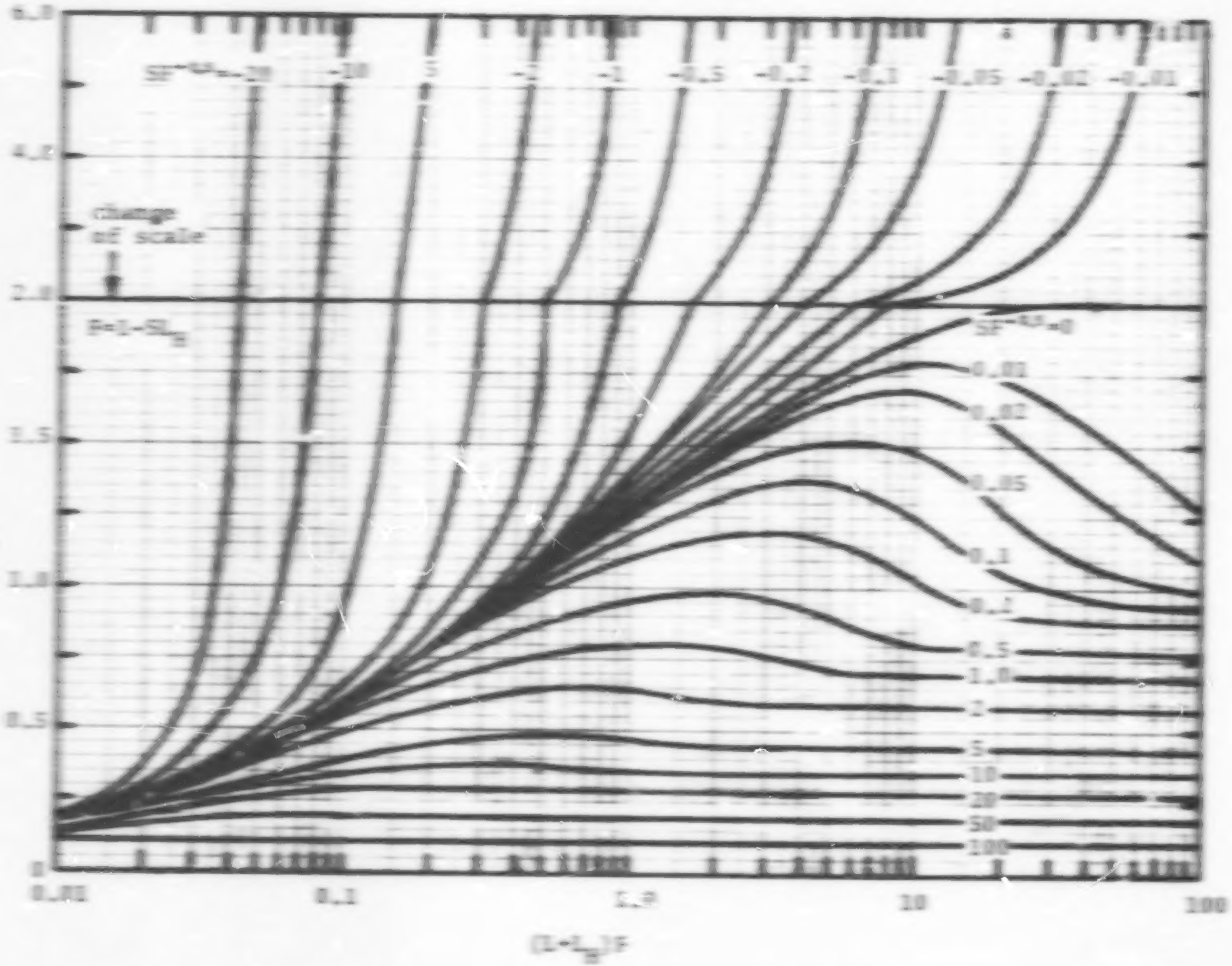

Figure 5-4. Chart for obtaining p_d^* for a rectangular duct.

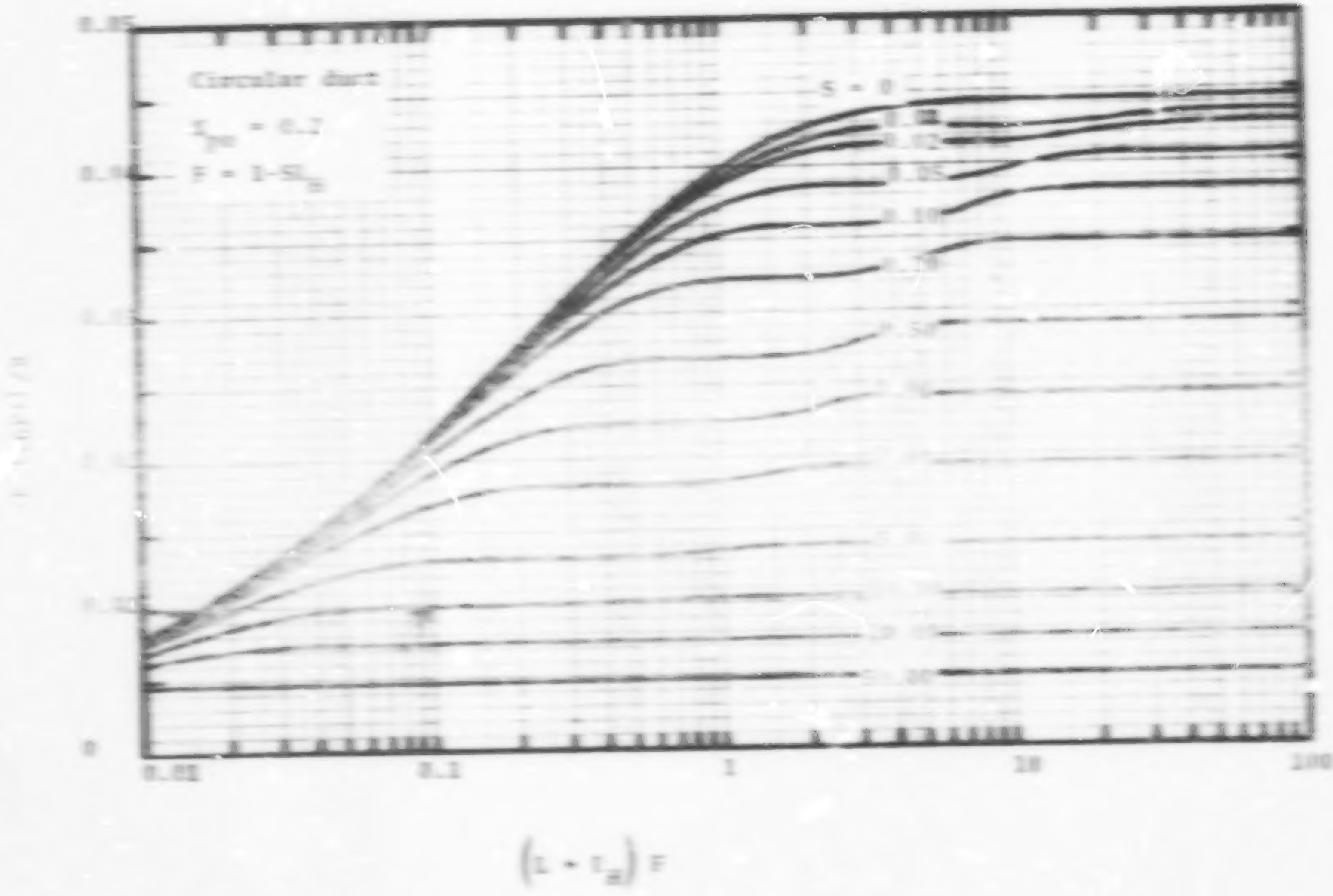

Figure 5-5. Chart for obtaining penetration for circular duct.

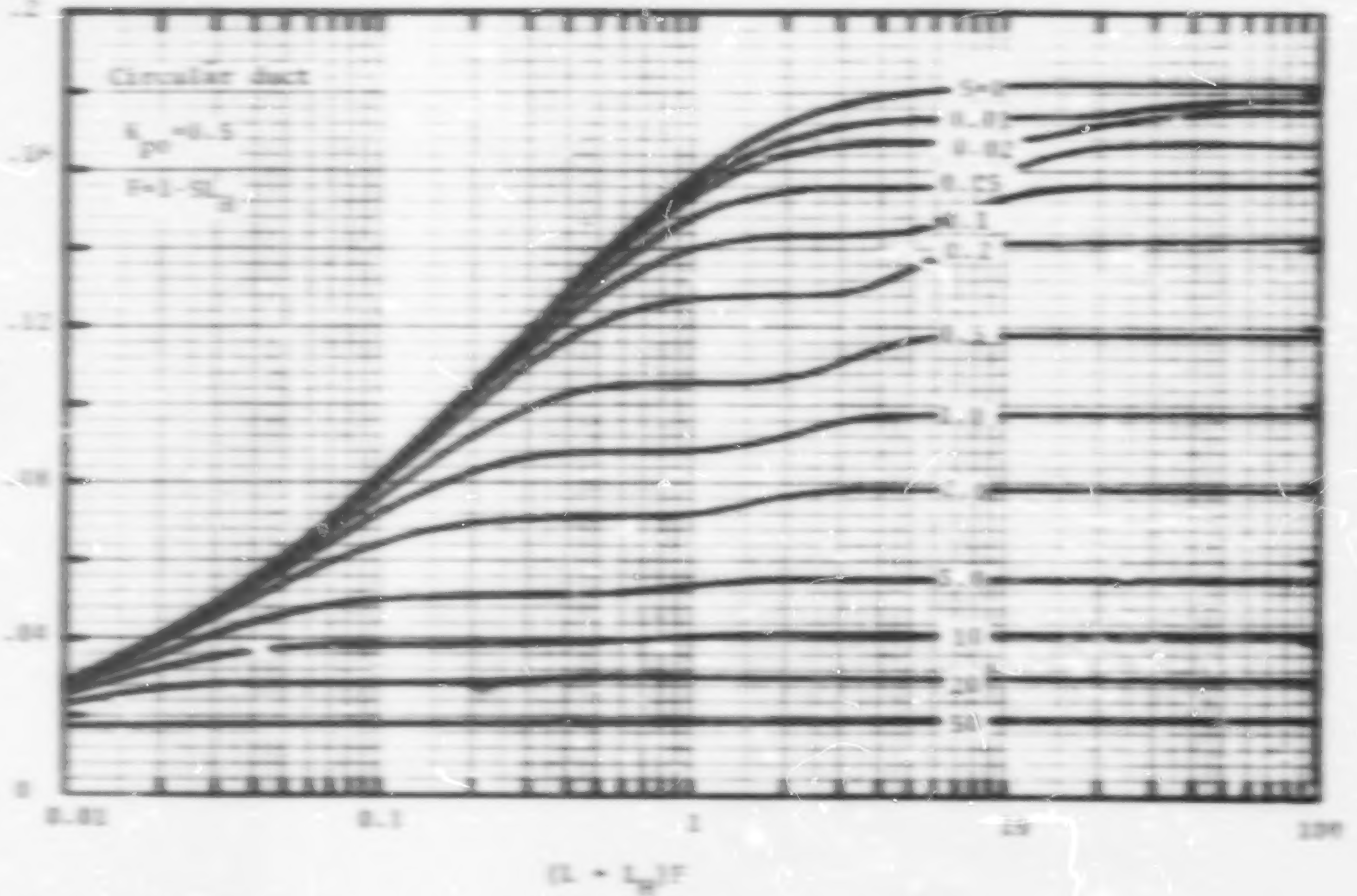

Figure 5-6. Chart for obtaining penetration for circular duct.

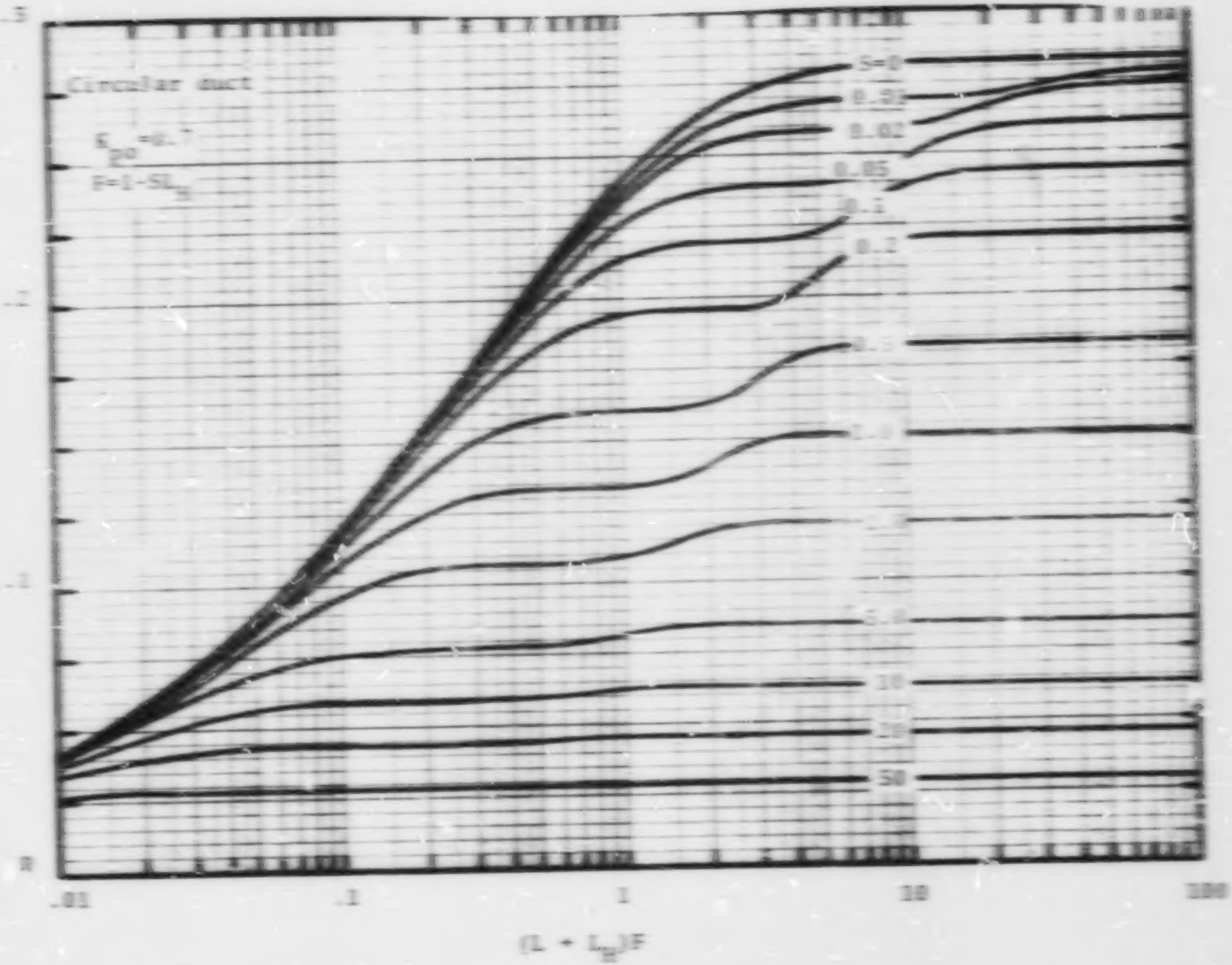

Figure 5-7. Chart for obtaining penetration for circular duct-

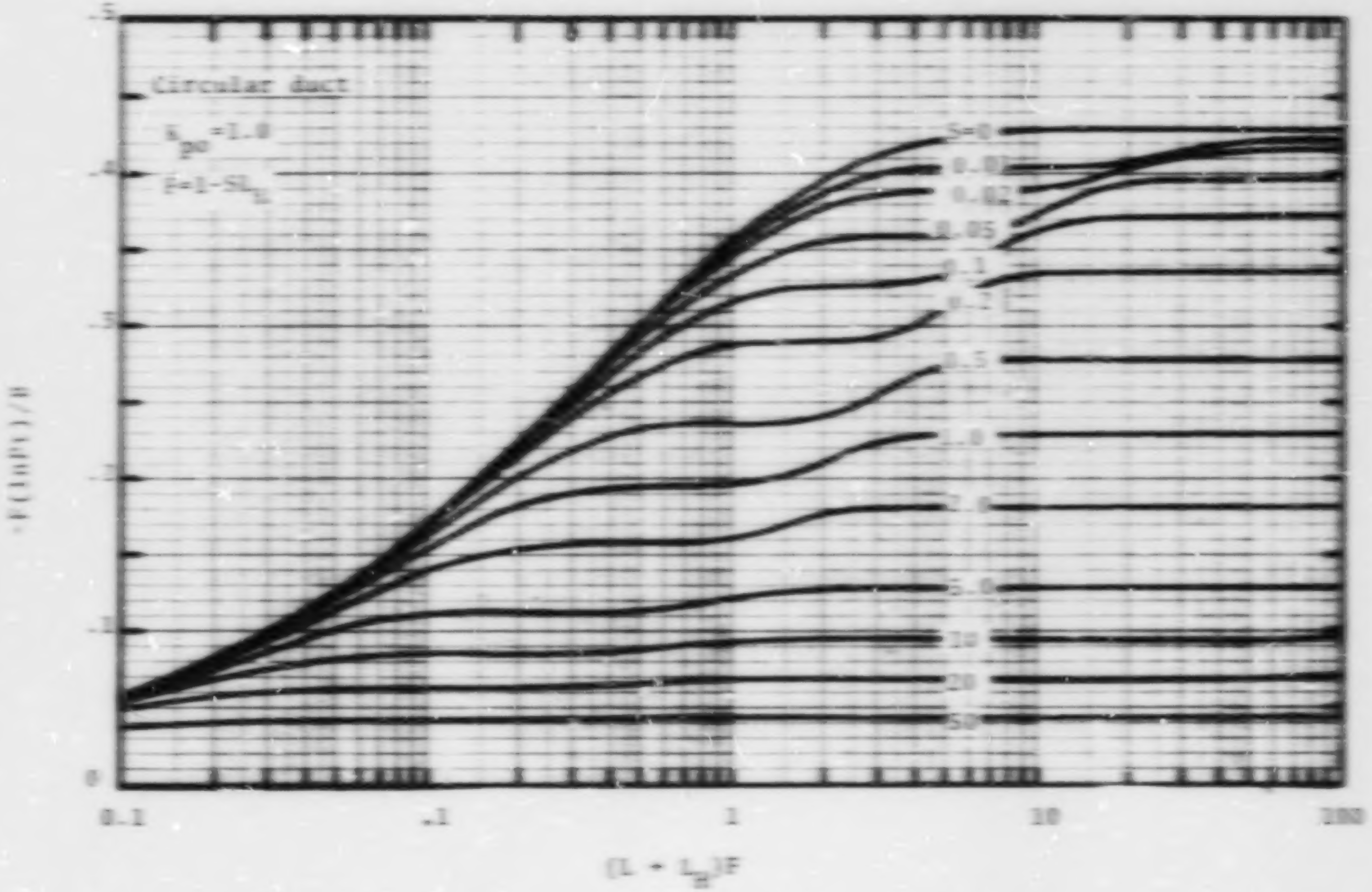

Figure 5-8. Chart for obtaining penetration for circular duct.

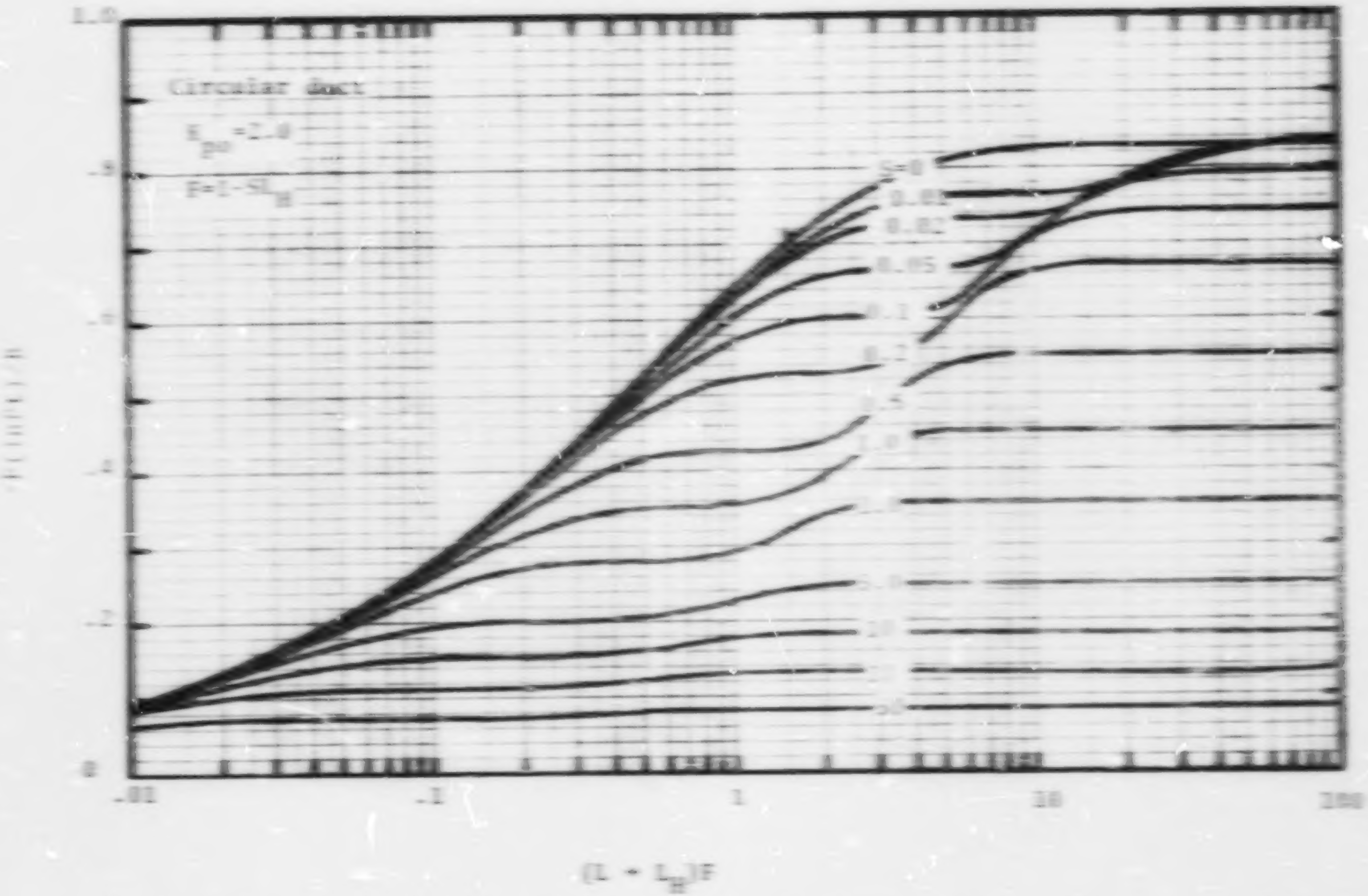

Figure 5-9. Chart for obtaining penetration for circular duct.

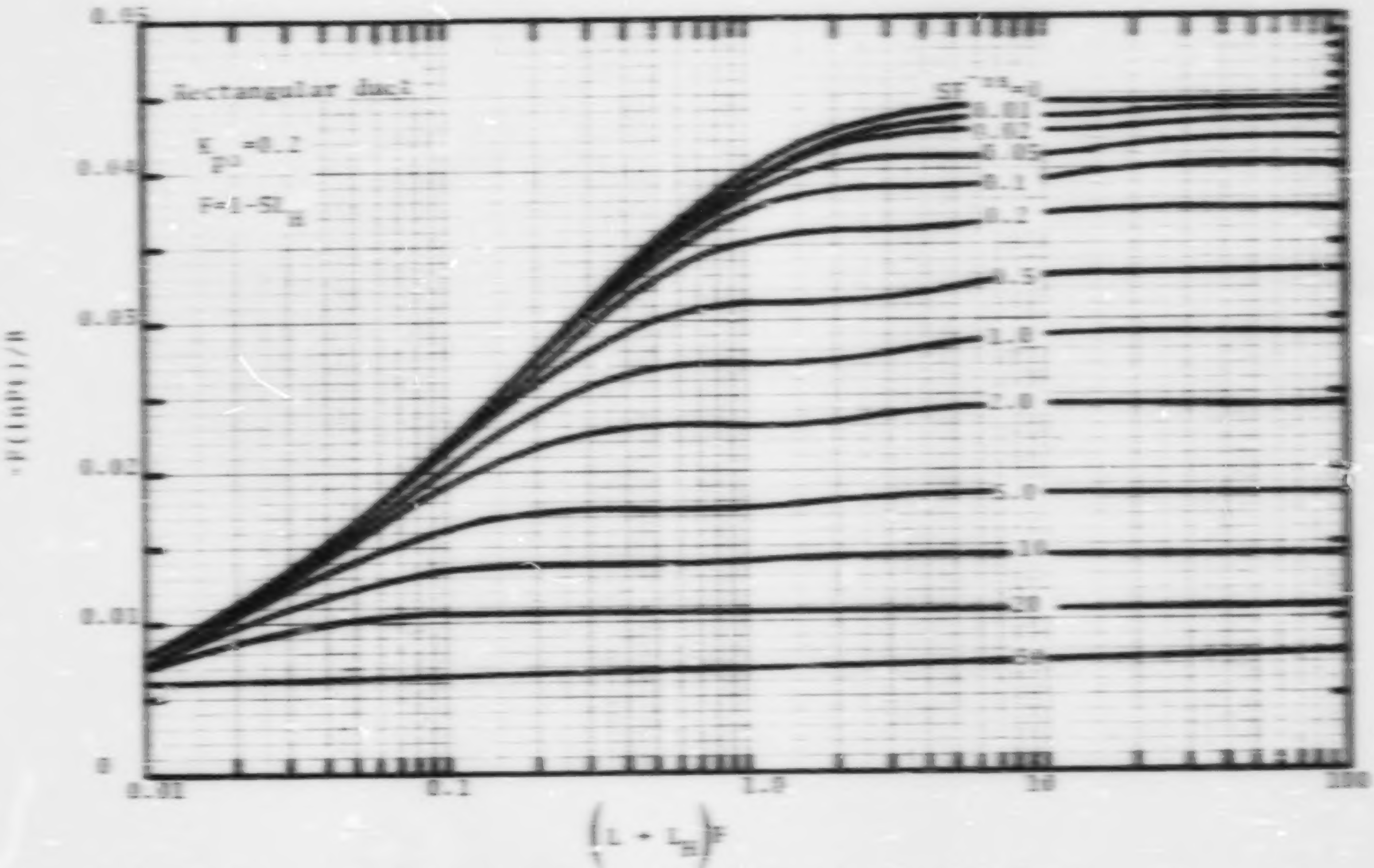

Figure 5-10. Chart for obtaining penetration for rectangular duct.

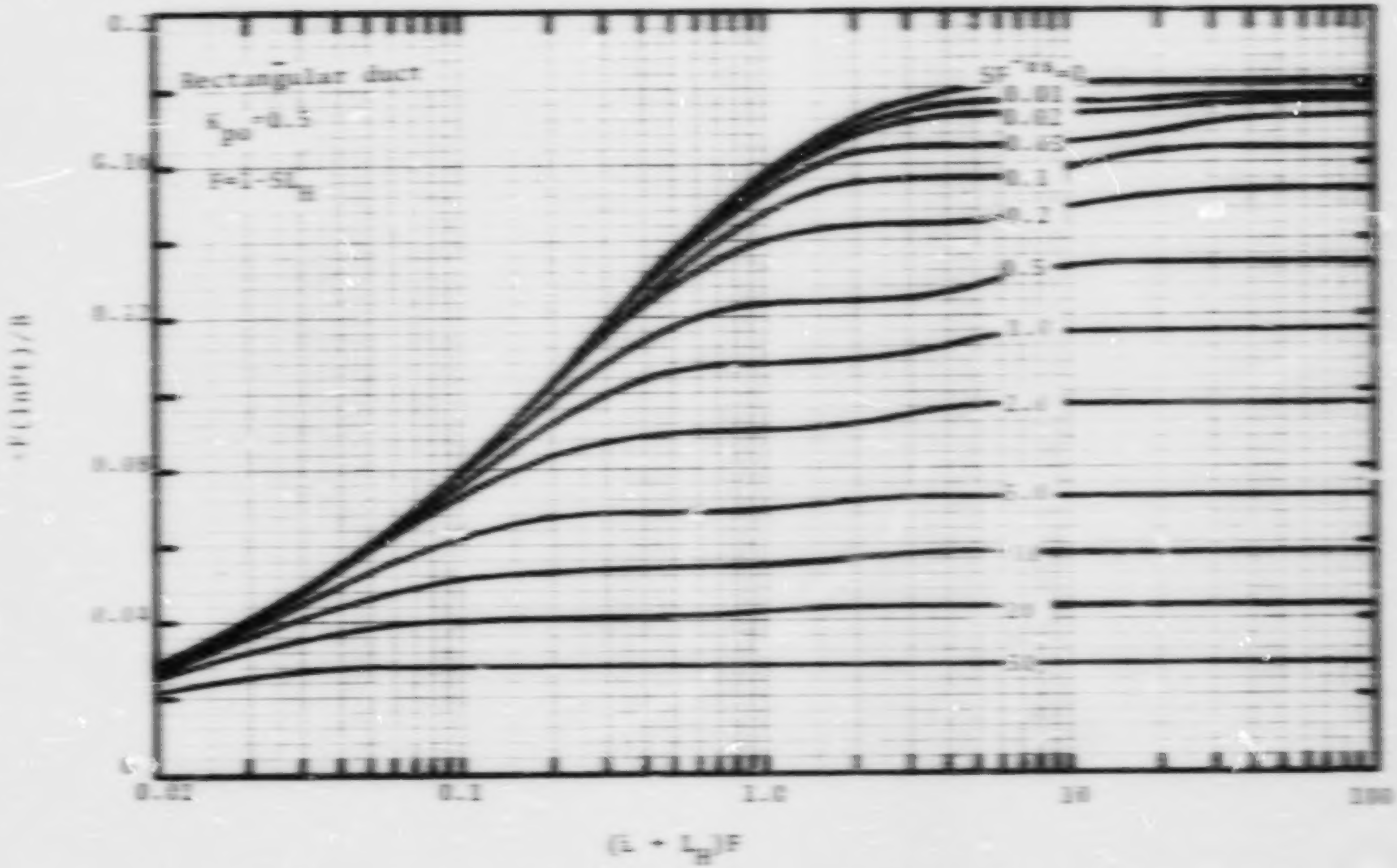

Figure 5-11.Chart for obtaining penetration for rectangular duct.

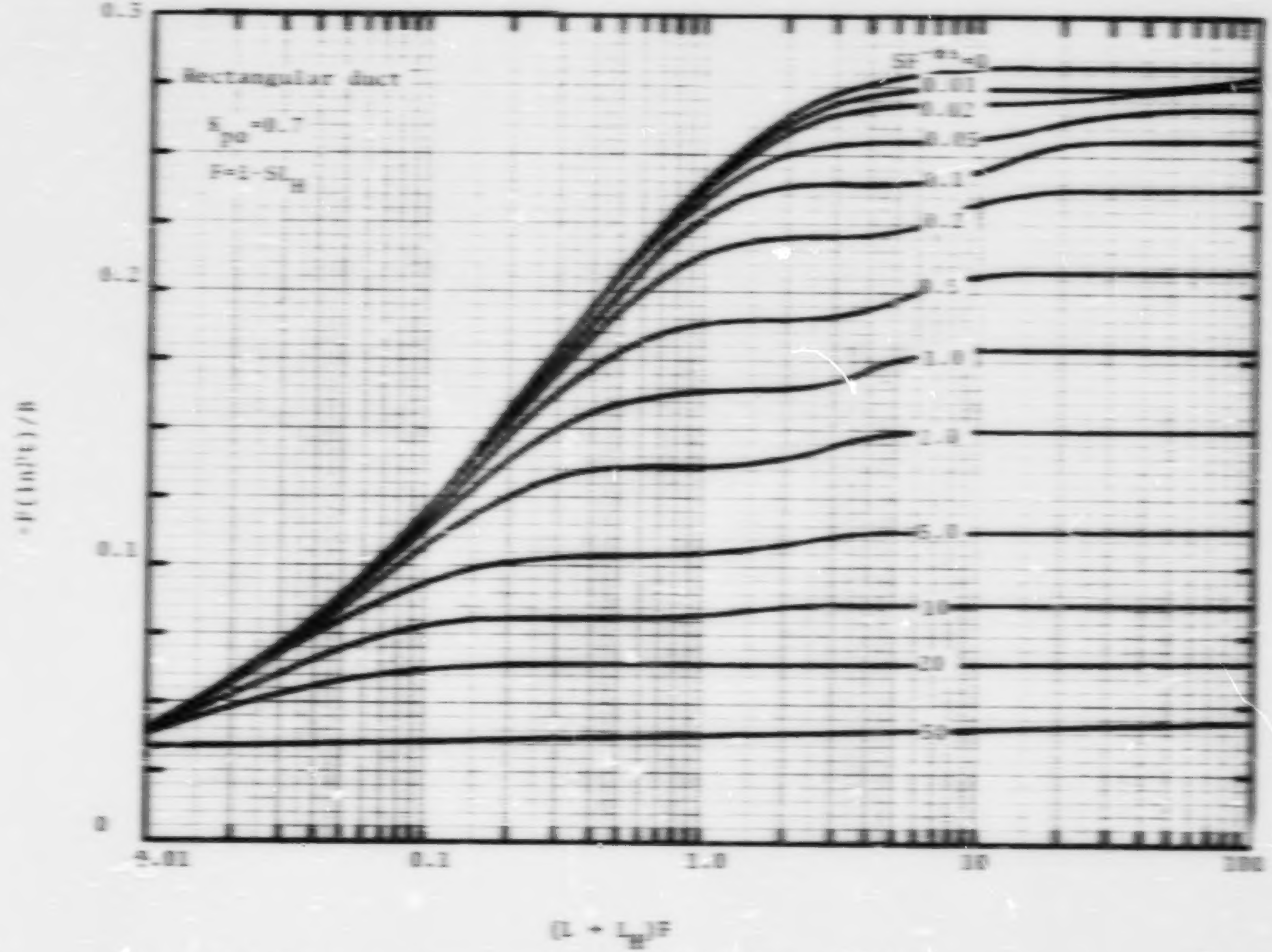

Figure 5-12. Chart to obtain penetration for rectangular duct.

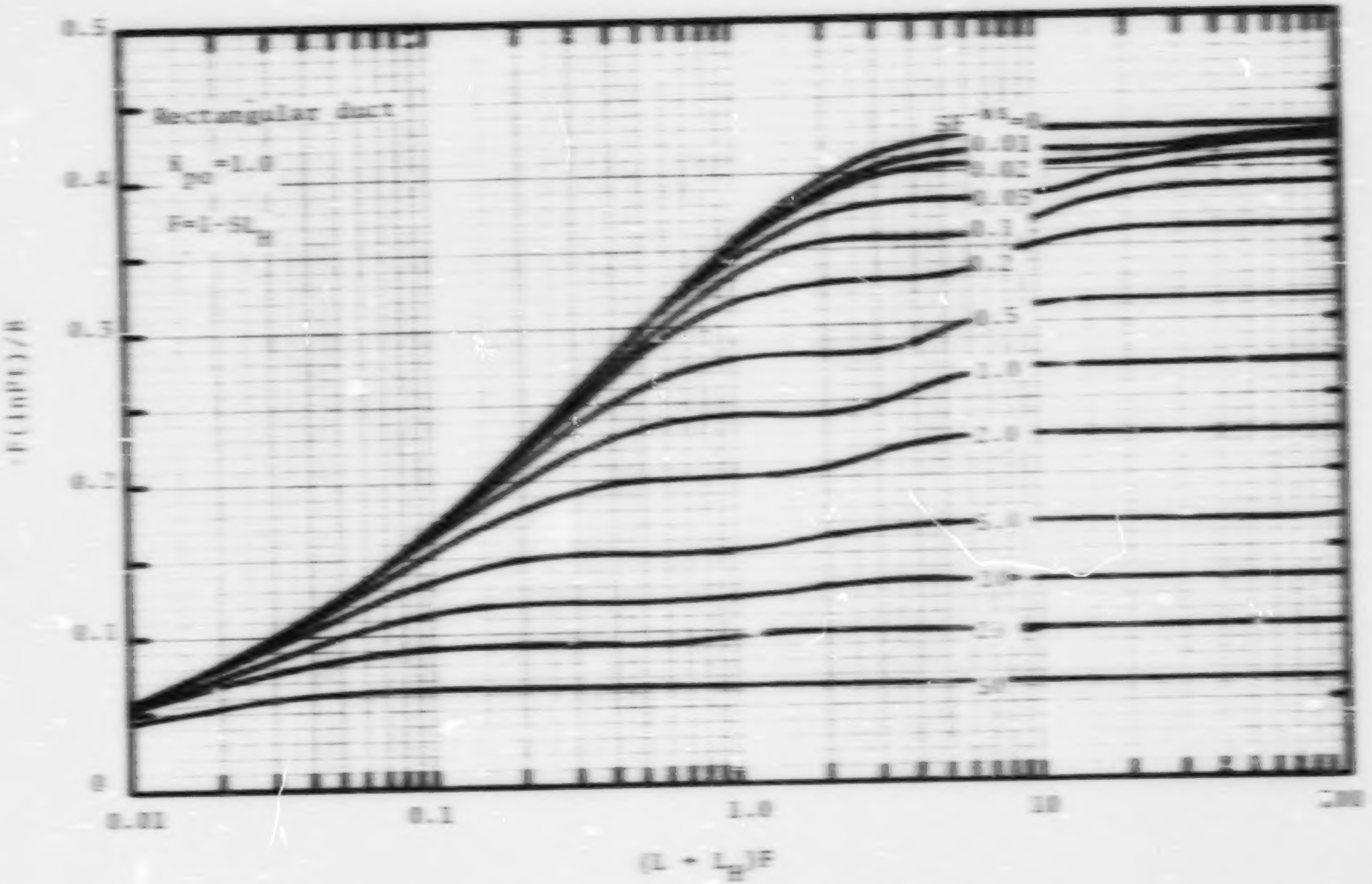

Figure 5-13. Chart to obtain penetration for rectangular duct.

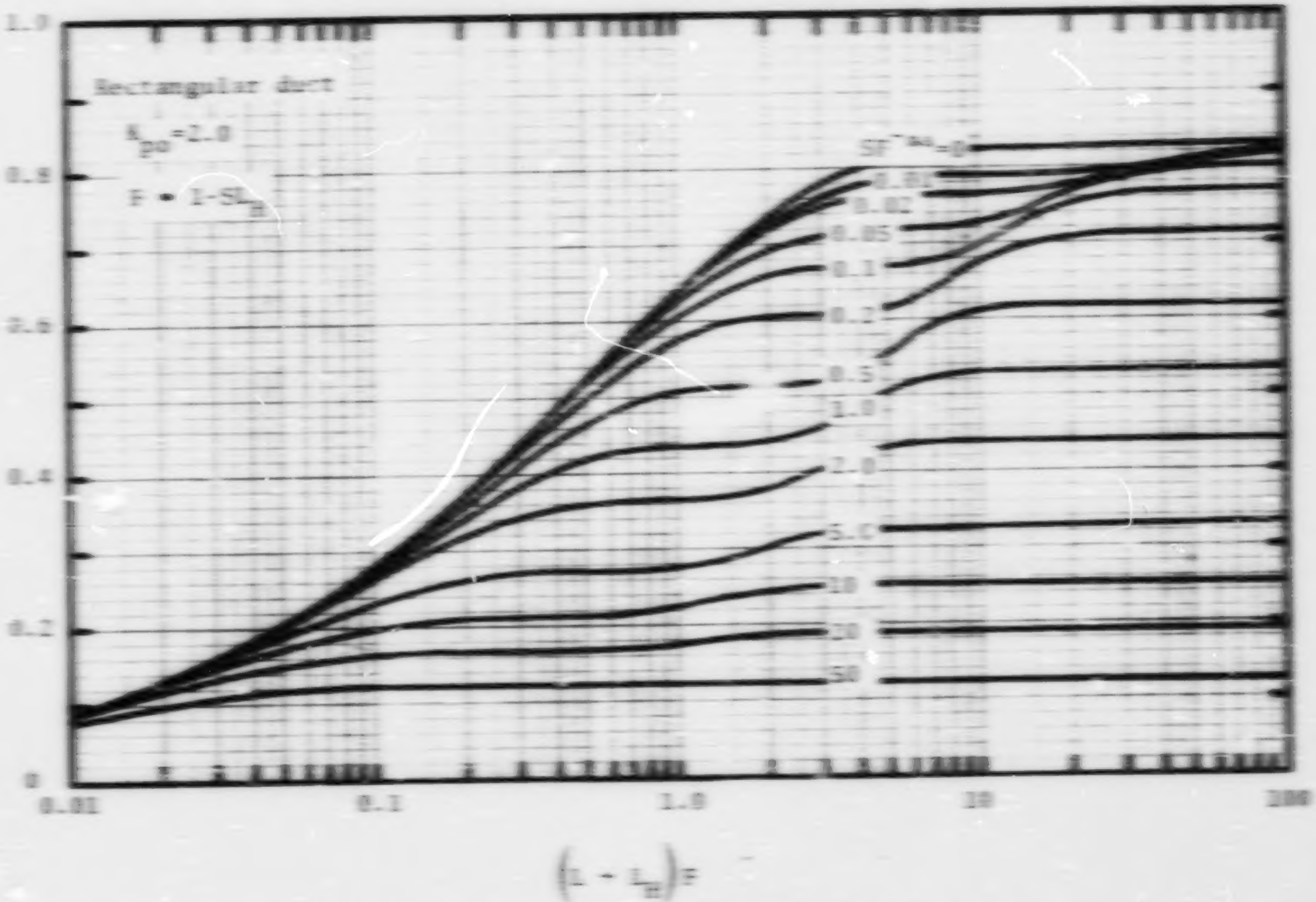

Figure 5-14. Chart to obtain penetration for rectangular duct.

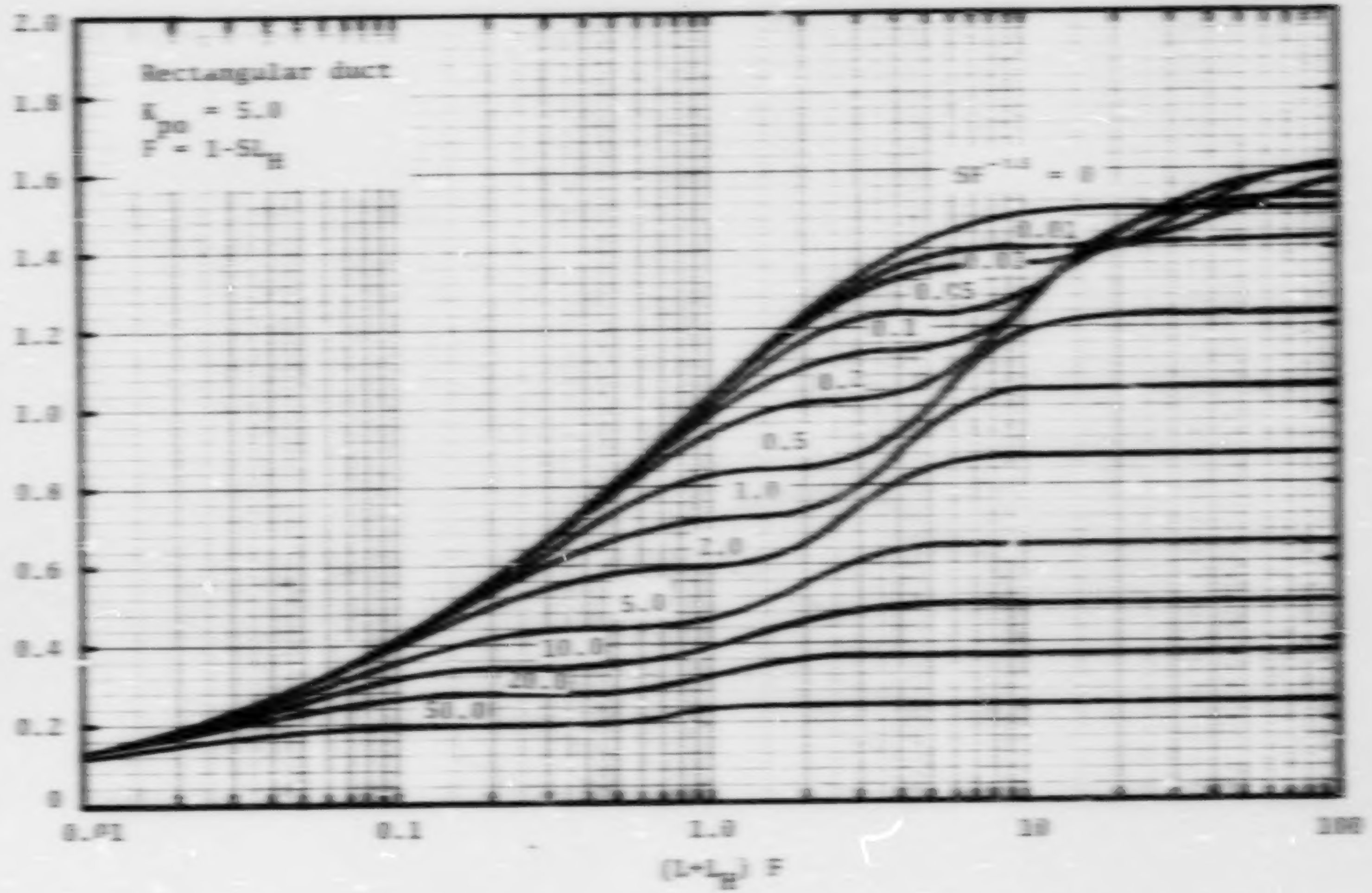

Figure 5-15. Chart to obtain penetration for rectangular duct.

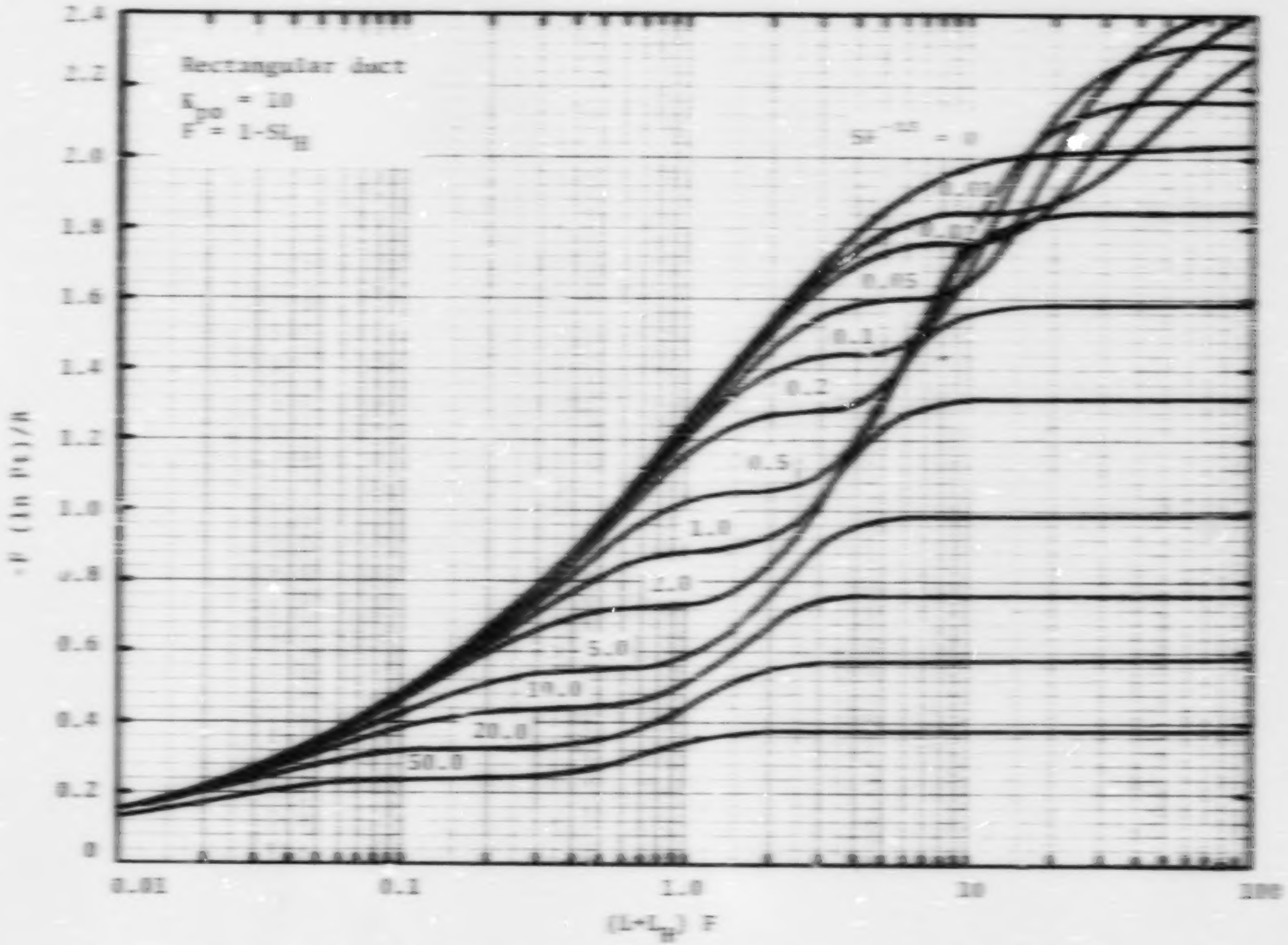

Figure 5-16. Chart to obtain penetration for rectangular bed.

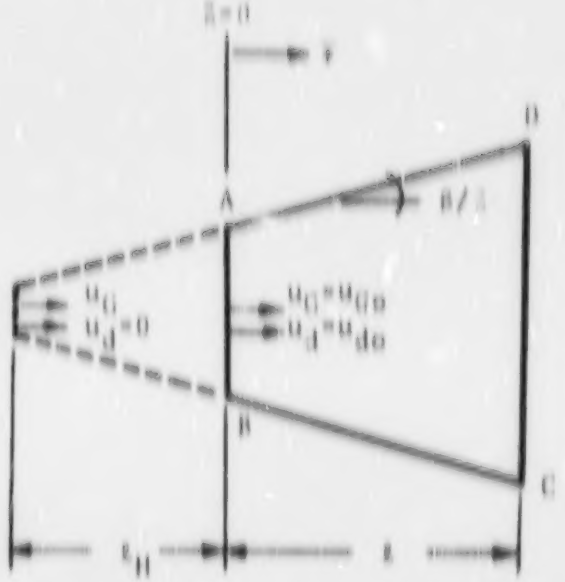
z=0
V
D
A
θ/2
F
E
u_G
$u_d=0$
$u_G=u_{Go}$
$u_d=u_{do}$
B
C
ℓ_H
ℓ

Figure 5-17. Concept of a hypothetical section.

If we adjust the length of the imaginary section in such a way so that the liquid drop velocity at the inlet of the imaginary divergent section is zero, then "Pt_{FECD}" and "Pt_{FEBA}" can be obtained from Figure 5-3 through 5-16 and penetration for the real section can be calculated from equation 5-35.

The length of the imaginary section "ℓ_H", can be determined by integrating equation 5-2 with the following boundary conditions:

$$\text{at} \quad z = 0,\ u_d = u_{do}$$

$$z = -\ell_H,\ u_d = 0$$

Figures 5-18 and 5-19 are the results of the integration for a circular duct and a rectangular duct respectively. "L_H" is the dimensionless counterpart of "ℓ_H" and is defined by,

$$L_H = \frac{\ell_H}{\frac{2}{3}\left(\frac{d_d}{C_{Do}}\right)\left(\frac{\rho_L}{\rho_G}\right)} \tag{5-36}$$

In calculating "Pt_{FECD}" and "Pt_{FEBA}", it is necessary to use the gas and liquid parameters at the inlet of the imaginary added on section, i.e., at $z=-\ell_H$. From the geometry of the duct, parameters at $z=-\ell_H$ are related to the known parameters at $z=0$, i.e., at the inlet of the real duct, by the following equations,

$$L' = (L+L_H)\,(1-SL_H)^{\,j/2} \tag{5-37}$$

$$S' = S\,(1-SL_H)^{\,-j/2\,-1} \tag{5-38}$$

$$u_d^{*\prime} = u_d^{*}\,(1-SL_H)^{j} \tag{5-39}$$

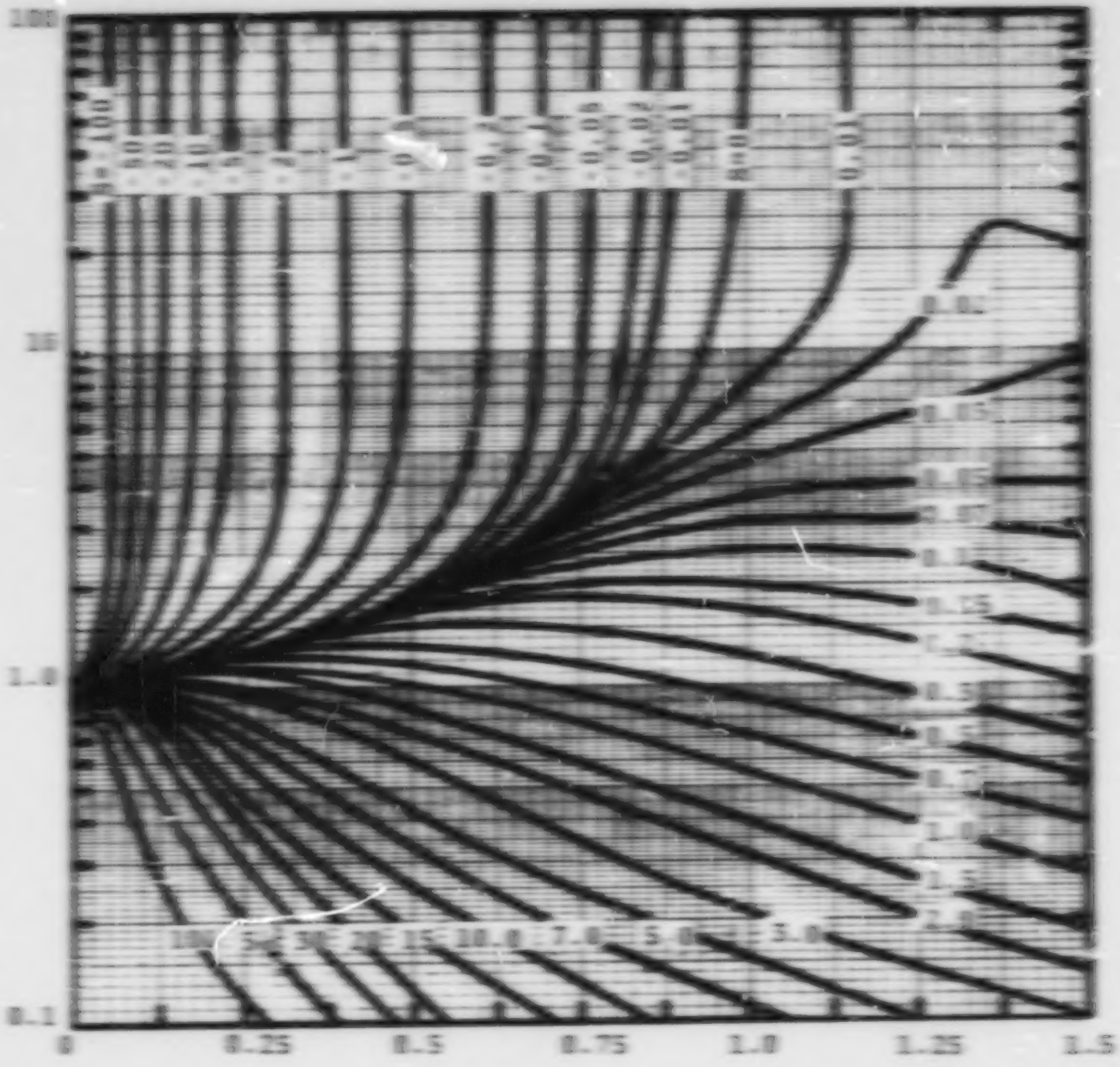

Figure 5-16. Chart for obtaining l_m for a circular duct.

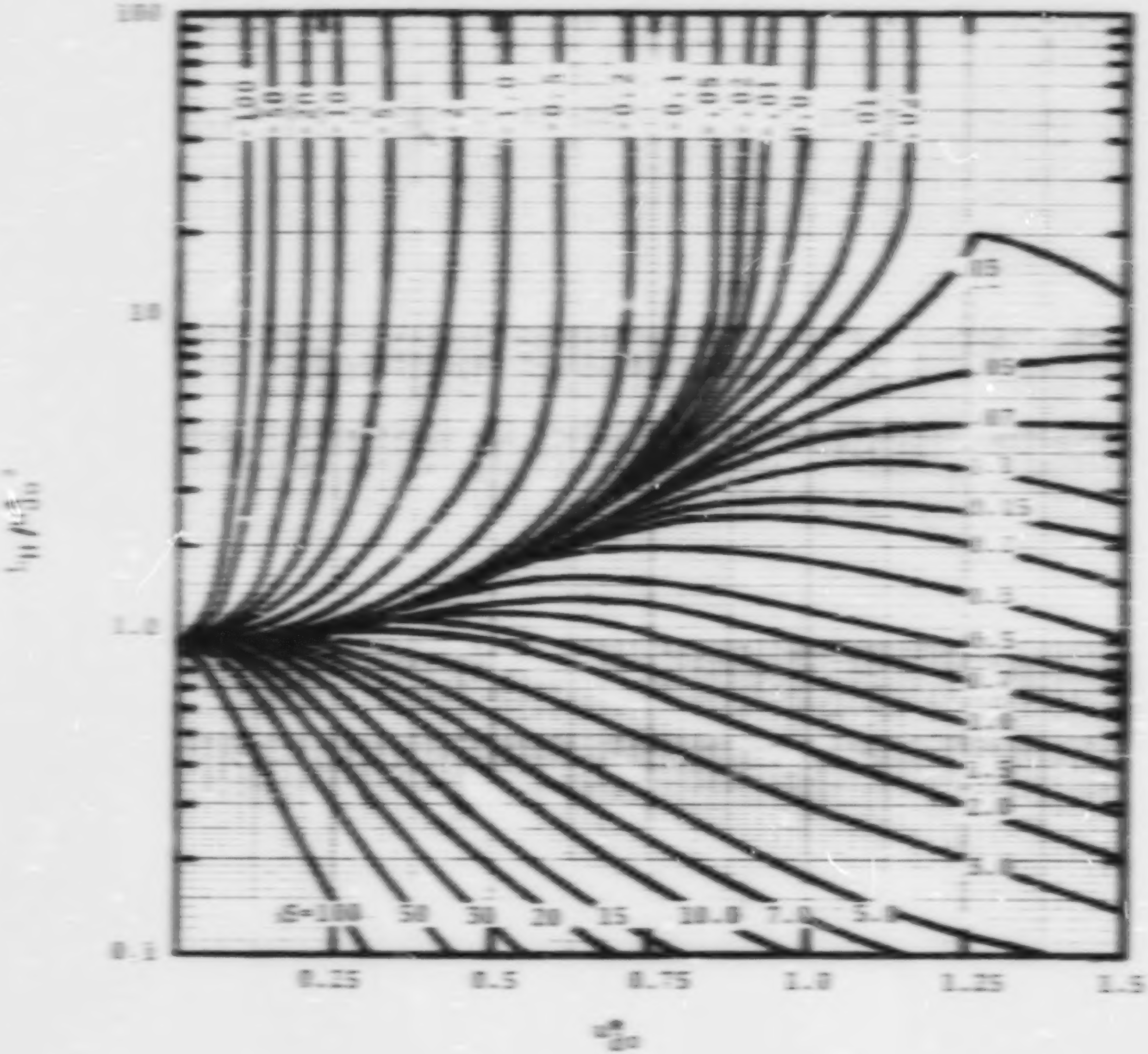

Figure 5-19. Chart for obtaining L_H for a rectangular duct.

$$\text{and } B' = B(1-8\ell_H)^{-1/2} \qquad (5\text{-}40)$$

where prime (') refers to $z = -\ell_H$. Detailed derivation of these equations is given in Appendix A.

SAMPLE CALCULATION

To illustrate the application of these figures to predict the performance of a venturi scrubber, we will calculate the pressure drop and particulate collection for the venturi scrubber shown in Figure 5-20. We will predict its performance for the following operating conditions:

Q_G = 800 Am^3/min
Q_L/Q_G = 1.33 ℓ/m^3
Gas temperature = 20°C

Particle Collection

Convergent Section - Water is injected at the start of the throat. Therefore, there is no particle collection in the convergent section.

Throat Section - The water is assumed to be injected with no axial momentum so that "u_{do}" is equal to zero. The gas velocity at the inlet of the throat is calculated to be 8,060 cm/sec. Thus, the drop diameter according to Nukiyama and Tanasawa is:

$$d_d = \frac{50}{u_G} + 91.8\left(\frac{Q_L}{Q_G}\right)^{1.5}$$

$$= 0.0107 \text{ cm}$$

Drop Reynolds number

$$N_{Re,o} = \frac{d_d\,(u_{Go}-u_{do})}{\nu}$$

$$= \frac{0.0107\,(8060-0)}{0.15} = 575$$

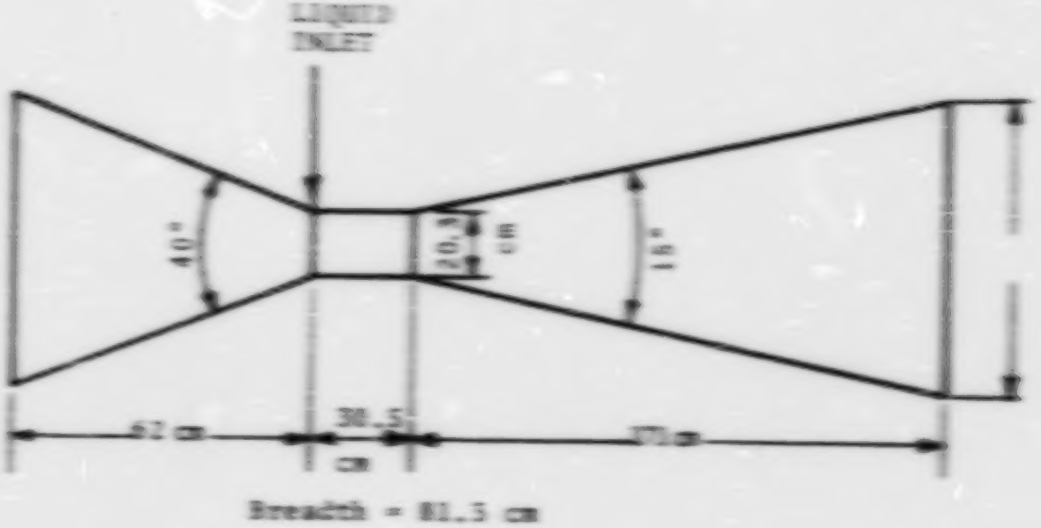
LIQUID INLET
40°
20.3 cm
15°
62 cm
30.5 cm
Breadth = 81.3 cm

Figure 5-37. Venturi scrubber for sample calculation.

From Standard curve, or from equation (5-8):

$$C_{Do} = 0.22 + \frac{24}{N_{Re,o}} (1 + 0.15\ N_{Re,o}^{0.6})$$

$$= 0.22 + \frac{24}{575} \left|1 + (0.15)(575)^{0.6}\right|$$

$$= 0.545$$

$$L = \frac{3}{2}\ \frac{l_t C_{Do}}{d_d} \left(\frac{\rho_G}{\rho_L}\right)\left(\frac{u_{Go} - u_{do}}{u_{Go}}\right)^{0.5}$$

$$= 2.79$$

$$B = \left(\frac{Q_L}{Q_G}\right)\left(\frac{\rho_L}{\rho_G}\right) \frac{1}{C_{Do}} \left(\frac{u_{Go}}{u_{Go} - u_{do}}\right)^{0.5}$$

$$= 2.03$$

For venturi throat, S=0. Since $u_{do}=0$, we have $l_H=0$ and F=1.

$$K_{po} = \frac{u_{Go}\ d_{pa}^2}{9\ \mu_G\ d_d} = \frac{(8060)\ (10^{-8})\ (d_{pa})^2}{(9)\ (1.8 \times 10^{-4})\ (0.0107)}$$

$$= 4.65\ d_{pa}^2$$

or $d_{pa} = \left(0.215\ K_{po}\right)^{0.5}$ μmA

Read "-F in Pt/B" from Figures 5-10 to 5-16 for L=2.79 and S=0 for various "K_{po}", we obtain the following:

K_{pa}	d_{pa}, μmA	-F ln Pt/B	Pt(d_{pa})
0,2	0,21	0,044	0,91
0,5	0,33	0,176	0,7
0,7	0,39	0,272	0,58
1	0,46	0,41	0,44
2	0,66	0,77	0,21
5	1,04	1,3	0,071
10	1,5	1,7	0,032

Divergent Section - At the exit of the venturi throat, the drop velocity is:

$$u_d^* F' = 0,78 \text{ (Figure 5-2)}$$

$$\text{i.e., } u_d = (0,78)\ (8060) = 6287 \text{ cm/s}$$

$$u_d^* = 0,78$$

At the start of the divergent section, gas and drop velocities are the same as at the throat exit. Therefore, at the beginning of the divergent section:

$$u_{Go} = 8060 \text{ cm/s}$$

$$\text{and } u_{do} = 6287 \text{ cm/s}$$

Drop Reynolds number is

$$N_{Re,o} = \frac{d_d\ (u_{Go} - u_d)}{\nu} = \frac{(0,0107)\ (8060 - 6287)}{0,15}$$

$$= 126$$

From Standard curve or by equation (5-8):

$C_{Do} = 0,95$

$$S = \frac{2}{3}\,\frac{\tan\theta}{R}\,\frac{d_d}{C_{Do}}\,\frac{\rho_L}{\rho_G}\left(\frac{u_{Go}}{u_{Go}-u_{do}}\right)^{0,7}$$

$= 0,177$

$$L = \frac{3}{2}\,x\,\frac{C_{Do}}{d_d}\,\frac{\rho_G}{\rho_L}\left(\frac{u_{Go}-u_{do}}{u_{Go}}\right)^{0,5}$$

$= 12,5$

We need "l_H" which can be found by using Figure 5-19,

$$\frac{l_H}{u_d^{2}} = 2,0$$

Therefore, $l_H = 2,0\ (0,78)^2 = 1,2$

$L + l_H = 13,7$

$F = 1 - Sl_H = 1 - 0,177\ (1,2) = 0,788$

Thus, $(L+l_H)F = 10,8$

$l_H F = 0,95$

and $SF^{-0,5} = 0,2$

$$K_{po} = \frac{u_{Go}\ d_{pa}^2}{9\ \mu_G\ d_d} = 4,65\ d_{pa}^2$$

or $d_{pa} = (0,215\ K_{po})^{0,5}$ μmA

$$B = \left(\frac{Q_L}{Q_G}\right)\left(\frac{\rho_L}{\rho_G}\right)\frac{1}{C_{Do}}\left(\frac{u_{Go}}{u_{Go}-u_{do}}\right)^{0,7}$$

$= 2,54$

Read "$-F \ln Pt/B$" from Figures 5-10 to 5-14 at $SF^{0.5}=0.2$ and $(L+L_H)F=10.8$ and 0.95 for various K_{po}, we obtain:

K_{po}	d_{pa}, µmA	$(-F \ln Pt/B)_{L+L_H}$	$Pt(d_{pa})_{L+L_H}$	$(-F \ln Pt/B)_{L_H}$	$Pt(d_{pa})_{L_H}$
0.2	0.21	0.057	0.83	0.035	0.89
0.5	0.33	0.148	0.62	0.142	0.63
0.7	0.39	0.233	0.47	0.213	0.50
1.0	0.46	0.35	0.32	0.315	0.36
2.0	0.66	0.68	0.11	0.57	0.16
5.0	1.04	1.25	0.018	0.93	0.05
10	1.5	1.75	0.0035	1.15	0.025

The penetration for the whole venturi scrubber is calculated with the help of equation (5-32), i.e.,

$$Pt(d_{pa}) = \frac{Pt(d_{pa})_{throat}\ Pt(d_{pa})_{L+L_H}}{Pt(d_{pa})_{L_H}}$$

d_{pa}, µmA	0.21	0.33	0.39	0.46	0.66	1.04	1.5
Pt	0.91	0.69	0.55	0.30	0.14	0.025	0.0045

Figure 5-21 shows the result of this calculation. For this particular scrubber geometry and operating conditions, the particle collection in the divergent section contributes little to the overall scrubber collection efficiency as shown in the figure.

Pressure Drop

We will use both the modified Calvert's equation and Boll's equation to predict the pressure drop of the sample venturi scrubber.

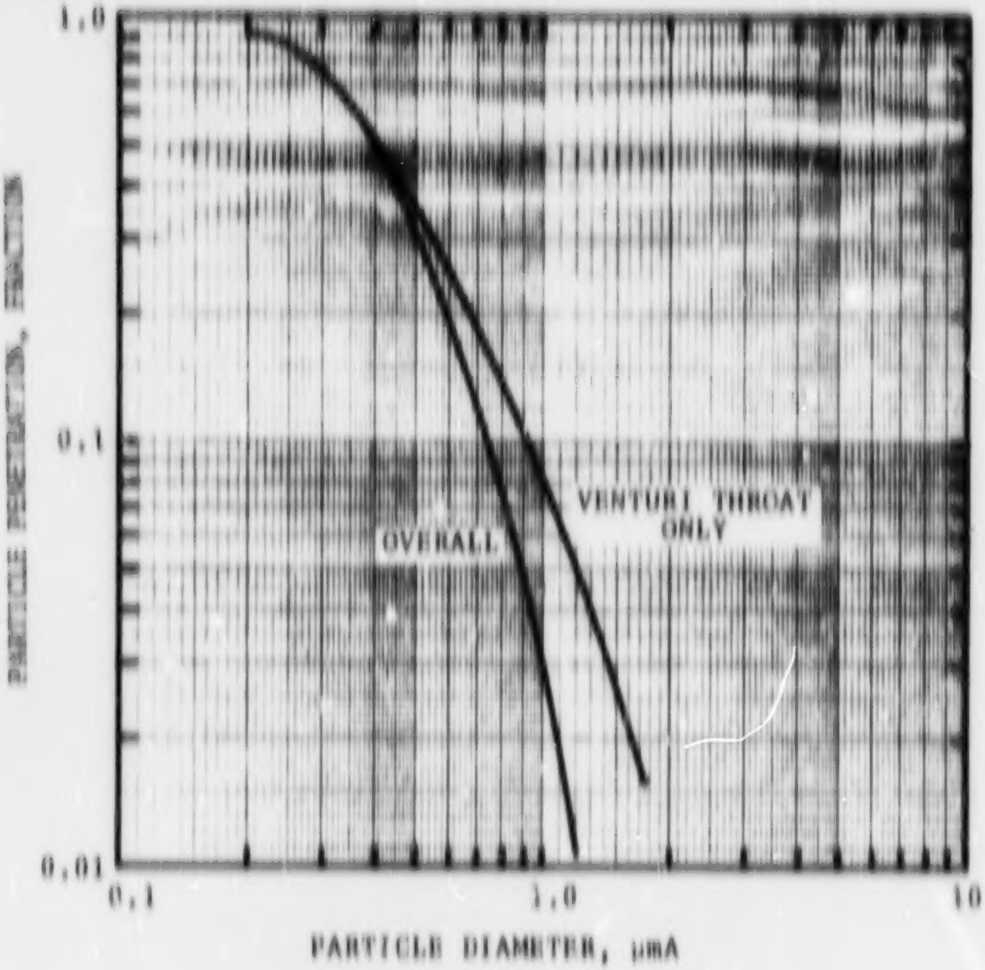

Figure 5-21. Predicted grade efficiency curve.

Modified Calvert's Equation - Modified Calvert's equation is:

$$\Delta P = 1{,}03 \times 10^{-3}\, u_d^{*}\, u_{Gt}^{2} \left(\frac{Q_L}{Q_G}\right)$$

For the present example, $u_{Gt} = 8060$ cm/s

$$\text{and} \quad \left(\frac{Q_L}{Q_G}\right) = 1{,}33 \times 10^{-3}\ \frac{m^3}{m^3}$$

Therefore, drop diameter by Nukiyama and Tanasawa:

$$d_d = \frac{50}{u_G} + 91{,}8\left(\frac{Q_L}{Q_G}\right)^{1.5}$$

$$= 0{,}0107 \text{ cm}$$

Drop Reynolds number

$$N_{Re,o} = \frac{d_d\ (u_{Go} - u_{do})}{\nu}$$

$$= \frac{0{,}0107\ (8060 - 0)}{0{,}15} = 575$$

From Standard curve, or from equation (5-8):

$$C_{Do} = 0{,}545$$

$$\text{and} \quad x = \frac{3\ \ell_t\ C_{Do}\ \rho_G}{16\ d_d\ \rho_L} + 1$$

$$= 1{,}35$$

$$u_d^{*} = 2\left|1 - x^2 + (x^4 - x^2)^{0.5}\right|$$

$$= 0{,}80$$

Therefore, pressure drop is:

$$\Delta P = (1{,}03\times10^{-7})(0{,}80)(8060)^2(1{,}35\times10^{-3})$$

$$= 71{,}5 \text{ cm W.C.}$$

Boll's Equation - The procedure to calculate the pressure drop using Boll's equation is to calculate wall friction loss and acceleration loss separately. The sum of the two losses is the total pressure drop.

(1) Convergent section

A. Wall friction

$$p_w^* = \frac{(M + 1)f}{d_{ho}^*} F_w \;, \quad f = 0{,}027$$

$$F_w = \frac{1}{A_r^2}\left| 1 + \frac{R^*(A_r - 1)(1+b^*+R^*)}{2(b^*+R^*)} \right|$$

$$\text{and} \quad A_r = \frac{\text{exit cross-sectional area}}{\text{inlet cross-sectional area}}$$

At the convergent section inlet:

u_{Go} = 2500 cm/s

$M = 0$

ℓ = 62 cm

b = 81,3 cm

R = (0,5)(65,4) = 32,7 cm

$$d_{ho} = \frac{2b(R + \ell \tan \theta)}{b + R + \ell \tan \theta} \qquad (5\text{-}15)$$

$$= \frac{(2)(81{,}3)\;32{,}7 + (62) \tan 20^\circ}{81{,}3 + 32{,}7 + (62) \tan 20^\circ}$$

$$= 65{,}8 \text{ cm}$$

By the definition of dimensionless parameters, we have:

$$h^* = \frac{81.3}{62} = 1.31$$

$$R^* = \frac{32.7}{62} = 0.527$$

$$d^*_{h0} = \frac{65.8}{62} = 1.06$$

$$A_r = \frac{(81.3)(20.3)}{(81.3)(65.4)} = 0.31$$

Therefore,

$$F_w = \frac{1}{(0.31)^2}\left[1 + \frac{0.527(0.31-1)(1+1.31+0.527)}{2(1.31+0.527)}\right]$$

$$= 7.48$$

$$p^*_w = \frac{\Delta p}{\frac{1}{2g_c}\,\rho_G\,u_{G0}^2} = \frac{(0.027)(7.48)}{1.06} = 0.19$$

$$\therefore \Delta p_w = \frac{(0.19)(1.2\times10^{-3})(2500)^2}{(2)(980)}$$

$$= 0.73 \text{ cm W.C.}$$

B. Acceleration loss

There is no water in this section, therefore acceleration loss is zero, i.e.,

$$\Delta p_d = 0$$

Total pressure drop in convergent section:

$$\Delta p = \Delta p_w + \Delta p_d = 0.73 \text{ cm W.C.}$$

(2) Throat section

A. Wall loss

At the throat inlet:

u_{Go} = 8060 cm/sec

h = 81.3 cm

R = (0.5)(20.3) = 10.2 cm

β = 0

d_{ho} = 18.1 cm

and $$M = \frac{Q_W}{Q_G}\ \frac{\rho_L}{\rho_G} = \frac{1.33\times10^{-3}}{1.2\times10^{-3}} = 1.1$$

$$d^*_{ho} = \frac{18.1}{30.5} = 0.593$$

A_r = 1

F_W = 1

Therefore,

$$F^*_W = \frac{(1.1 + 1)(0.027)}{0.593} = 0.0956$$

and $$\Delta P = \frac{(0.0956)(1.2\times10^{-3})(8060)^2}{(2)(980)}$$

$$= 3.8 \text{ cm W.C.}$$

B. Acceleration loss

From Nukiyama and Tanasawa correlation, we have:

d_d = 0.0107 cm

u_{do} = 0

Drop Reynolds number

$$N_{Re,o} = \frac{d_d(u_{Go} - u_{do})}{\nu} = \frac{(0.0107)(8060-0)}{0.15} = 575$$

From equation (5-8):

$$C_{Do} = 0.22 + \frac{24}{575}\left(1 + (0.15)(575)^{0.6}\right)$$

$$= 0.545$$

$$L = \frac{3}{2}\, z\, \frac{C_{Do}}{d_d}\left(\frac{\rho_G}{\rho_L}\right)\left(\frac{u_{Go}-u_{do}}{u_{Go}}\right)^{0.8}$$

$$= 2.79$$

For venturi throat, β=0, S=0, F=1.

From Figure 5-4, we obtain:

$$\frac{p_d^* F^2}{M} = 1.6 \qquad \text{for } (L+L_H)F = 2.79$$

Since $p_d^* = \dfrac{\Delta p_d}{\frac{1}{2g_c}\rho_G u_{Go}^2}$, we have

$$\Delta p_d = \frac{1.6M\,\rho_G\,u_{Go}^2}{2g_c F^2}$$

$$= \frac{(1.6)(1.1)(1.2\times10^{-3})(8060)^2}{(2)(980)}$$

$$= 70 \text{ cm W.C.}$$

Therefore, total pressure drop in venturi throat:

$$\Delta p = \Delta p_w + \Delta p_d = 2.79 + 70$$

$$= 72.79 \text{ cm W.C.}$$

(5) Divergent Section

A. Wall loss

At divergent section inlet:

$u_{Go} = 8050$ cm/s
$h = 81,3$ cm/s
$R = (0,5)(20,3) = 10,2$ cm
$\theta = 7,5°$
$M = 1,1$
$\ell = 171$ cm

$$d_{ho} = \frac{2h\ (R + \ell \tan \theta)}{h + R + \ell \tan \theta}$$

$$= \frac{(2)(81,3)\left|10,2 + (171)\ \tan 7,5°\right|}{81,3 + 10,2 + (171)\ \tan 7,5°}$$

$$= 46,7 \text{ cm}$$

$$d_{ho}^* = \frac{d_{ho}}{\ell} = \frac{46,7}{171} = 0,273$$

$$A_r = \frac{(81,3)(65,4)}{(81,3)(20,3)} = 3,22$$

$$R^* = \frac{R}{\ell} = \frac{10,2}{171} = 0,06$$

$$h^* = \frac{h}{\ell} = \frac{81,3}{171} = 0,475$$

and $$F_w = \frac{1}{3,22^2}\left|1 + \frac{0,06(3,22-1)(1+0,06+0,475)}{2(0,475+0,06)}\right|$$

$$= 0,115$$

$$p_w^* = \frac{(1,1+1)(0,027)(0,115)}{0,273} = 0,025$$

Since $p_W^* = \dfrac{\Delta p_W}{\frac{1}{2g_c}\,\rho_G\,u_{Go}^2}$, we have

$$\Delta p_W = \frac{(0.025)(1.2\times10^{-3})(8060)^2}{(2)(980)}$$

$$= 0.99 \text{ cm W.C.}$$

B. Acceleration loss

In the divergent section, liquid drop diameter is the same as in the throat, i.e., $d_d = 0.0107$ cm. At the divergent section inlet, drop velocity is equal to the velocity at the throat exit. From Figure 5-2, we obtain:

$$u_{d}^{*\prime} = 0.78 \quad \text{for } (1+L_H)F = 2.70 \text{ and } SF^{-0.5} = 0$$

$$\therefore u_{do} = (0.78)(8060)$$

$$= 6287 \text{ cm/s}$$

$$u_{Go} = 8060 \text{ cm/s}$$

Drop Reynolds number

$$N_{Re,o} = \frac{d_d(u_{Go}-u_{do})}{\nu}$$

$$= \frac{(0.0107)(8060-6287)}{0.15} = 126$$

Using equation 5-8, we obtain $C_{Do} = 0.93$

$$B = \frac{2}{3}\,\frac{\tan\beta}{R}\,\frac{d_d}{C_{Do}}\,\frac{\rho_L}{\rho_G}\left(\frac{u_{Go}}{u_{Go}-u_{do}}\right)^{0.5}$$

$$= 0.177$$

$$L = \frac{3}{2}\,z\,\frac{C_{Do}}{d_d}\,\frac{\rho_G}{\rho_L}\left(\frac{u_{Go}-u_{do}}{u_{Go}}\right)^{0.5}$$

$$= 12,5$$

From Figure 5-19, we obtain:

$$\frac{L_H}{u_d^{*2}} = 2,0$$

Therefore, $L_H = 2,0\ (0,78)^2 = 1,2$

$$L + L_H = 13,7$$

$$F = 1 - SL_H = 1 - 0,177\ (1,2) = 0,788$$

Thus, $(L+L_H)F = 10,8$

$$L_H F = 0,95$$

and $SF^{-0.5} = (0,177)(0,788)^{-0.5} = 0,199$

From Figure 5-4, we obtain

$$\left(\frac{P_d^* F^2}{M}\right)_{L+L_H} = 1,0$$

$$\left(\frac{P_d^* F^2}{M}\right)_{L_H} = 1,1$$

$$\therefore (P_d^*)_{L+L_H} = \frac{(1,0)(1,1)}{(0,788)^2} = 1,77$$

$$(P_d^*)_{L_H} = \frac{(1.1)(1.1)}{(0.788)^2} = 1.95$$

$$(P_d^*)_L = (P_d^*)_{L+L_H} - (P_d^*)_{L_H} = -0.179$$

Since $P_d^* = \dfrac{\Delta p_d^*}{\frac{1}{2g_c}\,\rho_G\,u_{G0}^2}$, we have

$$\Delta p_d^* = -\frac{(0.179)(1.2\times10^{-3})(8060)^2}{(2)(980)}$$

$$= -7.1 \text{ cm W.C.}$$

Negative pressure drop is equivalent to pressure recovery by the gas. Total pressure drop in the divergent section is then equal to:

$$\Delta p = 0.99 - 7.1 = -6.11 \text{ cm W.C.}$$

The pressure drop for the whole venturi scrubber is equal to the sum of convergent, throat and divergent section loss.

$$\Delta p \text{ (overall)} = 0.73 + 72.79 - 6.11$$
$$= 67.4 \text{ cm W.C.}$$

The difference in predictions by the modified Calvert's equation and by Boll's equation is 4.1 cm W.C. However, the modified Calvert's equation is simpler to use as proven by this calculation example.

PARTICLE COLLECTION IN THE VENTURI THROAT

For a venturi scrubber, most of the particle collection action occurs in the throat section where the relative velocity between particles and drops is highest. Thus, it would be desirable to obtain an expression for particle collection in a venturi throat.

For particle collection in a venturi throat, equation (5-23) reduces to:

$$-\frac{\ln Pt(d_p)}{B} = \int_0^L \frac{\left|1 - u_d^*\right|^2}{u_d^*\left[\left|1 - u_d^*\right| + \frac{0.7}{K_{po}}\right]^2}\, dz^* \qquad (5\text{-}41)$$

Equation (5-24) for liquid drop velocity becomes:

$$\frac{du_d^*}{dz^*} = \frac{(1-u_d^*)^{1.5}}{2u_d^*} \qquad (5\text{-}42)$$

We will solve these two equations for the special case $u_{do}^*=0$, i.e., initial liquid drop velocity is zero. By rearranging equation (5-42), we have:

$$dz^* = \frac{2u_d^*}{(1-u_d^*)^{1.5}}\, du_d^* \qquad (5\text{-}43)$$

By substituting equation (5-43) into (5-41), we obtain:

$$\frac{\ln Pt(d_p)}{B} = -2\int_0^{u_d^*} \frac{(1-u_d^*)^{0.5}}{\left(1 - u_d^* + \frac{0.7}{K_{po}}\right)^2}\, du_d^* \qquad (5\text{-}44)$$

The closed form solutions to equations (5-44) and (5-42) are:

$$\frac{\ln Pt(d_p)}{B} = \frac{1}{K_{po}\left(1-u_d^* + \frac{0.7}{K_{po}}\right)}\Bigg| 4\,K_{po}(1-u_d^*)^{1.5} + 4.2\,(1-u_d^*)^{0.5}$$

$$- 5.02\,K_{po}^{0.5}\left((1-u_d^*) + \frac{0.7}{K_{po}}\right)\tan^{-1}\sqrt{\frac{(1-u_d^*)K_{po}}{0.7}}\,\Bigg|$$

$$- \frac{1}{K_{po}\left(1 + \frac{0.7}{K_{po}}\right)}\left[4\,K_{po} + 4.2 - 5.02\,K_{po}^{0.5}\left(1 + \frac{0.7}{K_{po}}\right)\tan^{-1}\sqrt{\frac{K_{po}}{0.7}}\right]$$

(5-45)

and $u_d^* = 2\left|1 - x^2 + (x^4 - x^2)^{0.5}\right|$ (5-46)

where $x = \frac{3\ \ell_t\ C_{Do}\ \rho_G}{16\ d_d\ \rho_L} + 1 = \frac{1}{8}\ (L + 8)$ (5-47)

$$K_{po} = \frac{d_{pa}\ u_{Gt}^2}{9\ \mu_G\ d_d} \quad (5\text{-}48)$$

$$B = \left(\frac{Q_L}{Q_G}\right)\left(\frac{\rho_L}{\rho_G}\right)\frac{1}{C_{Do}} \quad (5\text{-}49)$$

ℓ_t = venturi throat length, cm

C_{Do} = drag coefficient for drops at the venturi throat inlet, dimensionless

"C_{Do}" is a function of drop Reynolds number and is obtained from "Standard Curve."

Drop Reynolds number is defined as:

$$N_{Re,d} = \frac{d_d\ u_{Gt}}{\nu} \quad (5\text{-}50)$$

For an infinite length venturi throat, u_d^* approaches unity and equation (5-45) reduces to:

$$Pt(d_p) = \exp\left[-B\ \frac{4\ K_{po} + 4.2 - 5.02\ K_{po}^{0.5}\left(1 + \frac{0.7}{K_{po}}\right)\tan^{-1}\sqrt{\frac{K_{po}}{0.7}}}{K_{po} + 0.7}\right] \quad (5\text{-}51)$$

Equations (5-45) and (5-51) were used to predict the particle collection for the venturi scrubber mentioned in the last section. Figure (5-22) shows the calculation results along with the grade efficiency curve obtained in the last section. As can be seen, there is little difference between the three curves. For this particular scrubber geometry, we can assume that the venturi throat is of infinite length and its particle collection is that predicted by equation (5-51).

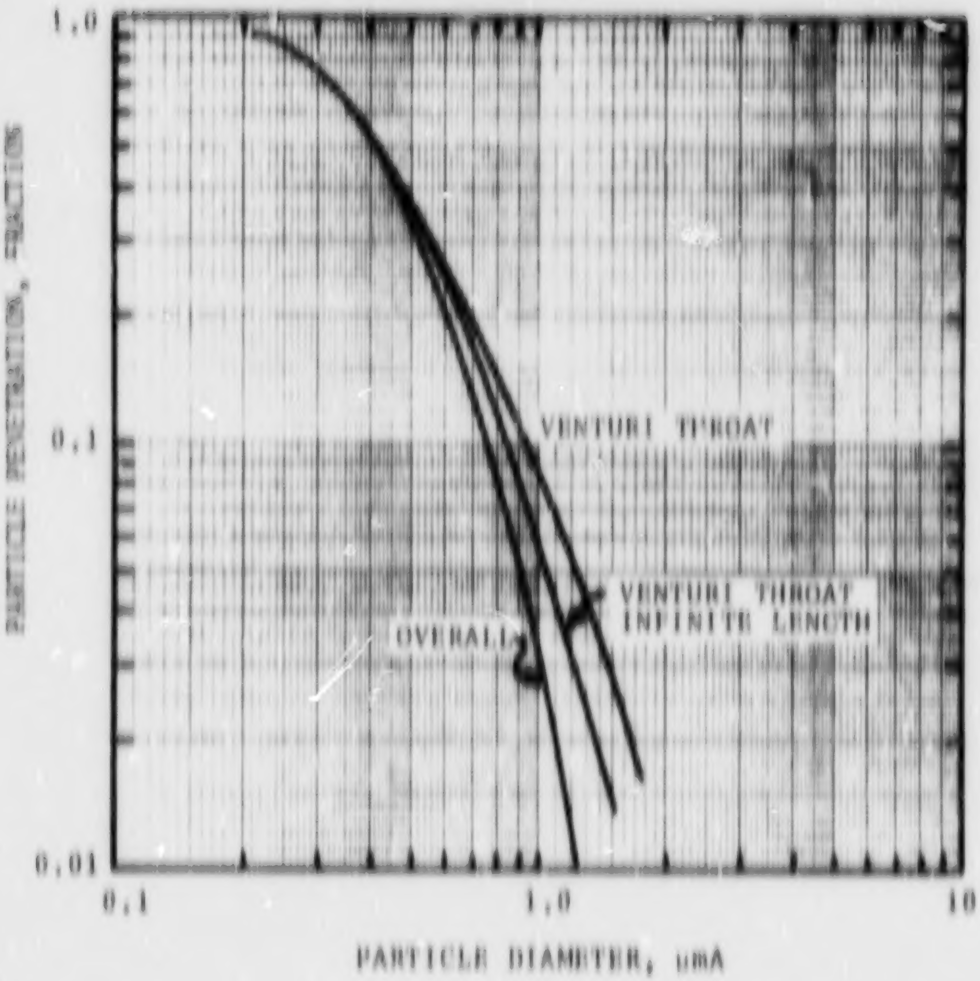

Figure 5-22. Predicted grade efficiency curve.

PARTICLE COLLECTION BY DIFFUSION

In all previous developments, particle collection by impaction is assumed to be the only collection phenomenon occurring in a venturi scrubber. This assumption is true for particles with diameters larger than 0.5 micron. Particles smaller than 0.1 μm in diameter are rarely collected by inertial impaction because they follow the gas streamlines surrounding the liquid drops. For particles in this size range, diffusional collection is usually the predominant collection phenomenon. In the following sections, we will derive an expression for the prediction of particle collection by diffusion in a venturi scrubber.

Again, we will use Calvert's differential equation as our starting equation. His equation is:

$$-\frac{dc}{c} = \frac{1.5\,|u_G - u_d|}{u_d\ d_d}\left(\frac{Q_w}{Q_G}\right)\eta\ dz \qquad (5\text{-}52)$$

where c = particle concentration, g/cm³
u_G = gas velocity, cm/s
u_d = drop velocity, cm/s
Q_w = liquid flow rate, cm³/s
Q_G = gas flow rate, cm³/s
η = single drop collection efficiency, dimensionless

According to Johnstone and Roberts (1949), single drop diffusional collection efficiency is given by the following equation:

$$\eta = \frac{4\ D_p}{|u_G - u_d|\ d_d}\left|2 + 0.552\ (N_{Re}^{0.5})\left(\frac{\nu_G}{D_p}\right)^{1/3}\right| \qquad (5\text{-}53)$$

where D_p = particle diffusivity, cm²/s
N_{Re} = drop Reynolds number, dimensionless
ν_G = kinematic viscosity of gas, cm²/s

By using the same dimensionless parameters defined earlier (equations (5-16), (5-17), (5-20) and (5-22) we have:

$$\eta = \frac{4\ D_p \left[2 + 0,552 \left(\frac{u_{Go}}{u_{Go} - u_{do}} \right)^{0.5} N_{Re,o}^{0.5} \left(\frac{\nu_G}{D_p} \right)^{1/3} \left| (1+8z^*)^{-1} - u_d^* \right| \right]}{d_d\ u_{Go}\ \left| (1+8z^*)^{-1} - u_d^* \right|} \tag{5-54}$$

and

$$-\frac{dc}{c} = \frac{4\ B\ D_p}{u_{Go}\ d_d} \frac{1}{u_d^*} \left| 2 + E \left| (1+8z^*)^{-1} - u_d^* \right|^{0.5} \right| dz^* \tag{5-55}$$

where

$$B = \frac{1}{C_{Do}} \left(\frac{Q_W}{Q_G} \right) \frac{\rho_L}{\rho_G} \left(\frac{u_{Go}}{u_{Go} - u_{do}} \right)^{0.5} \tag{5-56}$$

$$E = 0,552 \left(\frac{u_{Go}}{u_{Go} - u_{do}} \right)^{0.5} N_{Re,o}^{0.5} \left(\frac{\nu_G}{D_p} \right)^{1/3} \tag{5-57}$$

let

$$B_D = \frac{4\ B\ D_p}{u_{Go}\ d_d} \tag{5-58}$$

we have:

$$-\frac{dc}{c} = \frac{B_D}{u_d^*} \left| 2 + E\ (1+8z^*)^{-1} - u_d^* \right|^{0.5} \Big|\ dz^* \tag{5-59}$$

Upon integration, we obtain:

$$\frac{\ln Pt}{B_D}(d_p) = \int_0^1 \frac{2dz^*}{u_d^*} + \int_0^1 \frac{E}{u_d^*} \left| (1+8z^*)^{-1} - u_d^* \right|^{0.5} dz^* \tag{5-60}$$

Equation (5-60) is the final equation describing the particle collection by diffusion in a venturi scrubber. Plots similar to Figures 5-1 through 5-10 can be constructed.

For venturi throat (θ=0) and for the special case that initial drop velocity is zero (u_{do}^*=0), the analytical solution to equation (5-60) is:

$$\frac{\ln Pt}{B_p}(d_p)=8+2E\ \ln(1-u_d^*)-\frac{8}{\sqrt{1-u_d^*}} \qquad (5\text{-}61)$$

CHAPTER 6
COMPARING MODEL PREDICTIONS WITH PERFORMANCE DATA

There are numerous venturi scrubber performance data scattered in literature. However, most of these data are of little use in model comparison because either scrubber geometry information or particle information, e.g. size distribution and loading are not available. In the following sections, only those data with well defined scrubber geometry and particle parameters will be compared with the mathematical model.

Data by Calvert, et al

Calvert, et al (1975) measured the performance of an American Air Filter Kinpactor 52 venturi scrubber. The scrubber is used to control the emission from an asphalt aggregates dryer.

The scrubber operating conditions during the test were as follows:

1. Gas flow rates were as shown in the tabulation below.

		Outlet	
Gas Parameters	Inlet Duct	Scrubber Outlet Duct	Chimney
Temperature	149°C	57°C	49°C
Pressure during pitot runs	+75.5 cm W.C.	+0.5 cm W.C.	+0.02 cm W.C.
Actual m^3/min	790	-	670
ACFM	28,200	-	23,700
DS m^3/min	420	-	500
DSCFM	16,300	-	19,000
Vol % H_2O vapor	21	13	11.8

2. Water flow rate to the venturi scrubber was reported by the plant as approximately 1.06 m³/min (280 GPM). Water temperatures were 32°C (90°F) and 63°C (145°F) for the inlet and outlet streams, respectively.

The performance predicted by equation 5-23 is compared with experimental measurements in Figure 6-1. The prediction agrees with the average of the measurements.

Predictions by Calvert's equation for venturi scrubber are shown in Figure 6-2. As can be seen, the experimental results lie between predictions for f = 0.25 and 0.5. A "f" value of f = 0.4 will give better fit between Calvert's model and data than other values of "f".

Brink and Contant's Data

Brink and Contant (1958) obtained performance data on a Pease-Anthony venturi scrubber installed in a phosphoric acid plant. The dimensions of the scrubber are shown in Figure 4-8. Brink and Contant gave a grade efficiency curve for the following scrubber operating conditions:

1) Throat velocity of gas: 66.4 m/sec (218 ft/sec).
2) Liquid flow rate: 757 ℓ/min (200 GPM).

Figure 6-3 shows the model predictions for (1) particle collection occurring in the venturi throat, (2) combined particle collection in venturi throat and divergent section, (3) particle collection occurring in the venturi throat and the throat is of infinite length.

The particle diameters given by Brink and Contant are actual size. However, aerodynamic particle diameter is used in the mathematical model. Aerodynamic particle diameter is related to actual diameter by the following expression:

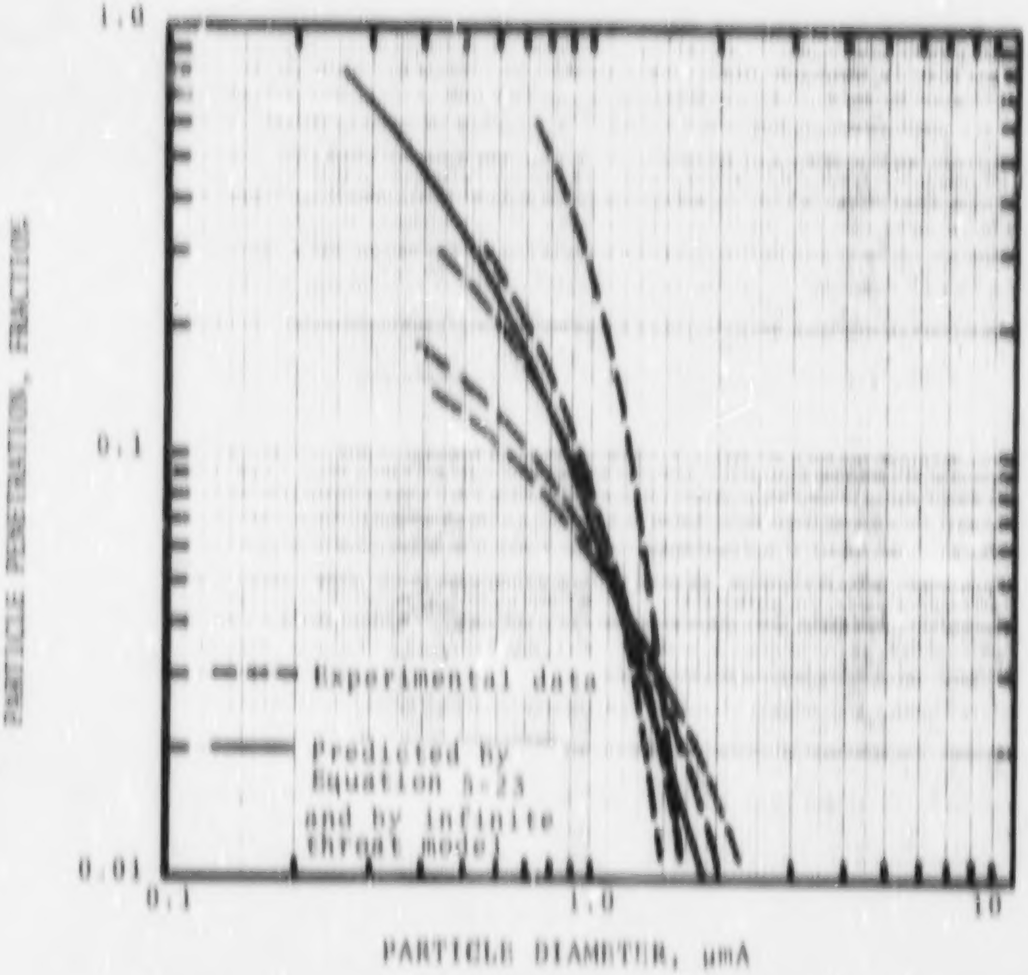

Figure 6-1. Experimental and predicted performance of AAF Kinpactor 32 Venturi scrubber.

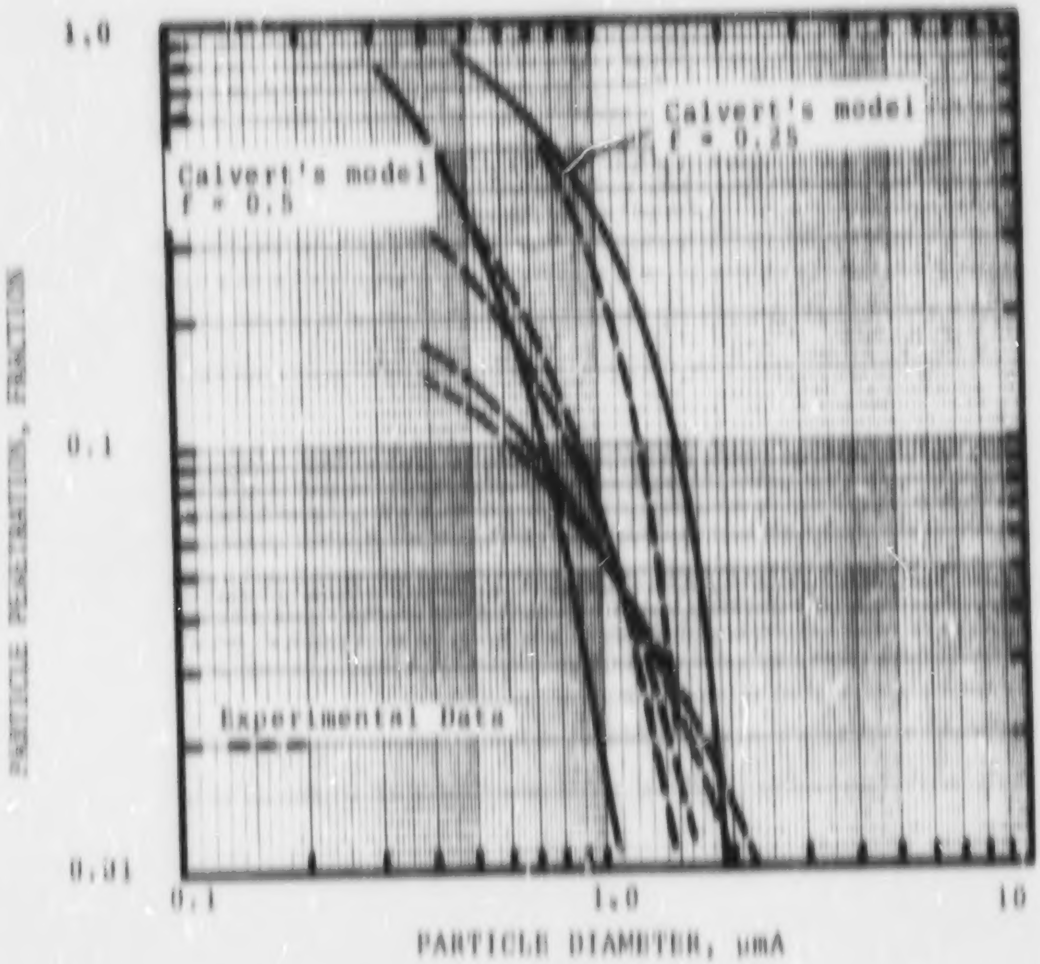

Figure 6-2. Experimental and predicted performance for AAF Kinpactor 32 Venturi scrubber.

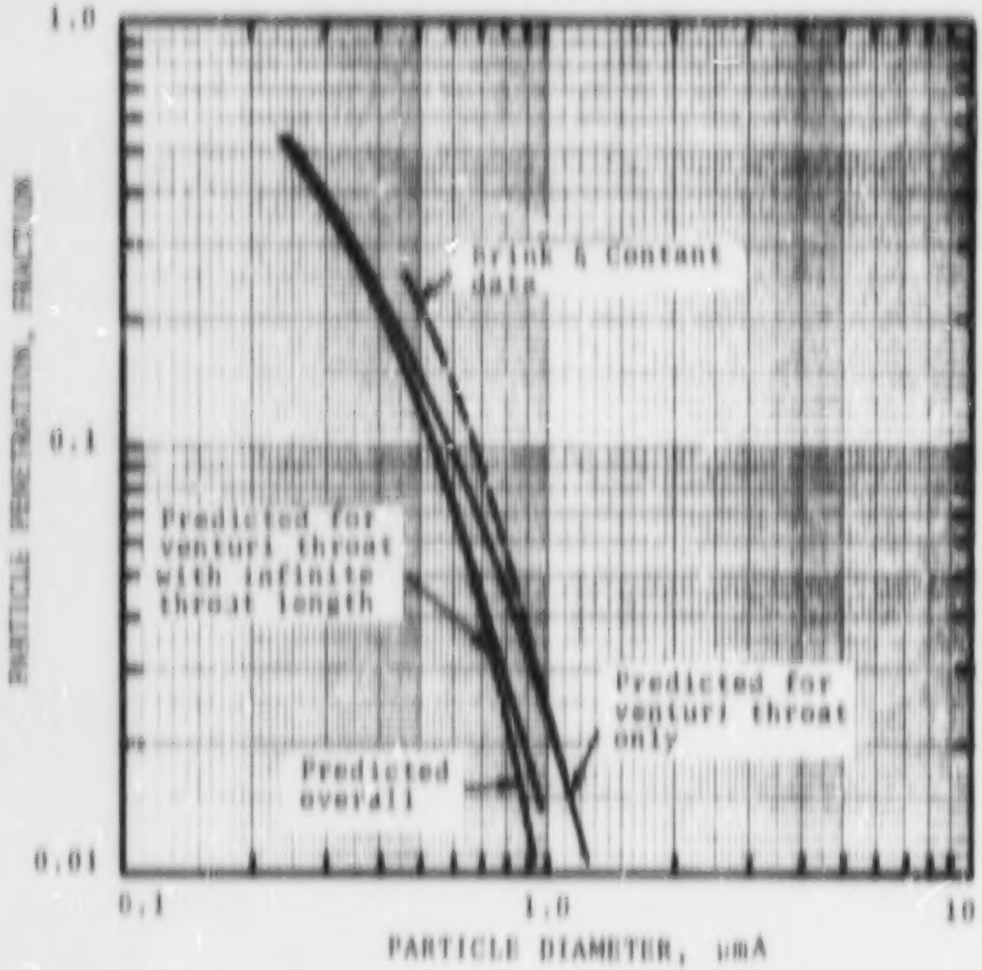

Figure 6-3. Predicted and experimental penetration for venturi scrubber used by Brink and Contant.

$$d_{pa} = d_p \left(\rho_p \, C' \right)^{0.5} \qquad (6\text{-}1)$$

where:

d_{pa} = aerodynamic particle diameter, μmA
d_p = actual particle diameter, μm
ρ_p = particle density, g/cm^3
C' = Cunningham slip factor, dimensionless

Aerodynamic diameter was transformed to actual diameter based on equation 6-1. A particle density of 2.6 (for MgP_2O_6) was assumed in the calculation.

As can be seen, the experimental data have a higher penetration than predicted. This discrepancy probably is caused by non-uniform liquid drop distribution as mentioned by Boll (1973). For this particular venturi scrubber, the prediction based on infinite throat length assumption is close to the prediction for the actual scrubber.

Data by Calvert et al

Calvert et al (1974) measured the performance of a Chemico venturi scrubber operating on the flue gas from a coal fired utility boiler. The scrubber might more accurately be described as a variable annular orifice type because its throat is formed by a movable "plumb bob" concentrically mounted in a conical "dental bowl."

The scrubber operating conditions during the test period were as follows:

1. Gas flow rates were as shown in the tabulation below and on the following page:

Duct	Inlet	Outlet
Temperature	163.0°C(325°F)	54.0°C(130°F)
Pressure during pitot run	60.0 cm Hg	60.0 cm Hg
A m^3/min	13,400	12,700
ACFM	4.75x10^5	4.5x10^5
DN m^3/min	6,300	7,150

Duct	Inlet	Outlet
DSCFM	2.4×10^5	2.7×10^5
% H_2O vapor (vol.)	6.0%	15.0%

The flow measured by the outlet velocity traverse is judged to be more reliable because the velocity distribution was much more regular than at the inlet. Based on 7,120 DNm^3/min (2.7×10^5 DSCFM), the inlet flow rate would be 15,300 Am^3/min (5.4×10^5 ACFM), which is 8% higher than the design flow rate of 14,200 Am^3/min (5×10^5 ACFM).

2. Slurry flow rate to the scrubber was reported by the plant as approximately 24.6 m^3/min (6,500 GPM).

Since the throat length and divergent angle for this scrubber were unknown, we will assume that it is equivalent to the venturi throat of infinite length. The throat velocity of the gas was calculated to be 42 m/sec and the liquid to gas ratio was 1.75 ℓ/m^3. Figure 6-4 shows the model prediction along with experimental data. The agreement between the two is reasonably well. Figure 6-5 compares data with predictions by Calvert's equation for venturi scrubber. A value of 0.5 for the empirical constant will make the model agree with data.

Data by Calvert et al

Calvert et al (1976) reported the performance test conducted on an APS electrostatic scrubber. When the charge inside the scrubber is turned off, the electrostatic scrubber becomes a venturi scrubber. The dimensions of the scrubber are shown in Figure 6-6. The measured performance of the scrubber is shown in Figure 6-7 along with predictions by equation 5-23 and by Calvert's equation for $f = 0.25$ and $f = 0.5$. The scrubber operating condition was:

1. $Q_L/Q_G = 1.4\ \ell/m^3$
2. $Q_G = 21\ Am^3/min$

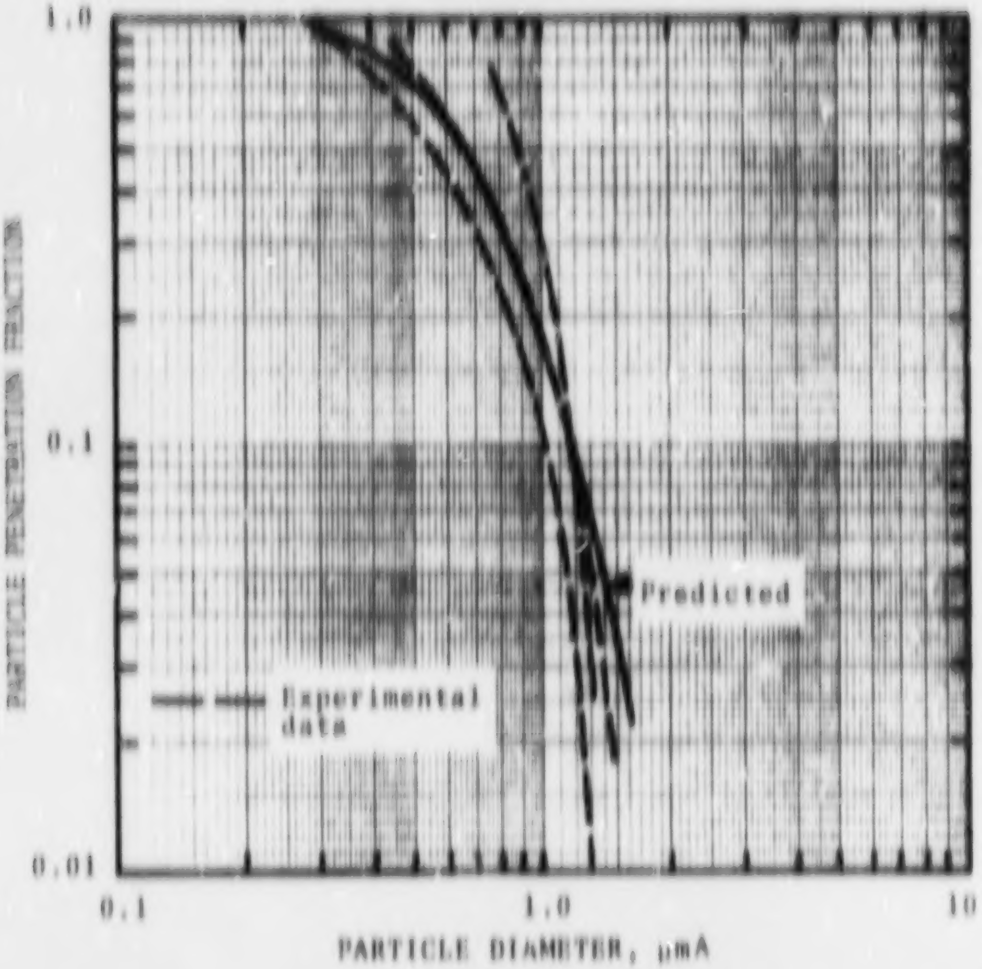

Figure 6-4. Predicted and measured penetration for Chemico venturi scrubber.

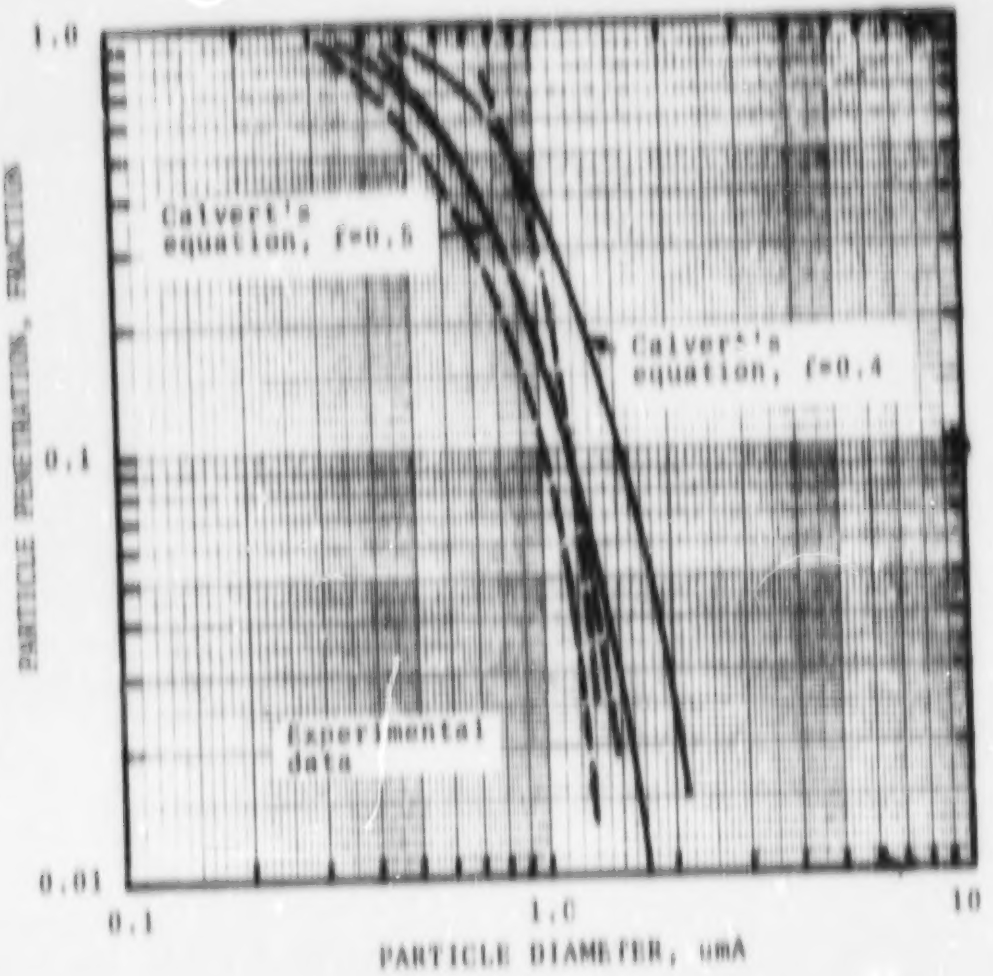

Figure 6-5. Predicted and experimental grade efficiency curve for Chemico venturi scrubber.

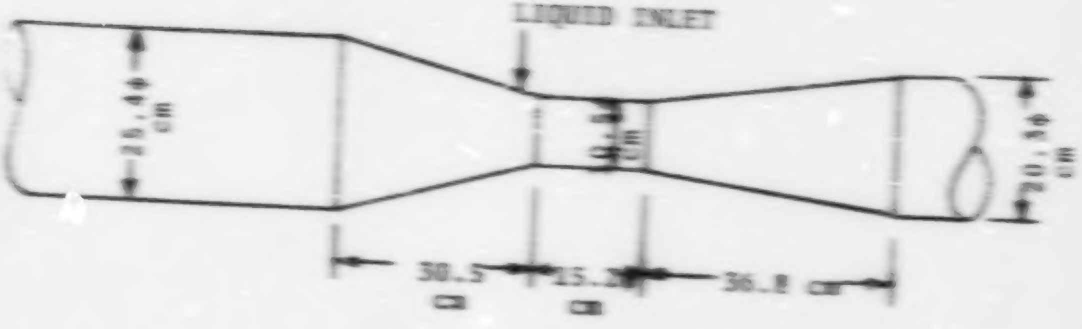
LIQUID INLET
25.40 cm
30.5 cm
15.2 cm
36.8 cm
20.30 cm

Figure 6-6 - APS Electrostatic Scrubber

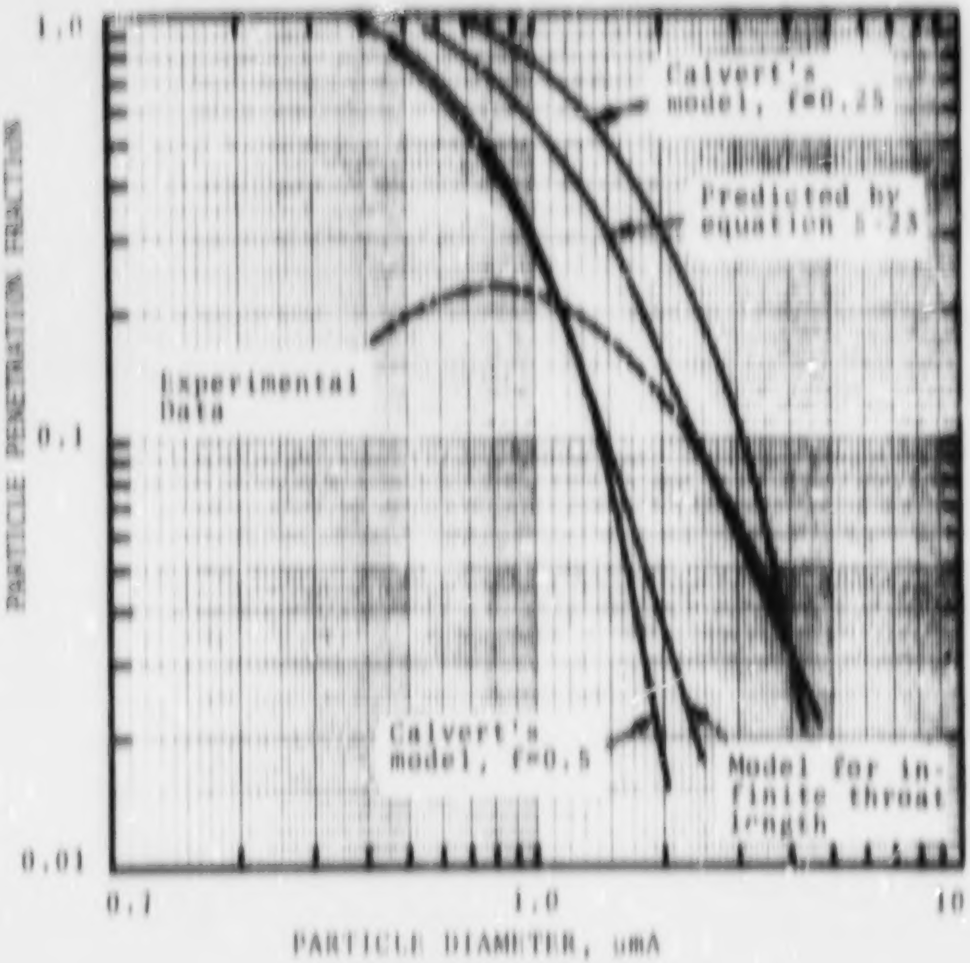

Figure 6-7. Experimental and predicted APS venturi scrubber performance.

As can be seen, in small particle regions, neither model agrees with experimental data. The models predict too high a penetration. Between the two models, equation 5-23 gives a better prediction than Calvert's equation.

Data by Calvert et al

Calvert et al (1974) obtained performance data on an Environeering Venturi-rod scrubber (Model A33 Hydro-Filter). This device consists primarily of several parallel rods which are positioned in a duct with some space between the rods so that gas can flow between them. Water is introduced upstream from the rod bed and is atomized by the gas stream as it flows between the rods. Strictly speaking, this scrubber is not a venturi scrubber but is one type of gas atomized spray scrubber.

The scrubber was installed to control the emission from an iron melting cupola. The scrubber operating conditions during the performance test runs were:

1. $Q_L/Q_G = 2.4\ \ell/m^3$
2. Gas velocity in the space betweed rods was calculated to be 196 m/s

This scrubber operates like a rectangular free jet. Since we do not know the expansion angle of the jet and the total jet length, we will assume that the scrubber operates like a venturi throat with throat length equal to five times and ten times the jet width. Figure 6-8 shows the calculation results along with experimental data. The experimental data lie in the area bounded by the curves for throat length equal to five times and ten times jet width.

CONCLUSIONS

Based on these comparisons, the following conclusions can be drawn:

1. If the venturi scrubber geometry is well defined, then the model prediction agrees with experimental data.

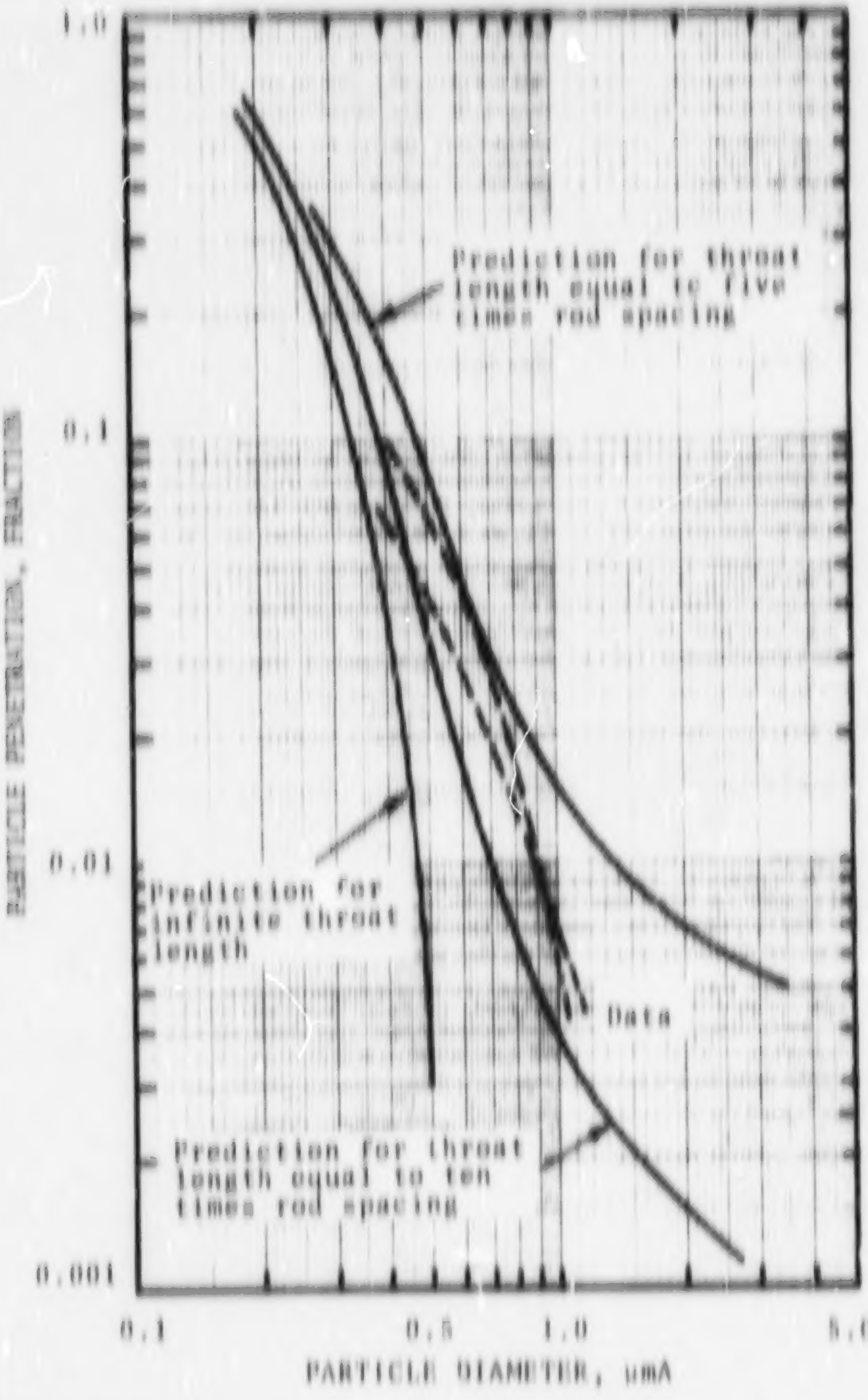

Figure 6-8. Predicted and experimental performance for venturi rod scrubber.

2. Equation 5-23 gives better predictions than Calvert's model. Another advantage of equation 5-23 is that it contains no empirical constants. However, Calvert's model is simpler to use than equation 5-23.

3. If the venturi scrubber throat length is long enough (dimensionless throat length, "L", larger than 2), then the scrubber performance can be approximated by the particle collection occurring in a straight tube of infinite length.

CHAPTER 7

DESIGN ANALYSIS

In this chapter, we will discuss the factors that affect the performance of a venturi scrubber, design techniques, and the optimization of the venturi scrubber design. Several factors have an influence on the performance and the design of a venturi scrubber. Some of these factors are:

1. Throat length of the scrubber
2. Throat velocity and liquid-to-gas ratio
3. The size distribution of the particles to be collected.

Effect of Inlet Particle Size Distribution on Performance

The overall (integrated) penetration, $\overline{Pt}$, of any device on a dust of any size distribution will be

$$\overline{Pt} = \frac{1}{W_c} \int_0^W Pt\ (d_p)\,dw \tag{7-1}$$

where $\overline{Pt}$ = overall penetration, fraction
$Pt\,(d_p)$ = penetration of particles with diameter d_p
W_c = total weight of particle, g
dw = particle weight corresponding to the interval $d\ (d_p)$ of particle size, g

The number and weight size distribution data for most industrial particulate emissions follow the log normal law. Hence, the two well established parameters of the log normal law law adequately describe the size distributions of particulate matter. These parameters are the geometric mean weight diameter, "d_{pg}", and the geometric standard deviation, "σ_g".

The log-normal particle distribution density is:

$$\frac{1}{W_o}\frac{dW}{d(\ln d_p)} = f(d_p) = \frac{1}{(2\pi)^{0.5}\ln\sigma_g}\exp\left[-\left(\frac{\ln d_p - \ln d_{pg}}{(2)^{0.5}\ln\sigma_g}\right)^2\right] \tag{7-2}$$

By combining equations 7-1 and 7-2, we have

$$\overline{Pt} = \int_{-\infty}^{+\infty} Pt\ (d_p)\ f\ (d_p)\ d\ (\ln d_p)$$

$$= \int_{-\infty}^{+\infty} Pt\ (d_p)\frac{1}{(2\pi)^{0.5}\ln\sigma_g}\exp\left[-\left(\frac{\ln d_p - \ln d_{pg}}{(2)^{0.5}\ln\sigma_g}\right)^2\right] d(\ln d_p) \tag{7-3}$$

For convenience we will use the following transformations. Let:

$$x = \frac{\ln d_p - \ln d_{pg}}{(2)^{0.5}\ln\sigma_g} \tag{7-4}$$

$$dx = \frac{1}{(2)^{0.5}\ln\sigma_g}d(\ln d_p) \tag{7-5}$$

Equation 7-7 in terms of x will become

$$\overline{Pt} = \frac{1}{(\pi)^{0.5}}\int_{-\infty}^{+\infty} Pt\ \exp\ (-x^2)\ dx \tag{7-6}$$

By substituting the expression for Pt (equation 5-23) into the above equation and performing the required integration, we can obtain the overall penetration for the whole particle population. This integration is tedious. Thus, the following simplification is made:

Based on the conclusion of the last chapter, the performance of a venturi scrubber can be approximated by the particle collection occurring in a straight tube of infinite length if the dimensionless throat length is larger than 2. Since most industrial venturi scrubbers have dimensionless throat length between 2 and 5, we will use the infinite throat length model to represent the performance of the venturi scrubber. The penetration for the venturi scrubber is then given by equation 5-46, i.e.,

$$Pt(d_p) = \exp\left[-B \frac{4K_{po} + 4.2 - 5.02\, K_{po}^{0.5} \left(1 + \frac{0.7}{K_{po}}\right) \tan^{-1}\sqrt{\frac{K_{po}}{0.7}}}{K_{po} + 0.7} \right] \qquad (7\text{-}7)$$

where $Pt(d_p)$ = penetration for particles with diameter d_p, fraction

B = dimensionless liquid-to-gas ratio parameter

$= \left(\frac{Q_W}{Q_G}\right)\left(\frac{\rho_L}{\rho_G}\right) \frac{1}{C_{Do}}$

K_{po} = inertial parameter

$= \frac{d_p^2\, \rho_p\, C'\, u_{Gt}}{9\, \mu_G\, d_d}$

d_p = particle diameter, cm

d_d = liquid drop diameter, cm

C' = Cunningham slip factor, dimensionless

u_{Gt} = gas throat velocity, cm/s

ρ_p = particle density, g/cm^3

ρ_L = liquid density, g/cm^3

ρ_G = gas density, g/cm^3

μ_G = gas viscosity, poise

The diameter for which collection efficiency is 50% is designated cut diameter "d_{pa50}", i.e.;

$$Pt = 0.5 \text{ when } d_p = d_{pa50}$$

In terms of cut diameter, equation 7-7 becomes

$$\ln(0.5) = -B \frac{4 K_{p50} + 4.2 - 5.02 K_{p50}^{0.5} \left(1 + \frac{0.7}{K_{p50}}\right) \tan^{-1} \sqrt{\frac{K_{p50}}{0.7}}}{K_{p50} + 0.7} \tag{7-8}$$

where "K_{p50}" is the inertial parameter for d_{pa50}

and is defined as

$$K_{p50} = \frac{u_{Gt}}{9} \frac{d^2_{pa50}}{\mu_G d_d} \tag{7-9}$$

By rearranging equation 7-8, we obtain

$$B = \frac{\ln(0.5)(K_{p50} + 0.7)}{4K_{p50} + 4.2 - 5.02 K_{p50} \left(1 + \frac{0.7}{K_{p50}}\right) \tan^{-1} \sqrt{\frac{K_{p50}}{0.7}}} \tag{7-10}$$

By substituting equation 7-10 into equation 7-8, we have

$$Pt(d_p) = \exp \left\{ - \frac{\ln (0.5) (K_{p50} + 0.7)}{(K_{po} + 0.7)} \left[\frac{4K_{po} + 4.2 - 5.02 K_{p50}^{0.5} \left(1 + \frac{0.7}{K_{po}}\right) \tan^{-1} \sqrt{\frac{K_{po}}{0.7}}}{4K_{p50} + 4.2 - 5.02 K_{p50}^{0.5} \left(1 + \frac{0.7}{K_{p50}}\right) \tan^{-1} \sqrt{\frac{K_{p50}}{0.7}}} \right] \right\} \tag{7-11}$$

From equation 7-4,

$$d_{pa} = d_{pg} \exp \left[(2)^{0.5} \sin \sigma_g \right]$$

By using this expression, we get for the inertial parameter,

$$K_{pa} = \frac{u_{Gt}\, d_{pa}^2}{9\, \mu_G\, d_d} = \frac{u_{Gt}\, d_{pg}^2 \exp\left[2(2)^{0.5} \sin \sigma_g\right]}{9\, \mu_G\, d_d} \qquad (7\text{-}12)$$

$$= b\, K_{pg}$$

where $b = \exp\left(2(2)^{0.5} \sin \sigma_g \right)$

$$K_{pg} = \frac{d_{pg}^2\, u_{Gt}}{9\, \mu_G\, d_d} \qquad (7\text{-}12a)$$

Since

$$\frac{K_{pss}}{K_{pg}} = \left(\frac{d_{pass}}{d_{pg}} \right)^2$$

let $Y = \dfrac{d_{pass}}{d_{pg}}$

then $K_{pss} = Y^2 K_{pg}$ (7-13)

By substituting equations 7-12 and 7-13 into equation 7-11 and after rearranging, we get,

$$Pt(d_p) = \exp \left\{ \frac{0.693\, (Y^2 K_{pg} + 0.7)}{(b\, K_{pg} + 0.7)} \left[\frac{4\, b\, K_{pg} + 4.2 - 5.02\, (b\, K_{pg})^{0.5} \left(1 + \frac{0.7}{bK_{pg}}\right) \tan^{-1}\sqrt{\frac{bK_{pg}}{0.7}}}{4\, Y^2\, K_{pg} + 4.2 - 5.02\, Y\, K_{pg}^{0.5} \left(1 + \frac{0.7}{Y^2 K_{pg}}\right) \tan^{-1}\sqrt{\frac{Y^2 K_{pg}}{0.7}}} \right] \right. \qquad (7\text{-}14)$$

By substituting equation 7-14 into equation 7-6, we have

$$\overline{Pt} = \frac{1}{\pi^{1/2}} \int_0^\infty \exp\left\{ -x^2 + \frac{0.693\,(Y^2 K_{pg} + 0.7)}{(b\,K_{pg} + 0.7)} \right.$$

$$\left. \left| \frac{4\,b\,K_{pg} + 4.2 - 5.02\,(b\,K_{pg})^{0.5} \left(1 + \frac{0.7}{b\,K_{pg}}\right) \tan^{-1} \sqrt{\frac{b\,K_{pg}}{0.7}}}{4\,Y^2\,K_{pg} + 4.2 - 5.02\,Y\,K_{pg}^{0.5} \left(1 + \frac{0.7}{Y^2 K_{pg}}\right) \tan^{-1} \sqrt{\frac{Y^2 K_{pg}}{0.7}}} \right| \right\} dx \qquad (7\text{-}15)$$

Equation 7-15 is the final equation relating the overall penetration "$\overline{Pt}$" to inlet particle size distribution (d_{pg}, σ_g) and to the inertial parameter for the mean particle diameter "K_{pg}".

Figures 7-1 through 7-5 are plots of "$\overline{Pt}$" versus (d_{mass}/d_{pg}) with "K_{pg}" as parameter for various "σ_g" values. These plots are exact solutions of equation 7-15, accounting for log-normal particle size distribution as given by equation 7-2.

The overall penetration can also be determined by knowing the size distribution and liquid-to-gas mass flow rate ratio. By substituting equation (7-12) into equation (7-7), we obtain,

$$Pt(d_p) = \exp\left[-B\, \frac{4\,b\,K_{pg} + 4.2}{b\,K_{pg} + 0.7} - \frac{5.02\,(b\,K_{pg})^{0.5} \left(1 + \frac{0.7}{b\,K_{pg}}\right) \tan^{-1} \sqrt{\frac{b\,K_{pg}}{0.7}}}{b\,K_{pg} + 0.7} \right] \qquad (7\text{-}16)$$

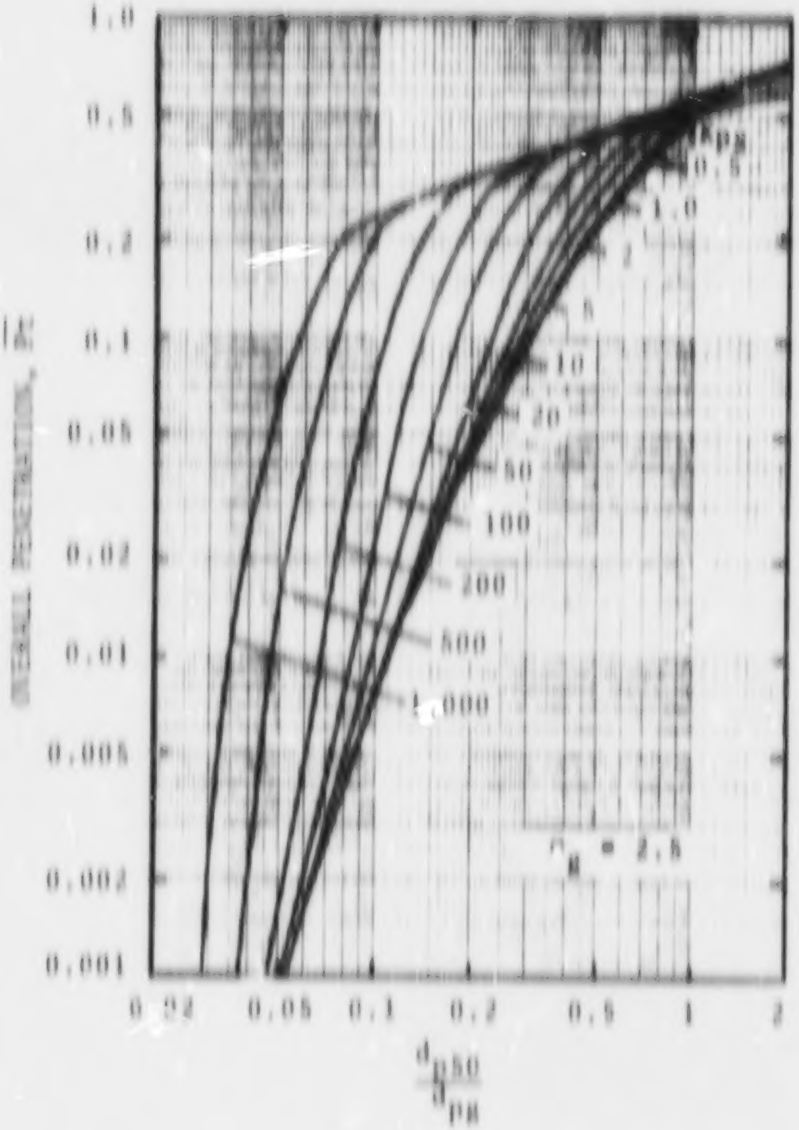

Figure 7-1. Venturi scrubber integrated penetration, "Pt" versus "d_{p50}/d_{pg}", with "K_{pg}" as parameter, "σ_g=2.5".

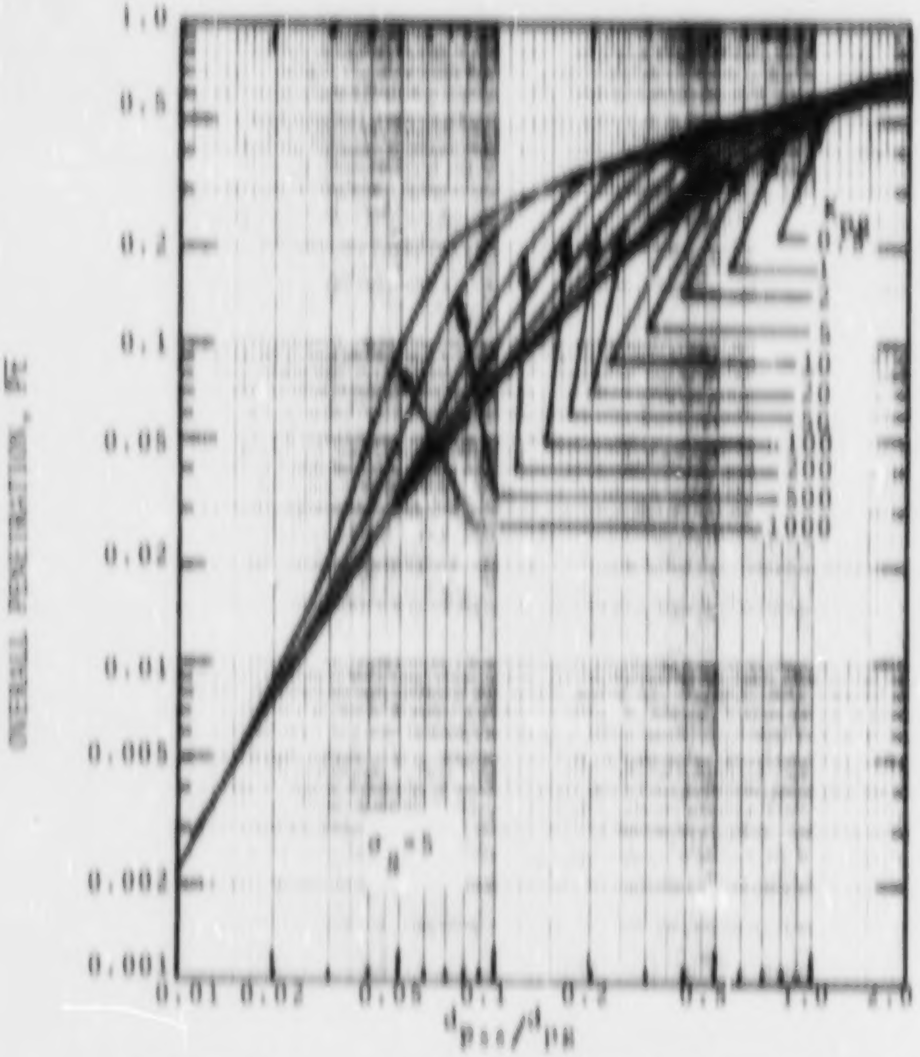

Figure 7-2. Venturi scrubber integrated penetration, $\overline{Pt}$ versus $d_{p_{ss}}/d_{pg}$, with K_{pg} as parameter, $\sigma_g = 5$.

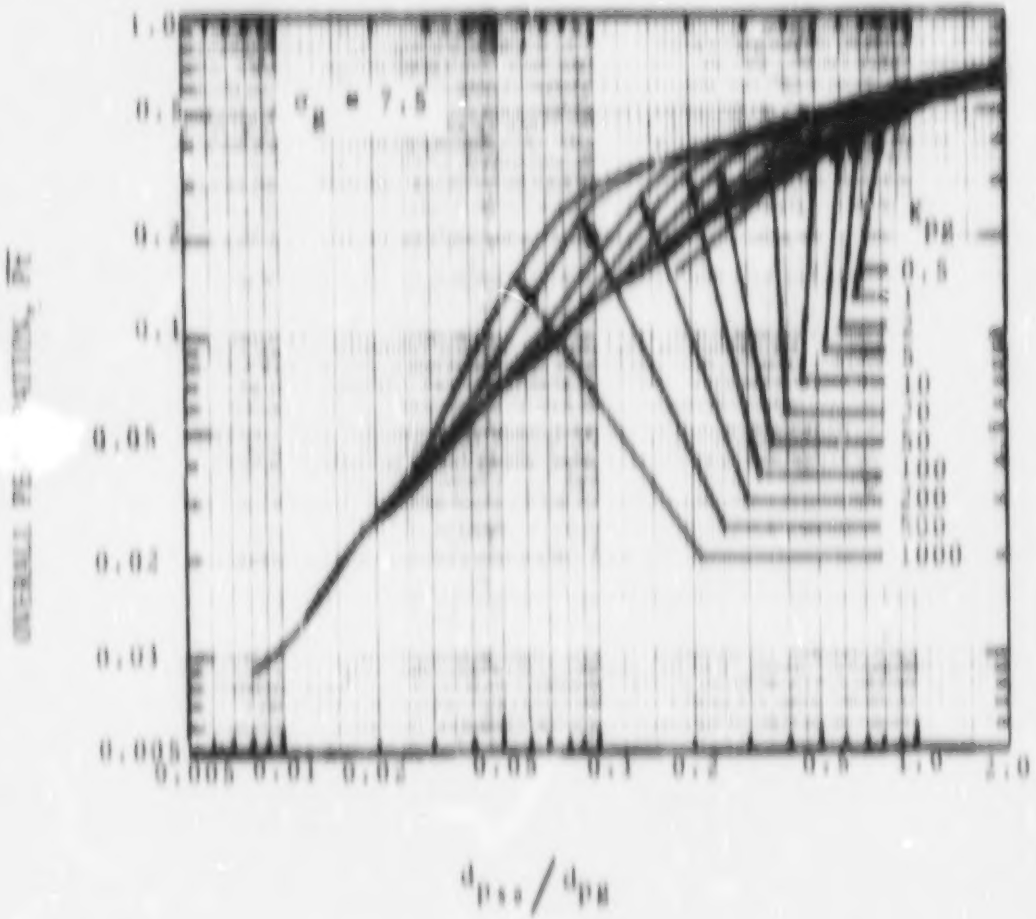

Figure 7-3. Venturi scrubber integrated penetration, $\overline{Pt}$ versus d_{pss}/d_{pg}, with K_{pg} as parameter, σ_g=7.5.

Equation 7-6 now becomes

$$\bar{P}t = \frac{1}{\pi^{0.5}}\int_0^\infty \exp\left\{-x^2 - B\left[\frac{4\,h\,K_{pg}+4.2}{h\,K_{pg}+0.7} - \frac{5.02\,(h\,K_{pg})^{0.5}}{h\,K_{pg}+0.7}\left(1+\frac{0.7}{h\,K_{pg}}\right)\tan^{-1}\sqrt{\frac{h\,K_{pg}}{0.7}}\right]\right\} dx \qquad (7\text{-}17)$$

Figures 7-4 through 7-7 are the solutions for equation 7-17.

Throat Length of the Scrubber

For a venturi scrubber, most of the particle collection occurs in the venturi throat. From the results of the last chapter, for a well-designed scrubber there is only a slight difference between the grade efficiency curves of the venturi throat and the whole venturi. Thus, in the following design analysis, we will assume that particle collection only occurs in the venturi throat. This approach will give us a conservative design.

For particle collection in a venturi scrubber, the collection efficiency is predicted by equations (7-45 to 7-47). Figure 7-8 shows the graphical form of this equation. This figure applies both to the circular duct and the rectangular duct.

Under a specific operating condition, the performance of the venturi scrubber depends on the throat length as revealed by Figure 7-8. The longer the throat, the more efficient the scrubber. This dependence is more profound for larger particles, i.e., larger K_{po}. Thus, in designing a venturi scrubber, we should use a long throat. However, we should not use a longer throat than necessary because the pressure drop will increase with increasing throat length. The final choice of throat length should be a compromise of the two. A close inspection of Figure 7-8 reveals that a dimensionless throat length of 2 to 3 would be sufficient. Further increase in the

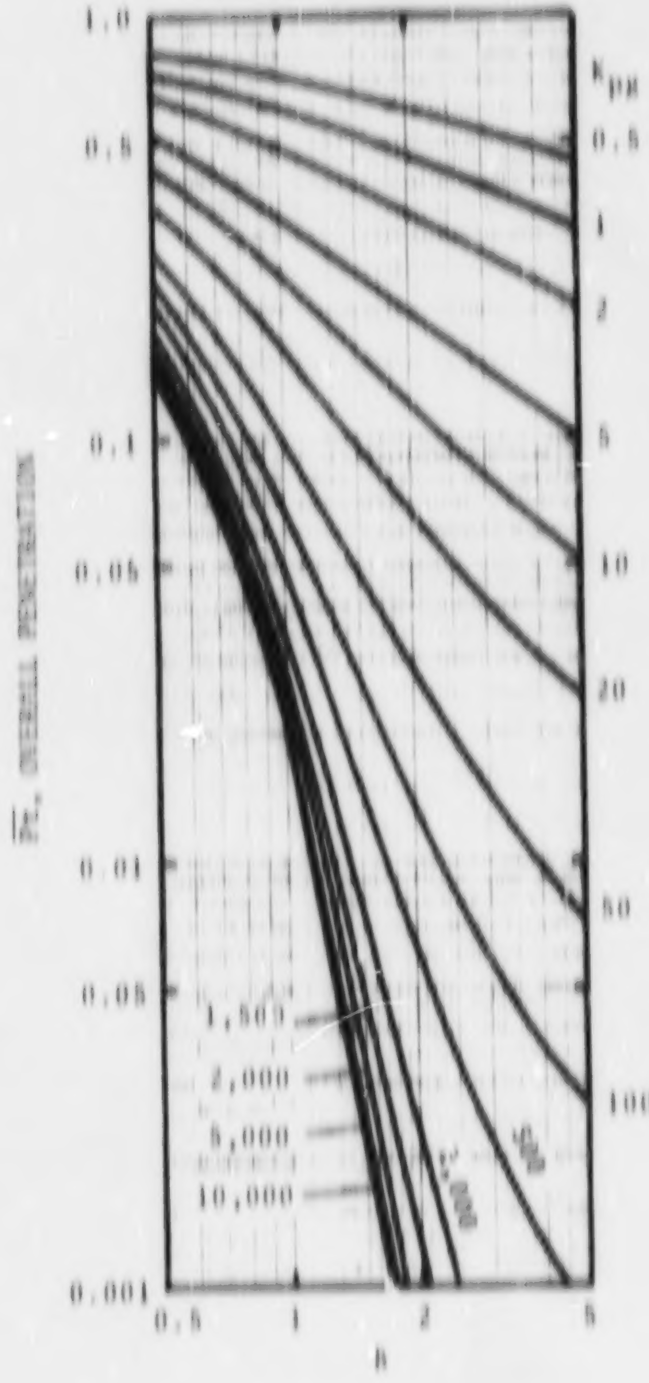

Figure 7-4. "$\overline{Pt}$" versus "B" with "K_{pg}" as parameter, "σ_g = 7.5".

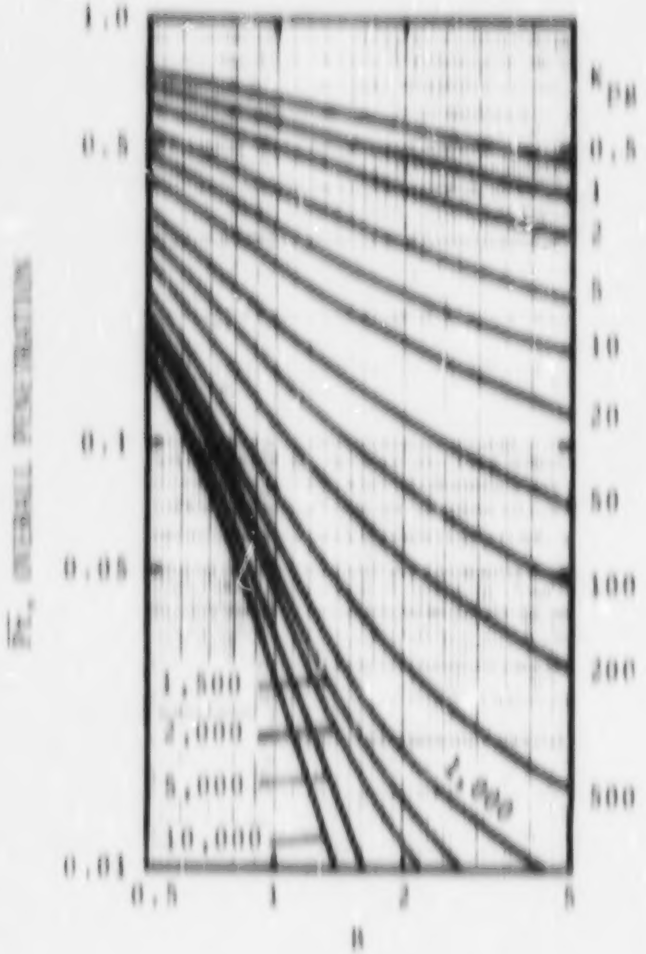

Figure 7-5. "$\overline{Pt}$" versus "B" with "K_{PB}" as parameter, "C_B = 5".

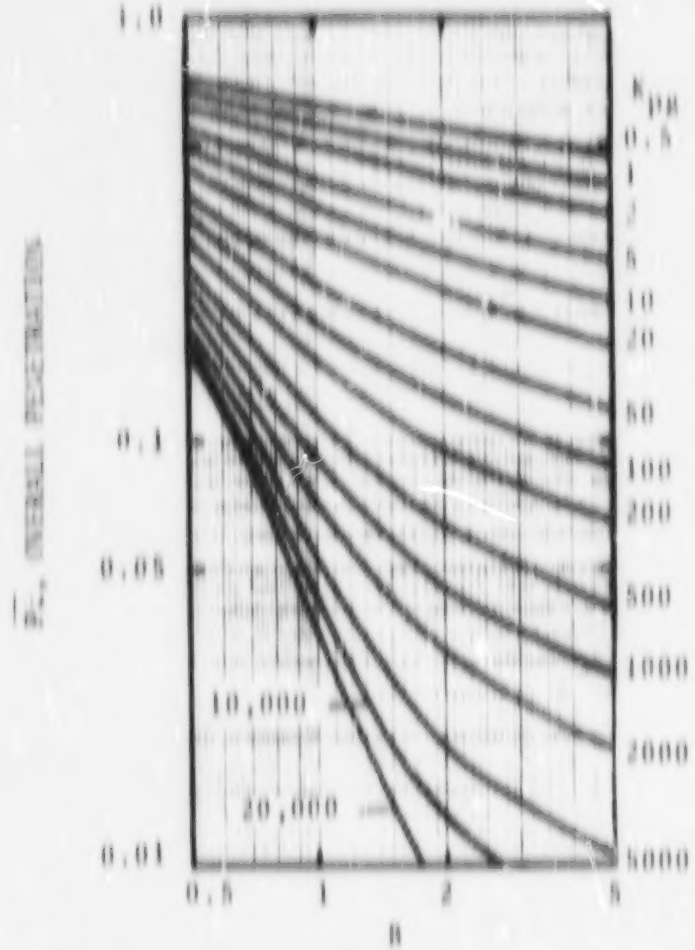

Figure 7-6. "$\overline{Pt}$" versus "R" with "K_{pg}" as parameter, "σ_g = 7.5".

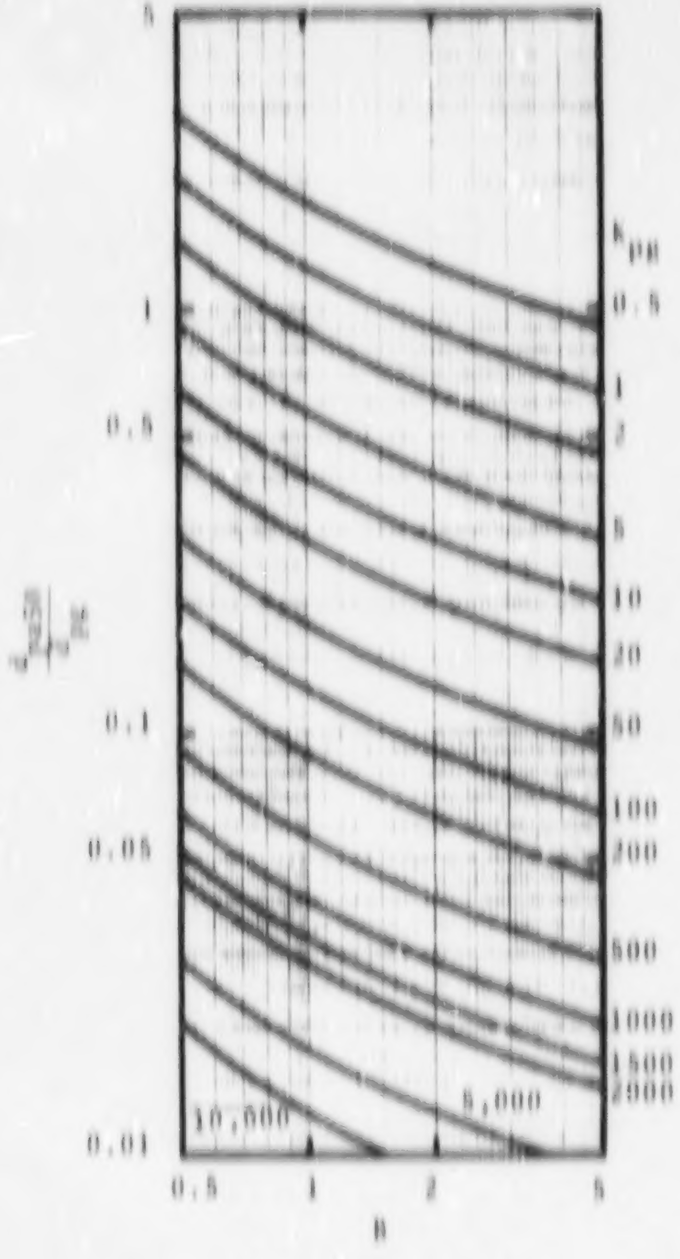

Figure 7-7. $\frac{d_{pa50}}{d_{pg}}$ versus "B" with "K_{pg}" as parameter.

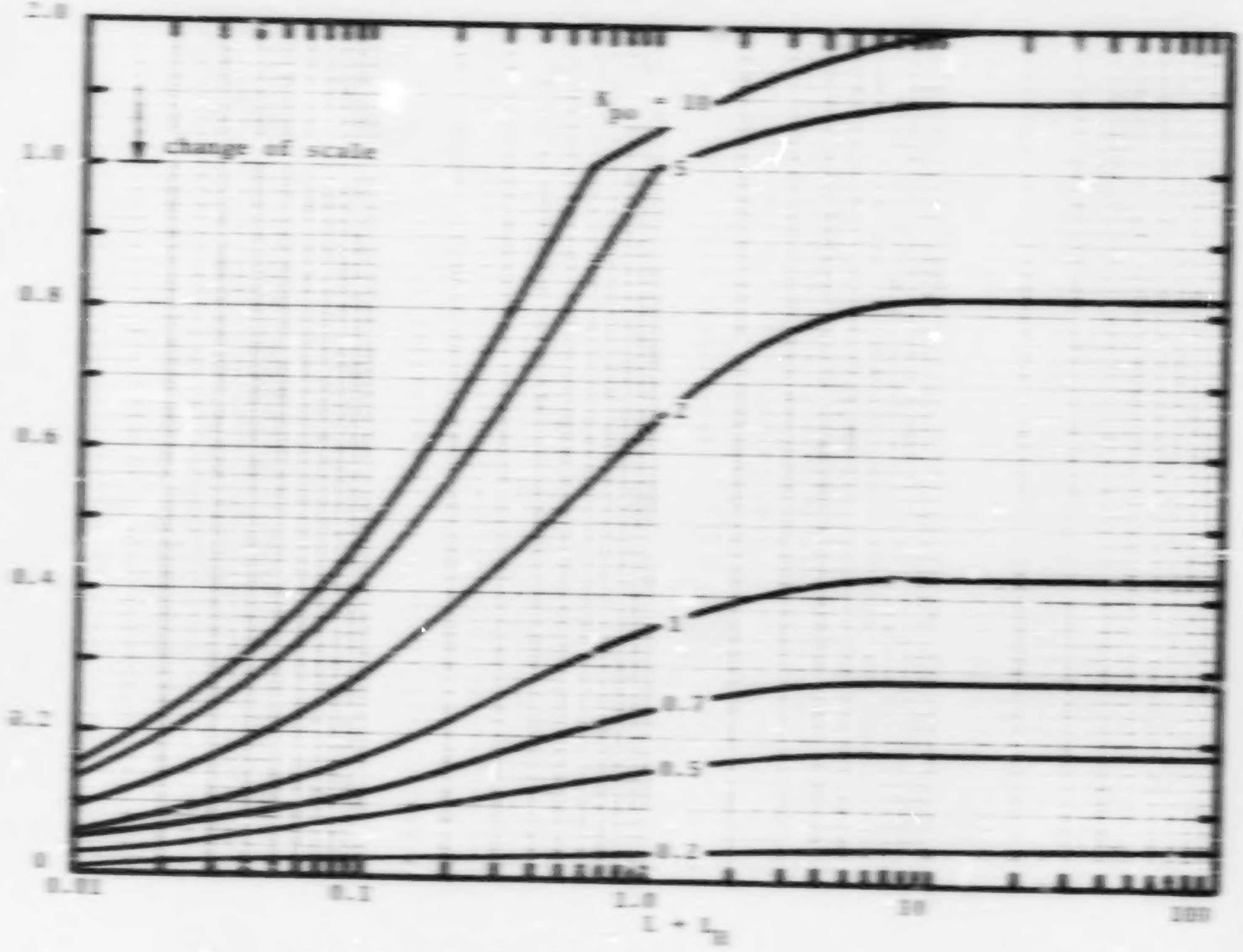

Figure 7-8. Effect of throat length on penetration.

dimensionless throat length will increase pressure drop with little gain in scrubber performance (Figure 7-9).

It is possible to predict the performance cut diameter, "d_{p50}" from Figure 7-8 if the scrubber operating condition is known. Figure 7-10 is a simplified plot of Figure 7-8. For an industrial-size venturi scrubber, "B" is usually larger than 1. As can be seen from Figure 7-10, the performance "K_{p50}" is almost constant for dimensionless throat length, "L", larger than 2, and "K_{p50}" becomes a function of "B" or liquid-to-gas mass flow-rate ratio. For a venturi scrubber with dimensionless throat length between 2 and 3, the correction factor "u_{de}" in the modified Calvert's pressure drop equation is approximately equal to 0.8. therefore, the expected pressure drop is

$$\Delta P \text{ (cm W.C.)} = 8.24 \times 10^{-4} \left[u_G \left(\frac{\text{cm}}{\text{sec}} \right) \right]^2 \left(\frac{Q_L}{Q_G} \right) \qquad (7\text{-}18)$$

Throat Velocity and Liquid-to-Gas Ratio

The principal collection mechanism occurring in a venturi scrubber is the collection by drops. It is a known fact that the target efficiency of a drop increases by decreasing the diameter and increasing the relative velocity between the gas and the drop. However, smaller drops accelerate faster than do bigger drops with the results that the relative velocity goes to zero earlier in the case of smaller drops. Consequently, there exists an optimum drop diameter for particle collection. Since atomized liquid drop diameter is a function of gas velocity and liquid-to-gas flow ratio, therefore, there exists an optimum combination of throat gas velocity and liquid-to-gas ratio.

Figure 7-11 shows the theoretical effect of throat gas velocity and liquid-to-gas flow rate ratio on the performance cut diameter of the venturi scrubber. Properties

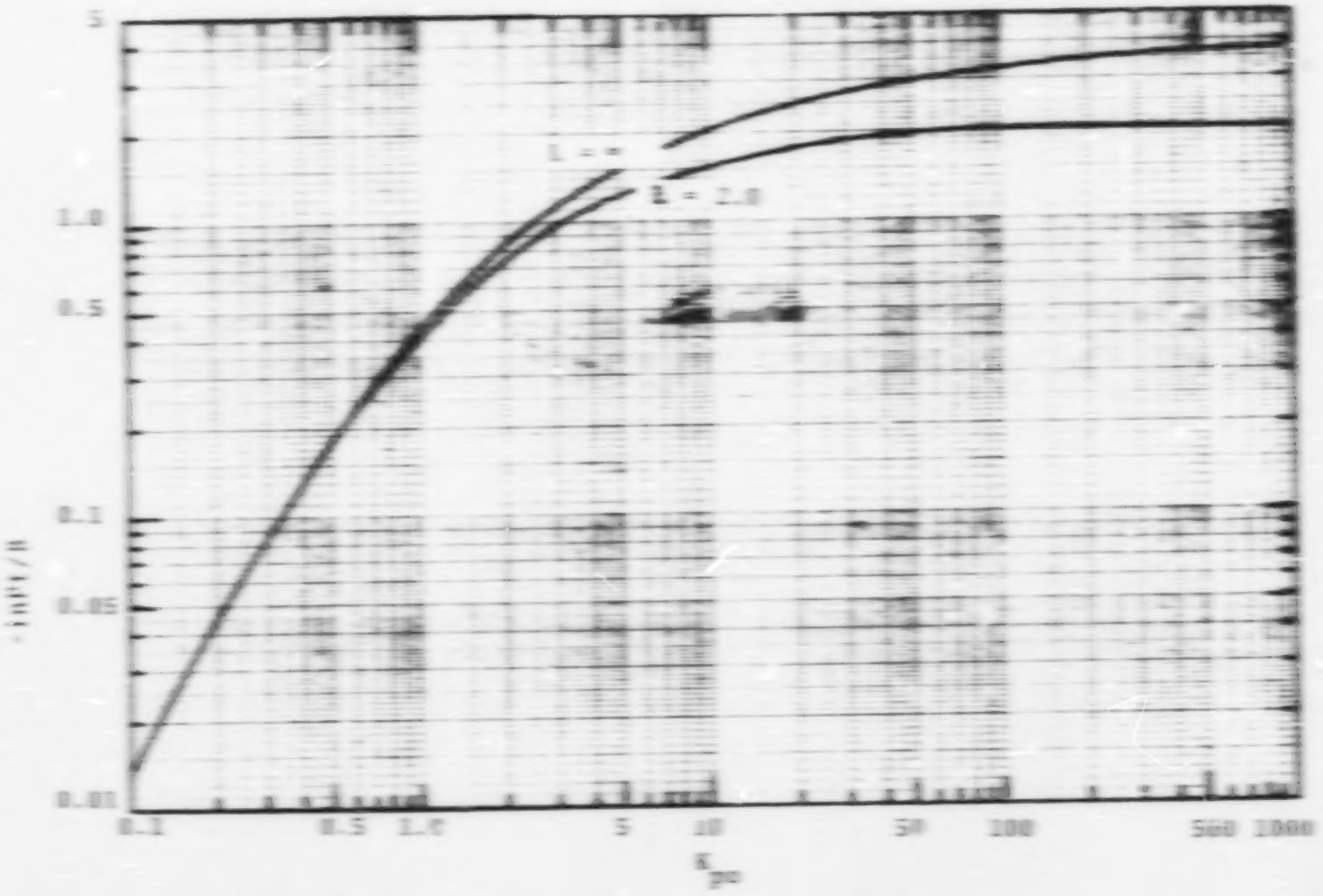

Figure 7-9. Effect of throat length on performance.

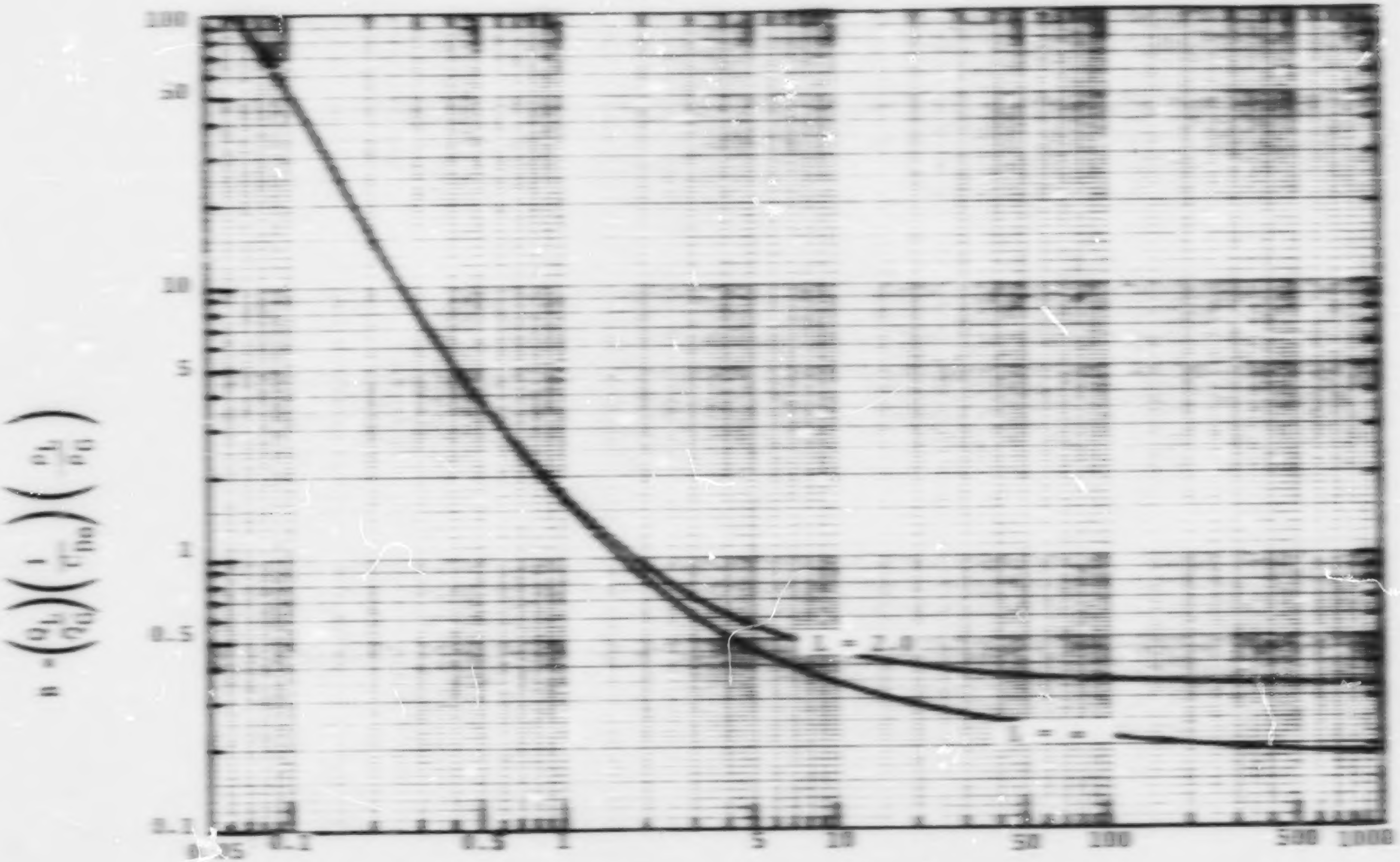

$$K_{po} = \frac{(d_{pa50})^2 u_G}{9 \mu_G d_d}$$

Figure 7-10. Predicted Venturi scrubber performance K_{po} vs. B.

of air and water at room temperature were used to construct this figure. For other liquid/gas combinations and conditions, one should construct different plots.

Optimum liquid drop diameter can easily be obtained from Figure 7-11. For instance, if the gas throat velocity is known, then the optimum drop diameter will be that which gives the smallest aerodynamic cut diameter.

If the scrubber required performance cut diameter is known, optimum throat velocity and gas-to-liquid ratio can be determined from Figure 7-11. Figure 7-12 shows the relationship between "B" and "K_{p50}". This curve was calculated from equation (7-8) and is applicable to all scrubber operating conditions. From this graph, we can calculate the anticipated cut diameter and pressure drop for various throat velocity and liquid-to-gas ratio combinations. Figure 7-13 shows such a calculation for air-water system at 25°C. Figure 7-14 is the cut diameter-pressure drop relationship with water flow rate as parameter for this system.

Design Procedure

The information presented in this chapter allows one to design a venturi scrubber to meet a required "Pt". The general method does not use Figures 7-13 and 7-14 since they represent the specific case of an air-water system at 25°C. If the conditions are close to those for these two figures then the procedure is simplified.

The general procedure is as follows:

1) Determine required cut diameters: First find the aerodynamic geometric mass mean diameter of the incoming dust at the temperature expected in the venturi. Then, construct a plot of K_{pg} vs d_{pa50} (required) by,

a) Obtaining several K_{pg} - B pairs using Figures 7-4 to 7-6 (depending on σ_g).

b) Knowing d_{pg}, obtain d_{pa50} for each of the K_{pg} - B pairs using Figure 7-7.

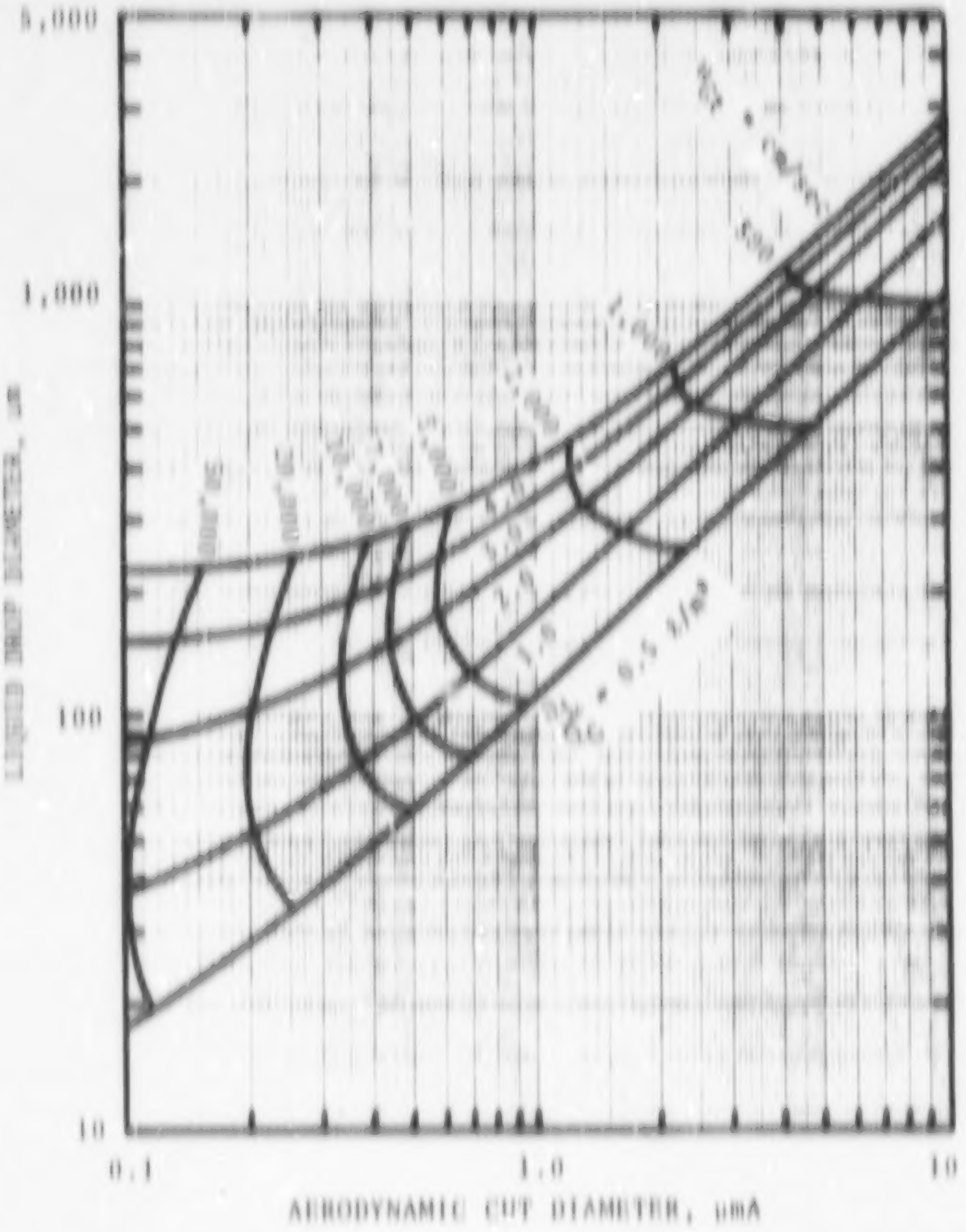

Figure 7-11. Effect of gas velocity and liquid to gas flow rate ratio on performance cut diameter.

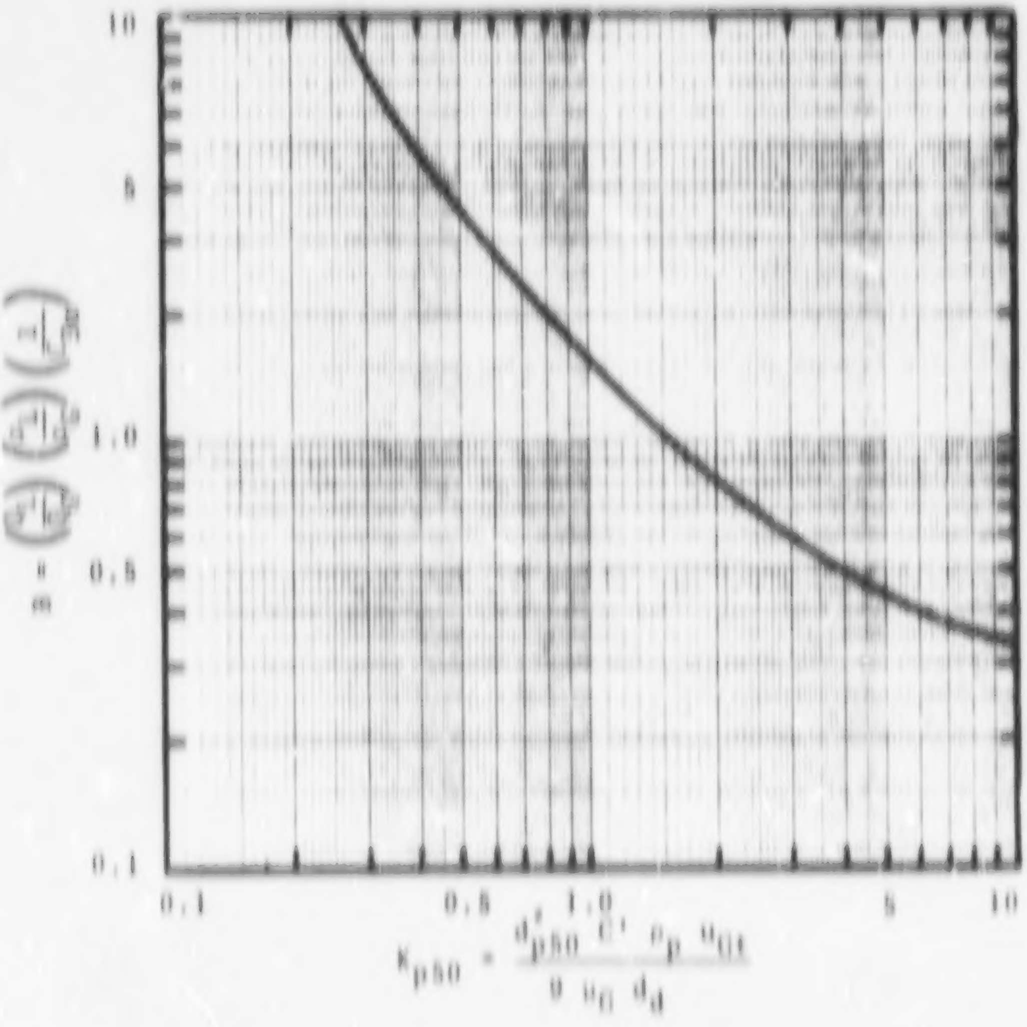

Figure 7-12. "B" vs "K_{p50}" for venturi throat of infinite length.

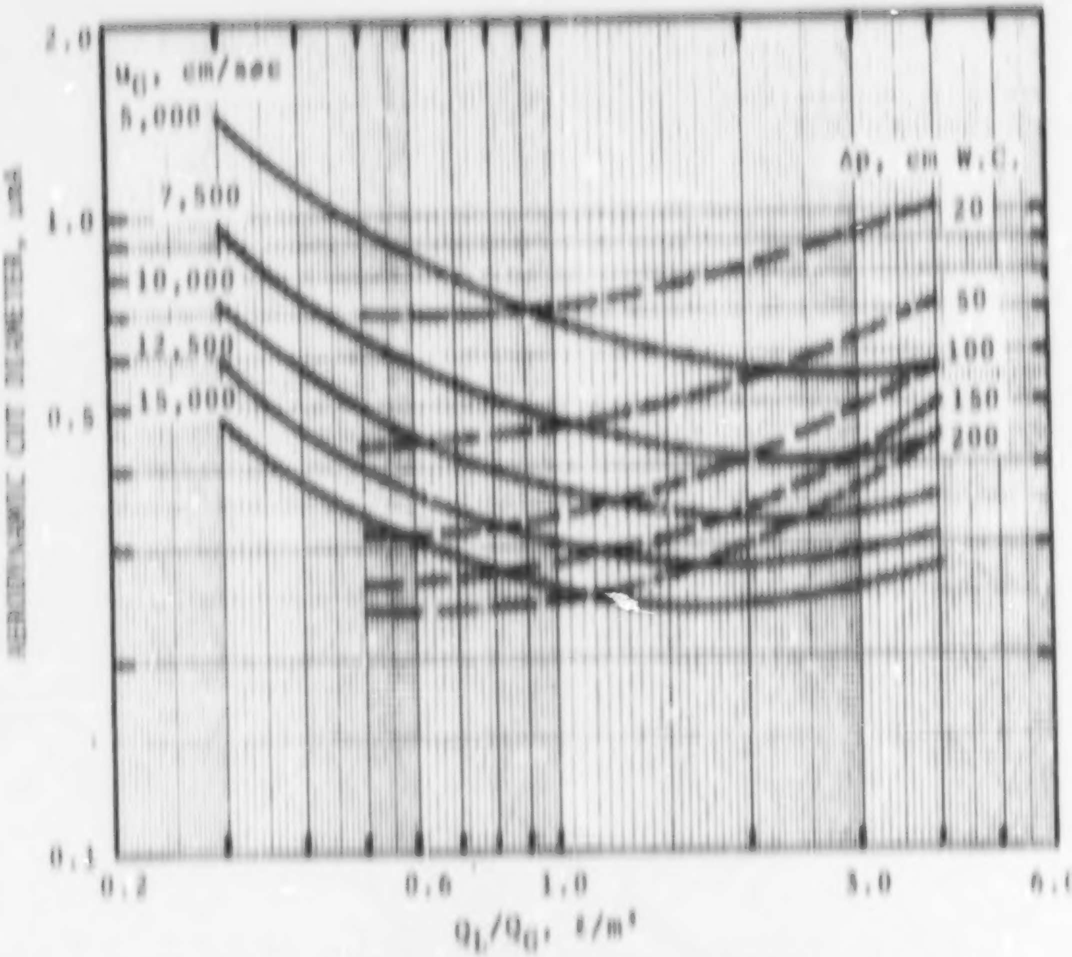

Figure 7-15. Predicted venturi performance, "d_{pa50}" vs. Q_L/Q_G with "u_G" and "ΔP" as parameter.

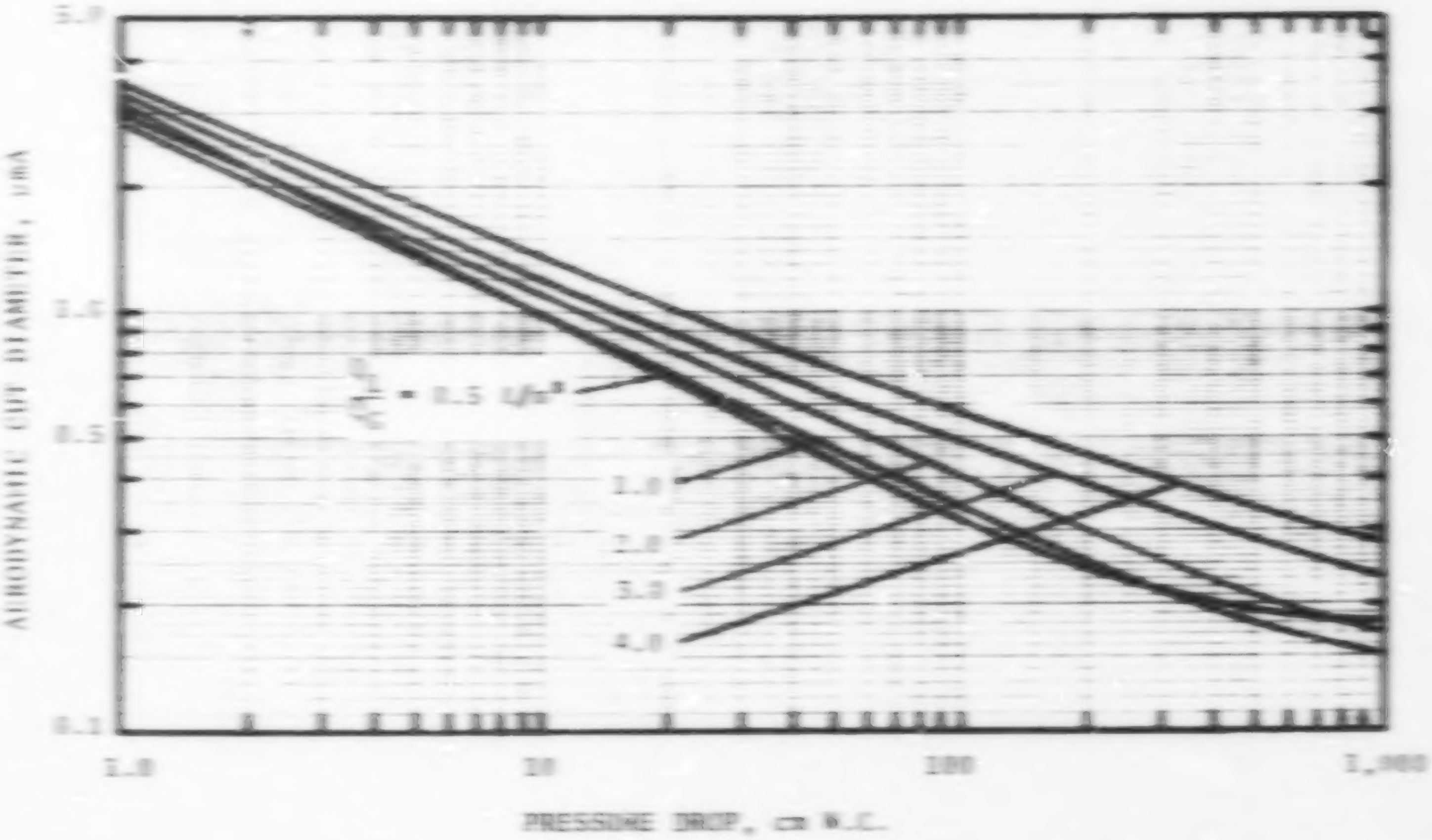

Figure 7-34. Aerodynamic cut diameter versus pressure drop with liquid to gas ratio as parameter.

2) Determine performance cut diameters: First determine viscosities, densities, and Nukiyama-Tanasawa coefficients for the venturi conditions. Then construct a number of performance curves corresponding to different Q_L/Q_G ratios as follows:

a) Select a "u_{Go}"
b) Drop diameter, d_d, from Nukiyama-Tanasawa relation (Table 5-2)
c) N_{Reo} from equation (5-7)(assuming $u_{do}=0$)
d) C_{Do} from equation (5-8)
e) Parameter B from equation (5-22) (assuming $u_{do}=0$)
f) K_{pss} from Figure 7-12
g) d_{pass} from equation (7-9)
h) K_{pg} from equation (7-13)
i) ΔP from equation (7-18)

Repeat steps (a) through (i) for several velocities. Plot performance K_{pg} vs d_{pass} curves on the same plot as the requirement curve from Step (1). Plot ΔP vs d_{pass} on a separate graph.

3) Determine required pressure drops: The intersections of the requirement and performance curves determine the proper design points. The corresponding pressure drops required can then be found from the plot of ΔP vs d_{pass}. The required pressure drops will correspond to a certain Q_L/Q_G ratios so that the fan costs versus the water and pumping costs can be compared to allow selection of the optimum design.

4) Determine throat cross-sectional area: Using the selected optimum combination of ΔP and Q_L/Q_G proceed as follows,

a) From the design K_{pg} solve equation 7-12a for u_{Gt} as a function of d_d.

b) Substitute this equation for d_d into the Nukiyama-Tanasawa relation and solve for u_{Gt}.

c) Divide the volume flow rate by u_{Gt} to get the throat cross-sectional area.

5) Determine throat length: Using the design velocity, perform steps (2a-d) and then, solve equation (5-47) for ℓ_t based on the desired L (2 to 3).

6) Determine convergence, divergence angles: These have little effect on particle collection but they do have some effects on pressure drop. Of the two, divergence angle is more important. Divergence angle should be designed such that,

a) Boundary layer separation does not occur

Momentum recovery occurs in the divergent section

The general procedure would be facilitated by use of a programmable calculator or a digital computer. As a check, or if the conditions are close to those of an air-water system at 25°C, Figures (7-11) and (7-14) can be used in an almost purely graphical procedure.

The graphical procedure is as follows (air-water at 25°C),

1) Determine required cut diameter: Same as general procedure.

2) Determine performance cut diameter: Use Figure 7-11 and equation (7-12a) to calculate the performance d_{pa50} vs K_{pg} curves for various Q_L/Q_G ratios.

3) Determine required pressure drops: Same as general procedure except use Figure 7-14 to find required pressure drop.

Steps (4-8) same as general procedure.

Venturi Design Example

The problem of designing a venturi scrubber to control dust from a typical asphalt plant dryer is illustrated.

The dust has a log-normal distribution of diameters described by a geometric standard deviation, σ_g = 5.0 and a geometric mass mean particle diameter, d_{pg} = 18 µm (physical). The particle density is 2.6 g/cm³. The flue gas flow rate is 567 Am³/min with a gas temperature of 116°C. The uncontrolled emission rate is 2,310 kg/hr.

Based on a local Air Pollution Control District rule for the amount of weight processed, the emission should not exceed 25 kg/hr. The required efficiency is then: (2,310-25)/2,310 x 100 = 98.9%. Thus, the design should meet an efficiency requirement of 99%.

Step 1. Specifying the required cut diameters: First, the aerodynamic geometric mean diameter must be found. For air at 116°C the Cunningham slip correction factor for 18 µm particles is C' = 1.013. Thus,

$$d_{pga} = 18\ (1.013 \times 2.6)^{0.5} = 29.2\ \mu mA$$

Next, a plot of the required cut diameters (d_{pa50}) for an overall penetration of 0.01 is made by using Figures 7-5 and 7-7. The points which are shown in Figure 7-15 as circles are listed below:

B	K_{pg}	d_{pa50} µmA
4.5	1,000	0.64
2.8	1,500	0.58
2.2	2,000	0.55
1.6	5,000	0.41
1.4	10,000	0.30

Step 2. Specifying the performance cut diameters: First the flow parameters must be found. For air at 116°C and water at 25°C,

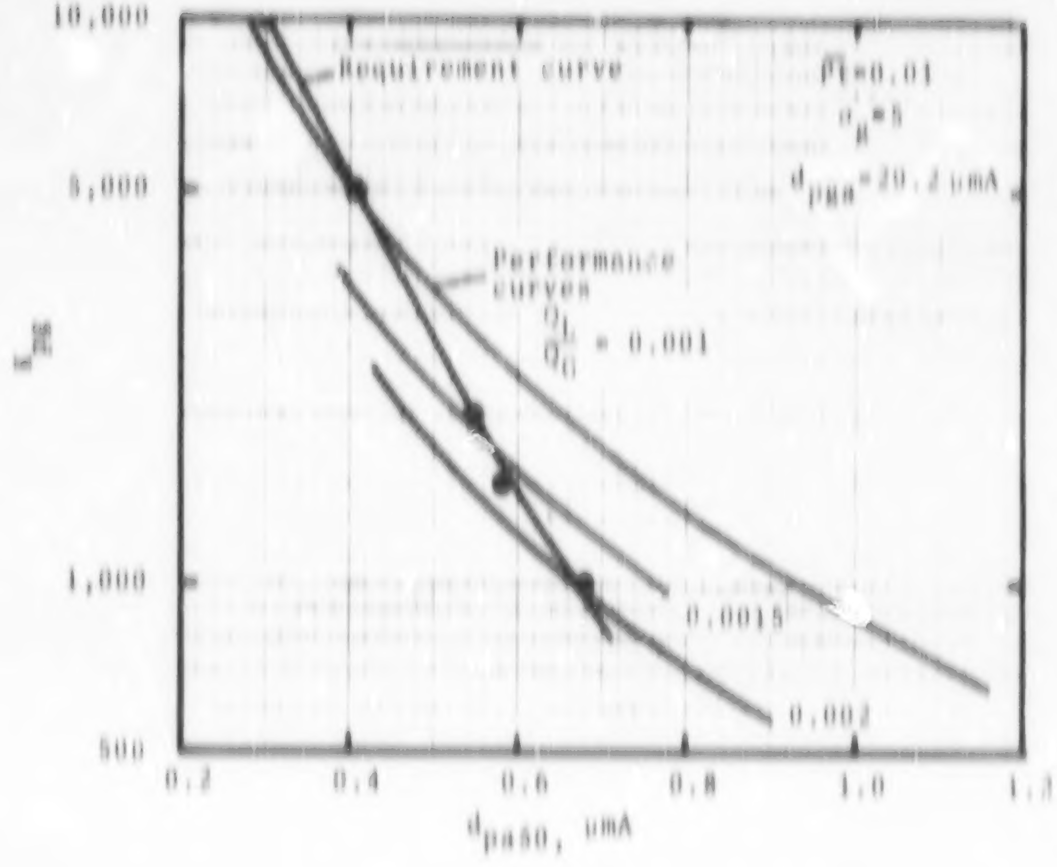

Figure 7-15. Impaction parameter vs aerodynamic cut diameter for a venturi design.

Gas Viscosity, μ_G = 2.23 x 10^{-4} g/cm·sec
Gas density, ρ_G = 0.907 kg/m³
Gas kinematic viscosity, ν_G = 0.246 cm²/sec
Liquid density, ρ_L = 997 kg/m³
so,

$$\frac{\rho_L}{\rho_g} = 1{,}099$$

and the Nukiyama and Tanasawa equation for drop size reduces to,

$$d_d(\text{cm}) = \frac{50}{u_{Go}(\text{cm/sec})} + 87\left(\frac{Q_L}{Q_G}\right)^{1.5}$$

Other design equations to be used are,

$$N_{Reo} = \frac{u_{Go}\ d_d}{\nu_G} \qquad (5\text{-}7)$$

$$C_{Do} = 0.22 + \frac{24}{N_{Reo}}\,(1 + 0.15\ N_{Reo}^{0.6}) \qquad (5\text{-}8)$$

$$B = \frac{1}{C_{Do}}\ \frac{Q_L}{Q_G}\ \frac{\rho_L}{\rho_G} \qquad (5\text{-}22)$$

$$K_{pss} = 0.2087 + \frac{0.946}{B} + \frac{0.48}{B^2}$$

0.5 ≤ B ≤ 5
(Based on Figure 7-12)

$$d_{pass} = \left(\frac{9\ K_{pss}\ \mu_G\ d_d}{10^4\ u_{Go}}\right)^{0.5} \times 10^4 \quad (\mu\text{mA}) \quad (7\text{-}3)$$

$$K_{pg} = K_{pss}\left(\frac{d_{pg}}{d_{pass}}\right)^2$$

and

$$\Delta P = 8.24 \times 10^{-5}\ u_{Go}^2\left(\frac{Q_L}{Q_G}\right)$$

Solution of these equations for various $\frac{Q_L}{Q_G}$ and u_{Go} can be greatly facilitated by use of a programmable calculator.

The solution to the design equations are plotted on Figures 7-15 and 7-16 for Q_L/Q_G ratios of 0.001, 0.0015, and 0.002.

Step 3. Determine the required pressure drops: The intersections of the performance lines with the requirement line in Figure 7-15 determine the cut diameters (both required and performance). These cut diameters are represented on Fig. 7-16 as triangles. The required pressure drops corresponding to these cut diameters are then,

$\frac{Q_L}{Q_G}$	d_{pass} μmA	ΔP cm W.C.
0.001	0.42	67
0.0015	0.57	40
0.002	0.675	32

Based on the flue-gas rate of 567 Am³/min these Q_L/Q_G ratios represent water requirements of 0.57 m³/min (150 gal/min) 0.87 m³/min (225 gal/min) and 1.13 m³/min (300 gal/min), respectively. Based on pump and water costs versus fan costs the designer can select the optimum design.

Step 4. Determine throat cross-sectional area. In order to carry out the calculation illustration we will assume that Q_L/Q_G = 0.002 and d_{pass} = 0.675 μmA is the optimum. From Figure 7-15 the required K_{pg} = 980.

$$K_{pg} = \frac{d_{pg}^2 u_{Gt}}{9 \mu_G d_d} = 980$$

$$u_{Gt} = \frac{9(980)(\mu_G)(d_d)}{d_{pa}^2} = \frac{9(980)(2.23 \times 10^{-5})d_d}{(29.2 \times 10^{-5})^2}$$

$$= 2.3 \times 10^5 d_d$$

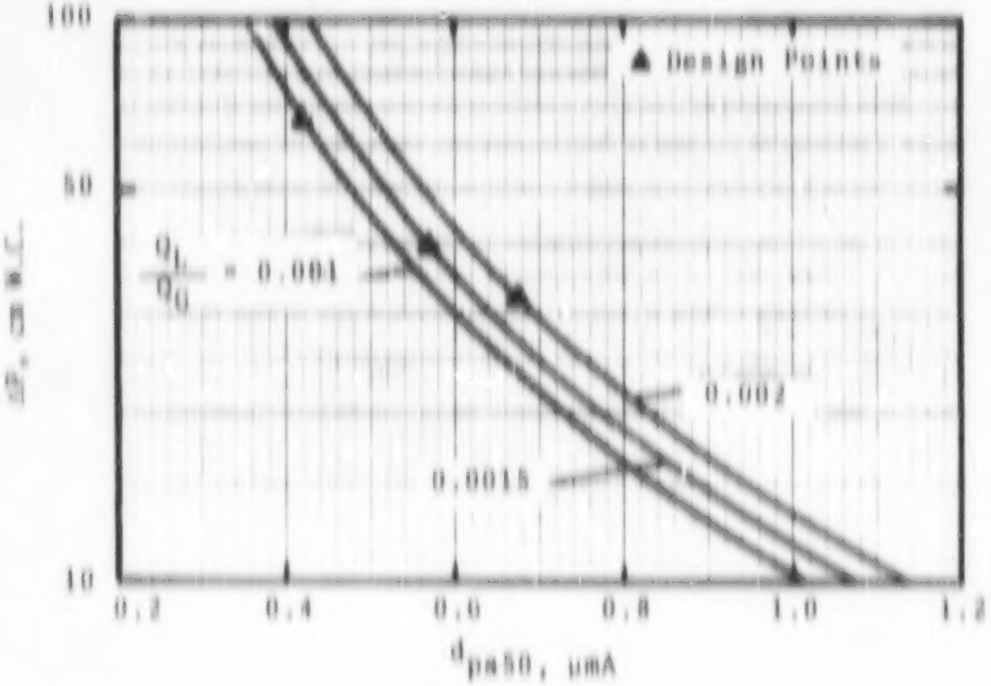

Figure 7-16. Pressure drop vs aerodynamic cut diameter for venturi design example.

From the Nukiyama-Tanasawa correlation for the present example,

$$d_d = \frac{50}{u_{Gt}} + 87\left(\frac{Q_L}{Q_G}\right)^{1.5} = \frac{50}{u_{Gt}} + 7.78 \times 10^{-3}$$

Substituting into the expression for "u_{Gt}" we have,

$$u_{Gt} = 2.3 \times 10^{5}\left[\frac{50}{u_{Gt}} + 7.78 \times 10^{-3}\right]$$

$$u_{Gt} = 5{,}300 \text{ cm/sec}$$

Throat cross-sectional area $= \frac{567 \times 10^{6}}{(60)(5300)} = 1{,}783 \text{ cm}^2$

Step 5. Determine throat length:

$$d_d = \frac{50}{5300} + 7.78 \times 10^{-3} = 0.0172 \text{ cm}$$

$$N_{Re} = \frac{u_{Gt}\, d_d\, \rho_G}{\mu_G} = \frac{(5300)(0.0172)(9.07 \times 10^{-4})}{2.23 \times 10^{-4}} = 370$$

$$C_{Do} = 0.62$$

Therefore, throat length $= \left(\frac{2}{3}\right)\left(\frac{0.0172}{0.62}\right)\left(\frac{1}{9.07 \times 10^{-4}}\right)(L)$

$$= 20.3L \text{ cm}$$

If design L = 2, then throat length = 40.6 cm

Suppose the gas temperature was 25°C, then the previously constructed performance curves (Figures 7-11 and 7-13) could be used.

__Step (1)__:

At 25°C $C' = 1.009$ for $d_p = 18$ μm so, $d_{pa} = 18 (1.009 \times 2.6)^{1/2} = 29.2$ μmA. Since this is the same d_{pa} as before, the $K_{pg} - d_{pa50}$ requirement pairs are the same.

__Step (2)__:

Using Figure 7-11 and the equation for K_{pg}, Figure 7-17 is generated. The shaded triangles represent the design points where the performance and required K_{pg}'s match. Thus the results, using Figure 7-14 are

$\frac{Q_L}{Q_G}$, ℓ/m³	d_{pa50} μmA	ΔP cm W.C.
1.03	0.30	140
1.1	0.41	74
1.55	0.55	44
1.85	0.58	40
2.8	0.64	44

These results are close to what we obtained using the general procedure and a higher temperature gas.

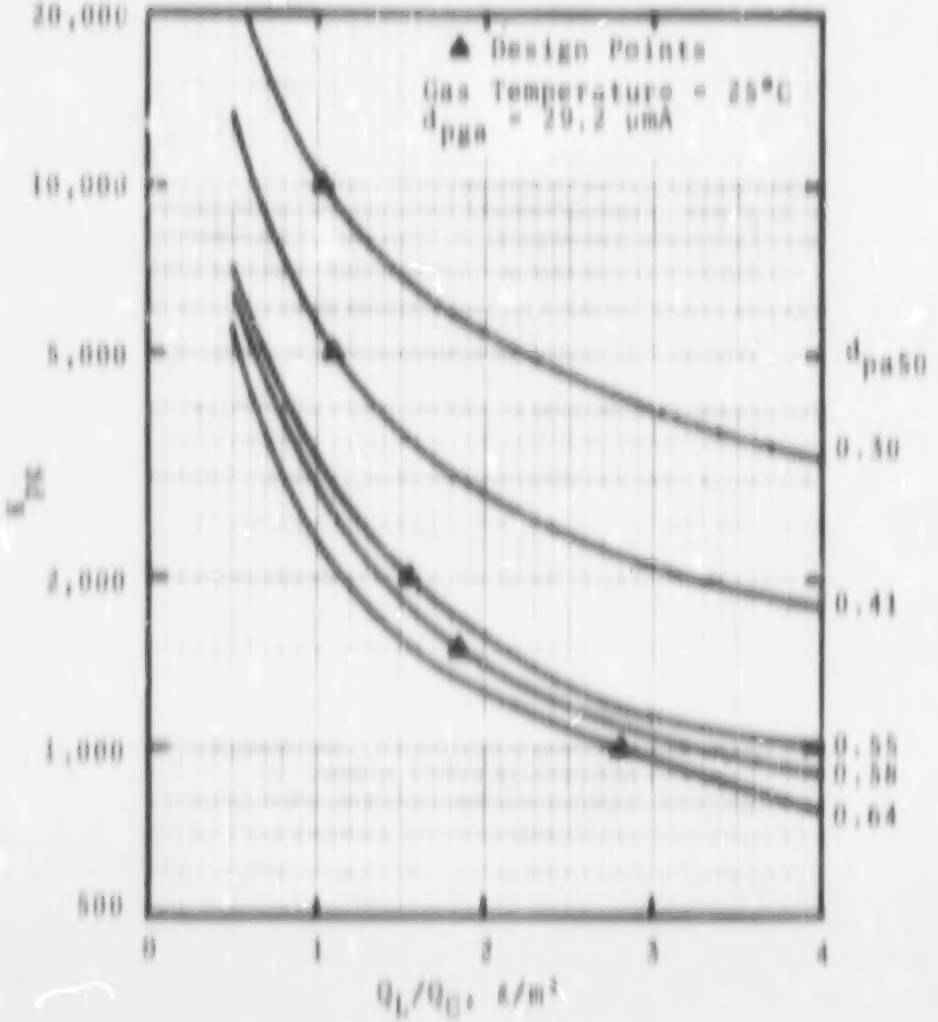

Figure 7.17. Impaction parameter vs Q_L/Q_G for venturi design example.

CHAPTER 8

ENTRAINMENT SEPARATOR

All scrubber systems include an entrainment separator, either as an integral part of the scrubber configuration or as a separate, clearly identifiable device. There are a number of devices which are commonly used as entrainment separators. Zigzag baffles, knitted mesh, packed beds, cyclone separators, and guide vanes causing rotation of the gas stream are frequently used for this purpose. Calvert et al (1975) had performed a detailed study of entrainment separators. The following is an abstract of their study.

ENTRAINED LIQUID INFORMATION

In order to design a proper entrainment separator, or to predict the collection efficiency of an entrainment separator, certain entrainment liquid information is needed. This includes:

1. Entrainment drop and size distribution.
2. Quantity or inlet loading.

An extremely important factor in choosing and designing an entrainment separator is drop size distribution. Different entrainment separators are limited to certain drop diameters, below which their efficiency falls off sharply. The size of the drops depends upon the way they were formed.

Entrainment rate and size distribution data for gas atomized spray scrubbers such as venturis have not been reported. Estimates can be made, as discussed below, but they are very rough because of uncertainties in predicting the characteristics of the initial atomization and the drop separation occurring within the venturi diffuser and similar flow elements.

Drop diameter can be predicted by means of the correlation by Nukiyama and Tanasawa (1938-40). For air and water at standard conditions the N+T correlation for Sauter mean diameter is:

$$d_s(\text{cm}) = \frac{50.0}{u_G(\text{cm/sec})} + 92.0\left(\frac{Q_W}{Q_G}\right)^{1.5} \qquad (8\text{-}1)$$

where: d_s = Sauter (volume-surface) mean diameter of drops, cm
u_G = air velocity relative to drops, cm/s
Q_W = water flow rate, m^3/s
Q_G = air flow rate, m^3/s

According to Steinmeyer in Perry (1973), the Sauter mean diameter is typically 70% to 90% of the mass median diameter. If the drop size distribution is log normal, this implies that the geometric standard deviation, "σ_g" is about 1.6 for 90% and 2.5 for 70%.

To illustrate the application of the above to the prediction of entrainment characteristics for a venturi scrubber, we can consider the case of a throat air velocity of 100 m/sec and water to air ratio of 1 ℓ/m^3 ($10^{-3} m^3/m^3$). The gas pressure drop would be about 80 cm W.C. and the Sauter mean diameter computed from equation (8-1) is 79 µm. From the typical ratios of mass median to Sauter diameter, we would expect the mass median drop diameter to range from 88 to 113 µm, with "σ_g" from 1.6 to 2.5, respectively. One would therefore predict that the cumulative entrainment concentration would be related to drop diameter within the range of high and low values tabulated on the following page.

Drop diameter, μm	4	5	10	15	20
High concentration, cm^3/m^3	0.035	0.11	2	8	20
Low concentration, cm^3/m^3	-	-	0.0025	0.06	0.6

If the entrainment contained 10% solids by weight, the residual particle concentrations after evaporation would be such that if one wanted to limit the particle loading due to entrainment to 0.01 g/m^3(0.0044 gr/ft^3) the separation of all entrainment larger than 5 μm diameter for the high estimate and 16 μm diameter for the low would be required. Since particle loadings of this magnitude can be significant for plume opacity, the example shows the efficiency with which entrainment must be controlled and the necessity for good data on entrainment size distribution and concentration.

DESIGN EQUATIONS FOR ENTRAINMENT SEPARATORS

The design and operation of most entrainment separators are governed by three factors:

1. Pressure drop
2. Collection efficiency
3. Reentrainment velocity and reentrainment rate

Knowledge of the pressure drop through a separation system is important in calculating the energy loss incurred and in selecting the proper pumps and other auxiliary equipment to overcome that energy loss.

Collection efficiency or overall collection efficiency is defined as the fractional collection of the droplets by the separator, i.e.

$$\eta = 1 - \frac{\text{effluent concentration}}{\text{influent concentration}}$$

When the gas velocity in the entrainment separator is high, some separated droplets in the separator will be reentrained in the gas stream. Because of this reentrainment, the observed collection efficiency of the separator is less than the primary collection efficiency which is defined as the efficiency an entrainment separator would have if reentrainment were not present.

Reentrainment velocity is the gas velocity at which drops are first observed to become reentrained in the gas. The onset of reentrainment will vary for different kinds of entrainment separators and different operating conditions. Reentrainment velocity determines the maximum allowable gas velocity in the separator. Reentrainment rate and drop size distribution are needed for the prediction of emissions from the system.

Once design equations predicting the primary efficiency, pressure drop, and reentrainment are available, the operating characteristics of the entrainment separator can be established.

Six different kinds of entrainment separators will be discussed in this section: cyclone, packed bed, zigzag baffles, tube bank, mesh, and sieve plate.

Cyclone

The cyclone is the most commonly used entrainment separator for venturi scrubbers. Commercially available cyclones in standard designs for entrainment separators have a maximum capacity of up to 141 m^3/sec (300,000 CFM) of gas. Efficiencies of about 95% are claimed for 5 μm diameter drops in a well-designed cyclone. Some manufacturers use a bundle of small cyclones (multicyclones), which can efficiently collect drops as small as 2 μm in diameter. However, this arrangement reduces the capacity of the device.

Primary Efficiency - Leith and Licht (1971) derived an equation to predict primary collection efficiency in conical bottom cyclones as pictured in Figure 8-1. With slight modification it can be applied to cylindrical cyclones.

The equation for predicting primary collection efficiency is:

$$\ln Pt = -2\left[\frac{\rho_d}{9\mu_G}\left(\frac{2d_d\ u_{tg}}{d_c}\right)^2 (n+1)t\right]^{\frac{1}{2n+2}} \qquad (8\text{-}2)$$

where:

$$n = 1 - \left[\frac{T}{283}\right]^{0.3}\left[1 - \frac{(0.393\ d_c)^{0.14}}{2.5}\right] \qquad (8\text{-}3)$$

Pt = penetration, fraction
ρ_d = drop density, g/cm³
μ_G = gas viscosity, poise
d_d = drop diameter, cm
u_{tg} = tangential velocity, cm/sec
t = mean residence time of the gas in the cyclone, sec
d_c = cyclone diameter, cm

The mean residence time of the gas stream in the cyclone is:

$$t = \frac{V_e}{Q_G} \qquad (8\text{-}4)$$

where:

V_e = effective volume of the cyclone, cm³
Q_G = volumetric gas flow rate, cm³/sec
$= u_G A$

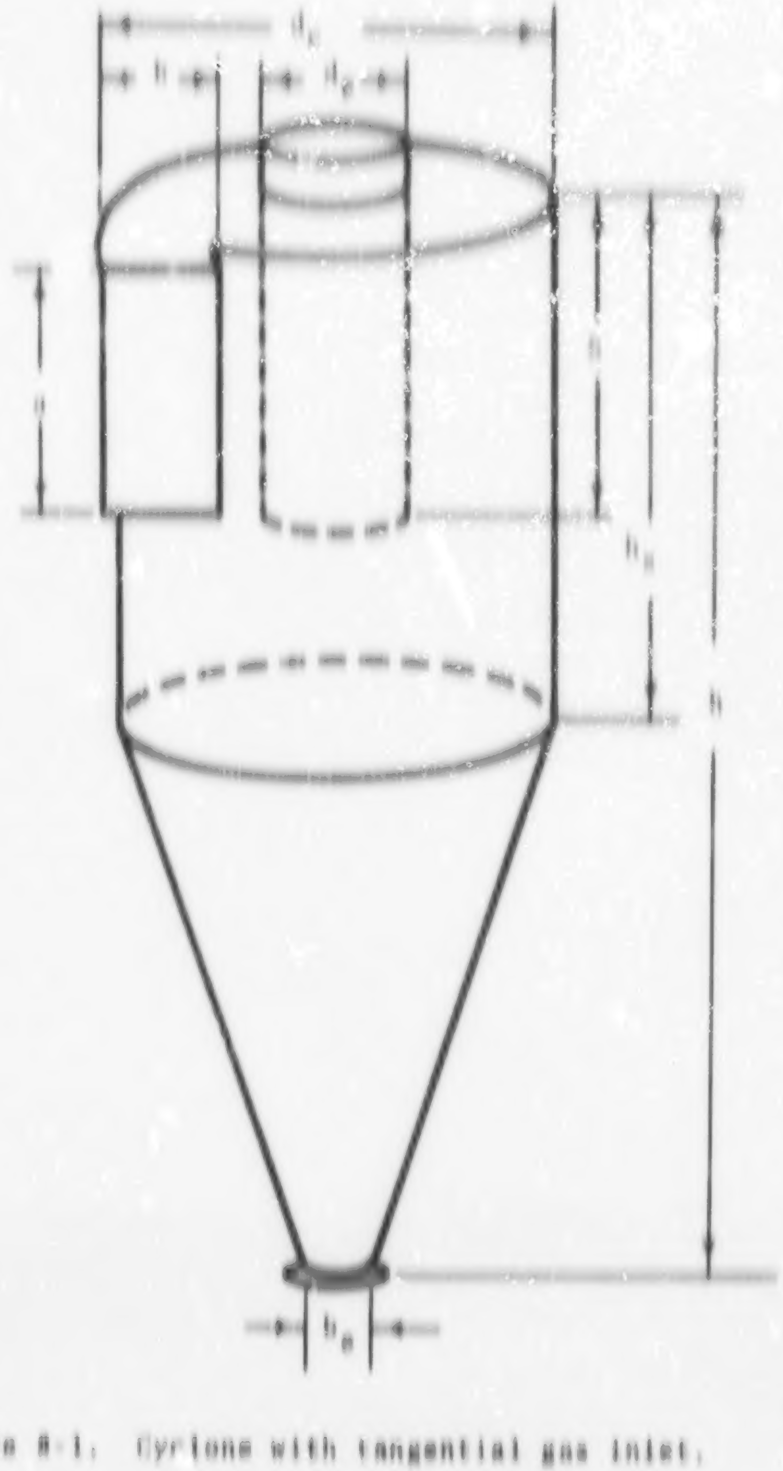

Figure 8-1. Cyclone with tangential gas inlet.

A = inlet area, cm²
u_G = inlet gas velocity, cm/sec

The effective volume of the cyclone, "V_e" is defined as the volume of the cyclone minus the volume occupied by the exit duct and exit gas core. The diameter of the exit gas core can be assumed equal to the diameter of the exit duct. Leith and Licht (1971) gave the following equations for the determination of effective volume of a conical bottom cyclone:

$$V_e = V_1 + 1/2\ V_2 \qquad (8\text{-}5)$$

where:

V_1 = annular shaped volume above exit duct inlet to mid-level of entrance duct

$$= \frac{\pi}{4}\left(S - \frac{a}{2}\right)\left(d_c^2 - d_e^2\right) \qquad (8\text{-}6)$$

V_2 = volume of cyclone below exit duct inlet to the natural length of the cyclone

$$V_2 = \frac{\pi d_c^2}{4}\left(h_s - S\right) + \frac{\pi\left(L+S-h_s\right)d_c^2}{12}\left(1 + \frac{d}{d_c} + \frac{d^2}{d_c^2}\right) - \frac{\pi d_e^2 L}{4} \qquad (8\text{-}7)$$

where:

$$d = d_c - \left(d_c - B_c\right)\left(\frac{S+L-h_s}{H-h_s}\right) \qquad (8\text{-}8)$$

and L = natural length of the cyclone

$$= 2.3d_e \left(\frac{d_c^2}{ab}\right)^{1/3} \qquad (8\text{-}9)$$

a, b, d_c, d_e, S, h, h_s are cyclone dimensions defined in Figure 8-1.

Pressure Drop-Shephard and Lapple (1940) derived an equation for a cyclone with inlet vanes for pressure drop as a function of inlet gas velocity and the cyclone inlet and outlet dimensions:

$$\Delta P = 0.000513\ \rho_G \left(\frac{Q_G}{ab}\right)^2 \left(\frac{7.5\ ab}{d_e^2}\right) \qquad (8\text{-}10)$$

where:

ΔP = pressure drop, cm W.C.
ρ_G = gas density, g/cm³
Q_G = gas volumetric flow rate, cm³/sec
a = cyclone inlet height, cm
b = cyclone inlet width, cm
d_e = cyclone exit pipe diameter, cm

Equation (8-10) can be modified by writing it as a function of the geometric average of the gas velocity at the cyclone inlet and outlet:

$$\Delta P = 0.000513\rho_G v_{Ave}^2 \qquad (8\text{-}11)$$

Shepard and Lapple also developed an equation for a cyclone without inlet vanes:

$$\Delta P = 0.000513\rho_G \left(\frac{Q_G}{ab}\right)^2 \left(\frac{16ab}{d_e^2}\right) \qquad (8\text{-}12)$$

Packed Bed

Packed beds of standard design with a capacity of up to 65 m^3/sec (140,000 CFM) are available. They can remove drops as small as 3 μm in diameter at 80-90% efficiency. Superficial gas velocities range from 75 to 240 cm/sec, and pressure drop is generally low, 0.05-0.1 cm W.C. per cm of bed length.

Cross flow beds are claimed to have high drainage efficiency and therefore are less prone to plugging. Upstream washing is recommended to avoid plugging if solids are present in the drops to be removed.

Packing in different materials, shapes and sizes is available. Various rings are claimed to have high collection efficiency and low pressure drop.

Packed beds are often used for mass transfer because of their high interfacial area. Thus they are sometimes employed when simultaneous mass transfer and entrainment separation are desired.

Primary Efficiency - Jackson and Calvert (1966) and Calvert (1968) have developed a theoretical relationship between particle collection efficiency and packed bed operating parameters:

$$Pt = 1 - \exp\left[\frac{-\pi}{2(j+j^2)\ (\varepsilon - H_d)}\ \frac{Z}{d_c}\ K_p\right] \qquad (8\text{-}13)$$

$$K_p = \frac{\rho_p\ d_d^2\ u_G}{9\ \mu_G\ d_c}$$

where:

j = ratio of channel width to packing diameter
H_d = fractional liquid hold-up in the bed
ε = bed porosity, fraction (Table 8-1)
Z = bed length, cm

d_c = packing diameter, cm
u_G = superficial gas velocity, cm/sec
d_d = drop diameter, cm

The experimental data of Jackson (1964) were analyzed to determine appropriate values of "j" to use in equation (8-13) with all quantities in the equation known except "j", which was calculated. The results are given in Table 8-2 which lists "j" values for various types and sizes of packing material. For the manufactured packing materials, "j" is fairly constant at about 0.16-0.19. The very low value of 0.03 for coke may be due to the small passages within the coke itself, which make each large piece of coke function effectively as a number of smaller pieces.

Pressure Drop - Perry (1963) gives a generalized pressure drop and flooding correlation plot which appears as Figure 8-2, where a dimensional group of function $\frac{G^2 F \Psi \mu_L^{0.2}}{\rho_G \rho_L g}$, (centipoise) $^{0.2}$, is plotted against a dimensionless group of function $\frac{L}{G}\left(\frac{\rho_G}{\rho_L}\right)^{1/2}$, where "G" and "L" refer to the gas and liquid mass fluxes respectively. "Ψ" is the ratio of water density to entrained liquid density. Values for the packing factor, "F", for dumped pieces, stacked pieces and grids are given in Tables 8-3 and 8-4. If "F" is not known, $\frac{a}{\epsilon}$, may be used instead.

Tube Bank

Tube banks made of streamlined struts have been used as entrainment separators but no experience with round tubes has been reported. Particle collection efficiency and pressure drop for round tube banks have been studied and the characteristics appeared promising for entrainment separation application.

TABLE 8-1

BED POROSITY, ε, FOR VARIOUS PACKING MATERIALS

Name Size (cm)	Stoneware Raschig Rings	Carbon Raschig Rings	Steel Raschig Rings (1/16" wall)	Stoneware Berl Saddles	Stoneware Intalox Saddles	Steel Pall Rings
1.27	0.57*	0.71*	--	--	--	--
1.9	0.67	--	--	0.65	--	--
2.54	0.68	0.75	0.92	0.69	0.70	0.93
3.8	0.68	0.67	0.92	0.70	0.81	0.94
5.1	0.75	--	--	--	--	--

*Treybal (1955) All other data from Perry (1963)

TABLE 8-2

EXPERIMENTAL VALUES OF j, CHANNEL WIDTH AS FRACTION OF PACKING DIAMETER

Size (cm)	Type of Packing	j
1.27	Berl Saddles, marbles, Raschig Rings, Intalox Saddles	0.192
2.54	Berl Saddles, Raschig Rings, Pall Rings	0.190
3.8	Berl Saddles, Raschig Rings Pall Rings	0.165
7.6 - 12.7	Coke	0.03

Adapted from Jackson (1964) and Calvert (1968)

Table B-3. PACKING FACTORS, "F", FOR DUMPED PIECES (m²/m³)

	Nominal size of packing, cm										
	(0.64)	(0.95)	(1.27)	(1.59)	(1.9)	(2.5)	(3.2)	(3.8)	(5)	(8)	(10)
Raschig rings, ceramic											
.16 cm wall	5,250	3,280									
.32 cm wall						510					
.63 cm wall								430	210		
.95 cm wall										121	28
Raschig rings, carbon											
.16 cm wall	5,250		1,340								
.32 cm wall					827	525					
.63 cm wall								430	210		
.79 cm wall										118	
Raschig rings, metal											
.08 cm wall	2,300	1,280	980	560	510	380					
.16 cm wall			1,340	950	720	450	360	272	187	105	
Lessing rings, porcelain											
.32 cm wall						(869)					
.63 cm wall									(360)		
Lessing rings, metal											
.08 cm wall			(1,060)		(630)						
.16 cm wall						(472)	(387)	(205)	(200)		

Table B.3. PACKING FACTORS, "F", FOR DUMPED PIECES (m²/m³) (continued)

	Nominal size of packing, cm										
	(0.64)	(0.95)	(1.27)	(1.59)	(1.9)	(2.5)	(3.2)	(3.8)	(5)	(8)	(10)
Partition rings										262	100
Pall rings, plastic				318		171		105	82		
Pall rings, metal				230		158		92	66		
Berl saddles	2,950		790		560	360		215	148		
Intalox saddles, ceramic	2,380	1,080	660		475	322		171	131	72	
Intalox saddles, plastic						108			69	52	
Super Intalox, ceramic						200			100		
Tellerettes									130		

Parentheses denote a value of a/ε³, rather than empirical F.

Table 8-4. PACKING FACTORS, "F", FOR GRIDS AND STACKED PIECES (m^2/m^3).

	Nominal size of packing, cm							
	2.5	3.8	5	8	10	13	14	15
Wood grid	20	11	8.2	5.9	4.9			
Metal grid	8.2							
Grid tiles						118		
Checker brick, $\varepsilon=0.55$							135	
Raschig rings, ceramic								
.63 cm wall			95	16				
.93 cm wall				36	12.8			
Raschig rings, metal				21				
Partition rings, diameter								
7.6 cm length				(1,200)	(725)			
10.2 cm length					(705)			(410)
15.2 cm length								(375)
Partition rings, square set								
7.6 cm length				(690)	(460)			
10.2 cm length					(450)			(275)
15.2 cm length								(260)

Parentheses denote a value of a/ε^3, rather than empirical F.

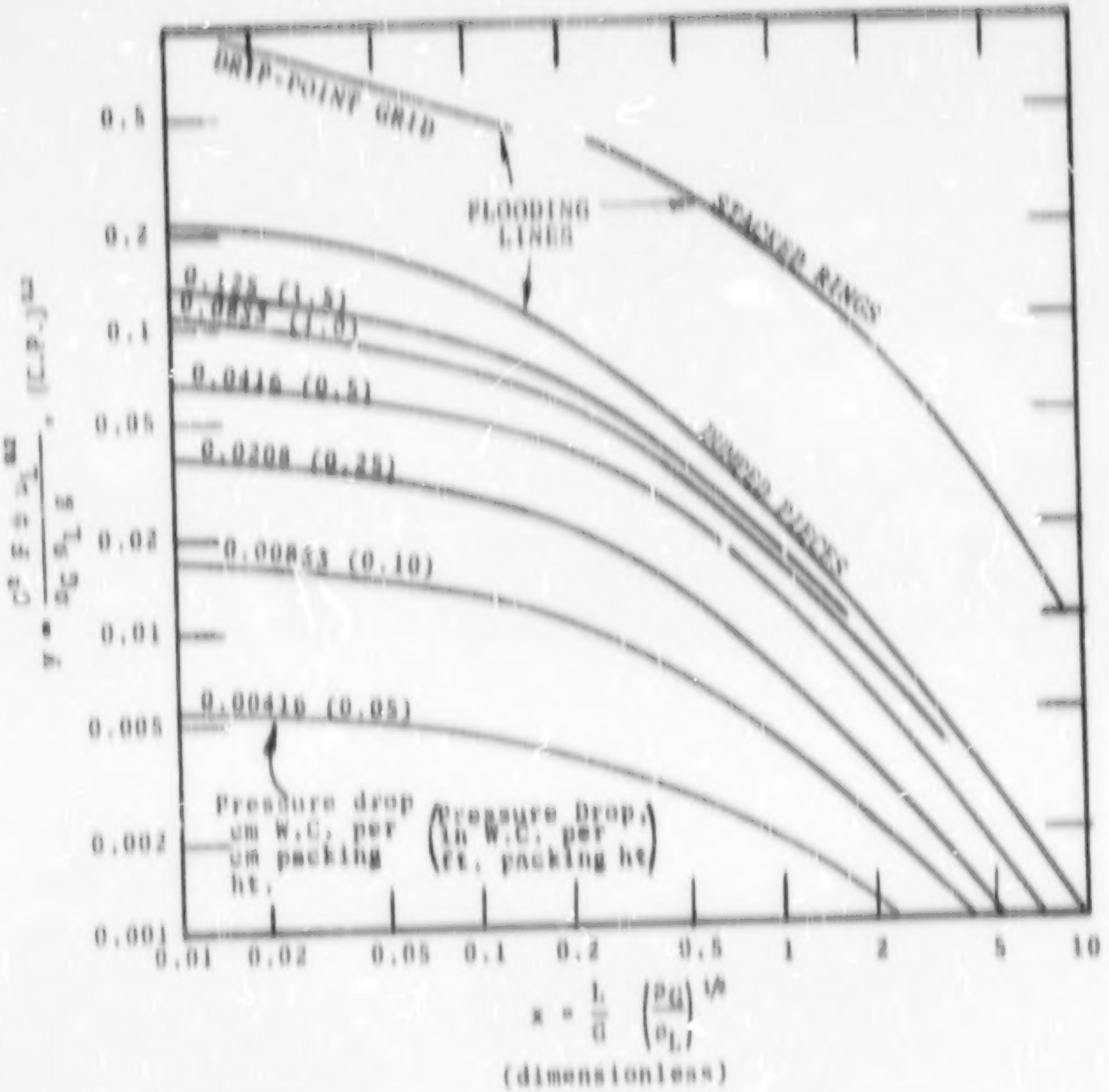

Figure 8-2. Generalized flooding and pressure drop correlation for packed beds (Perry, 1963).

Primary Efficiency - Calvert and Lundgren (1970) found that the collection efficiency for closely packed rods is given by the equation for rectangular jet impaction. The collection efficiency of each stage of impaction can be found in Figure 8-3. Each row of tubes except the first represents one stage of impaction. "β" is used as a parameter in Figure 8-3 and is defined by:

$$\beta = 2\ \ell/b \tag{8-14}$$

where:

b = jet orifice width

ℓ = distance between orifice and impingement plane

"K_p", the inertia parameter, is defined with drop radius, "r_p", rather than diameter.

Efficiency for the bank of tubes is given by:

$$E = 1 - (1-\eta_j)^N \tag{8-15}$$

where:

η_j = collection efficiency for a given particle diameter in one stage of rectangular jet impingement

N = number of stages in the tube bank = (number of rows) -1

If the tubes are widely spaced, the target efficiency, "η", can be calculated from Figure 8-4. In this case the efficiency for the entire tube bank is:

$$E = 1 - (1-\eta\frac{a'}{A})^n \tag{8-15}$$

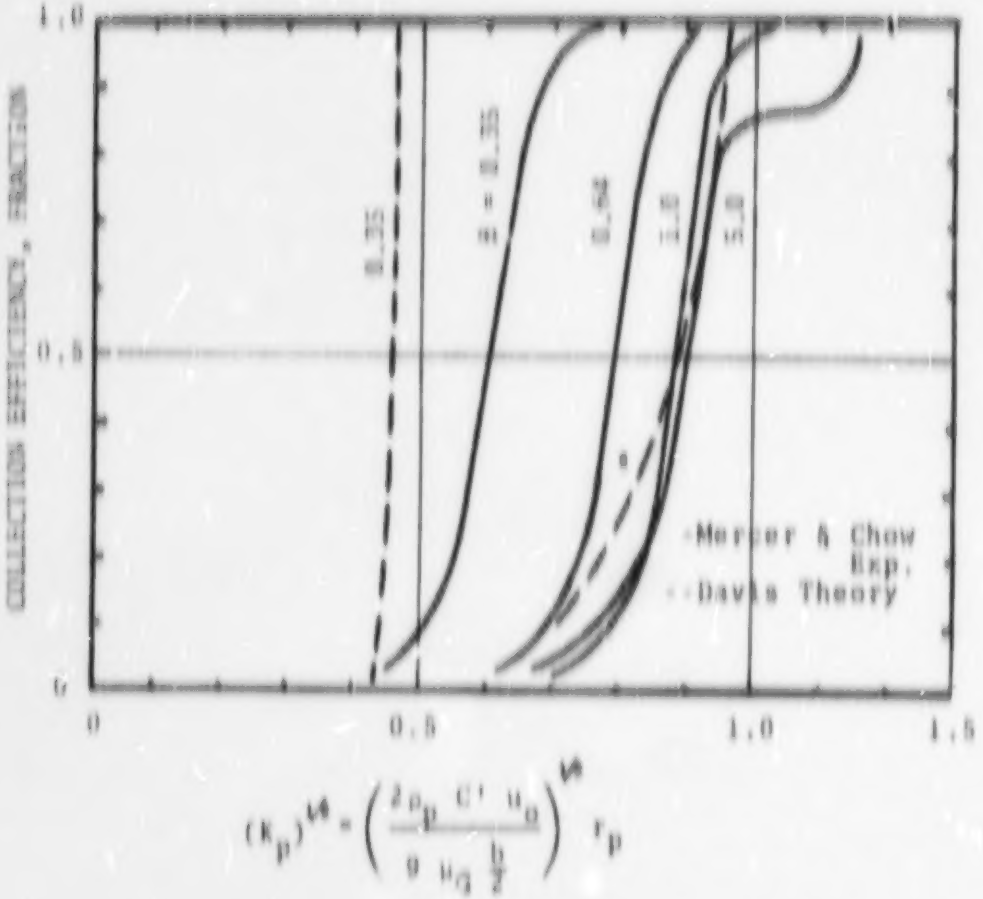

Figure 8-3 Theoretical and experimental collection efficiencies of rectangular aerosol jets.

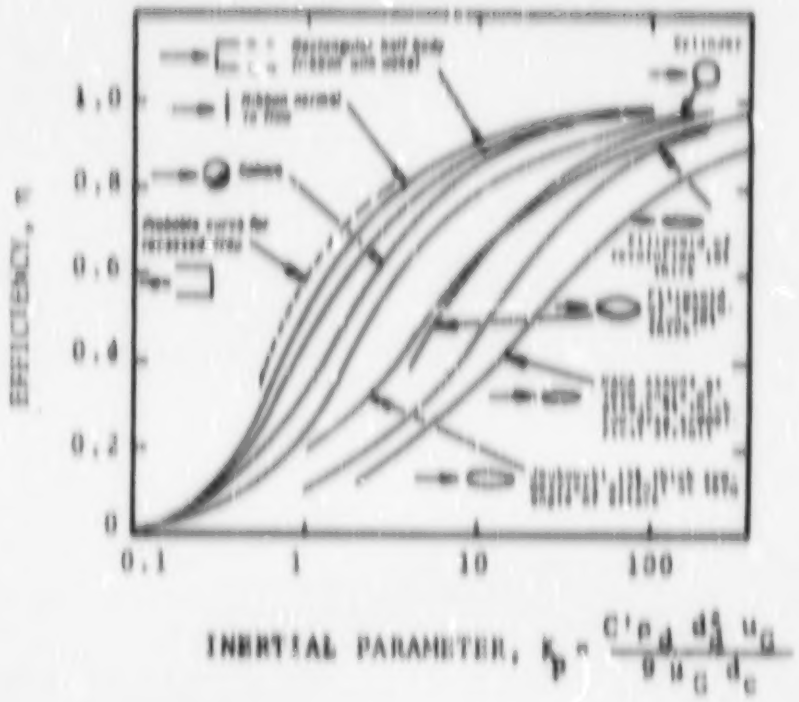

Figure 8-1. Theoretical impaction efficiency as a function of inertial parameter for different targets.

where:

a' = cross-sectional area of all the tubes in one row

A = total flow area

n = number of rows

Pressure Drop - Pressure drop for gas flow normal to banks of round tubes can be predicted by means of Grimison's correlations (Perry, 1973). As an approximation, Lapple (Perry, 1973) suggests that 0.72 velocity heads are lost per row of tubes in arrangements of the kind commonly used in heat exchangers. Calvert and Lundgren (1970) found that for closely spaced tube banks Lapple's approximation agreed satisfactorily with experimentally determined pressure drops.

Houghton and Radford (1939) studied streamline strut banks and found that for a center-to-center spacing of 2 strut widths (i.e. open space = strut width) the pressure drop was about 0.16 velocity heads per row. This can be expressed as:

$$\Delta P = 0.16\ N\ \rho_G\ (5.3 \times 10^{-4})\ (u_G')^2\ \text{cm W.C.} \qquad (8\text{-}16a)$$

where:

u_G' is the actual gas velocity

Mesh

Knitted mesh of varying density and voidage is widely used for entrainment separators. There are basically three different kinds of mesh: (1) Layers with crimp in the same direction - each layer is actually a nested double layer. (2) Layers with crimp in alternate directions - this results in an increase in voidage, reduced sheltering, a decrease in pressure drop per unit length and an increase in target efficiency per layer. (3) Spirally wound layers - the pressure drop is lower by about 2/3 than in layers with crimp in the same direction, but the creeping of fluids, which contributes to reentrainment, is expected to be higher.

Standard mesh 10-15 cm thick having a density of about 0.15 g/cm^3 is used to remove drops larger than 5 μm in diameter. Gas velocities range from 0.3 to 5 m/sec and liquid flow rate is limited by the drainage capacity of the mesh to 2.5 x 10^{-3} g/sec cm^2 of mesh. A lower density mesh made of standard wires is used when 10-20% higher flow rates are desired.

Often two mesh type separators in series are used to remove drops in the 1-5 μm diameter range. The first mesh, normally made of fine wires, coalesces the small drops, and the second mesh, made of standard wires, removes them. The first mesh is operated beyond the flooding velocity and the second under flooding velocity. A major disadvantage with this arrangement is a pressure drop which may reach 25 cm W.C.

Some manufacturers use two or three stages of mesh, the first being coarser and the final being finer, to remove large and small drops successively.

A mesh type separator has the advantage that it can be made to fit vessels of any shape. Any materials which can be drawn into the shape of a wire can be used for fabrication. However, mesh separators are limited in application because they plug easily. This can be avoided by upstream washing, which will decrease removal efficiency and increase pressure drop.

Primary Efficiency-Bradie and Dickson (1969) present the following expression for primary efficiency in mesh separators:

$$E = 1 - \exp \left(- \frac{2}{3} \frac{1}{\pi} a_{\ell} t_{\ell} \eta \right) \qquad (8\text{-}17)$$

where:

a_{ℓ} = specific area of mesh, surface area of wires per unit volume of mesh pad, cm^2/cm^3

t_{ℓ} = thickness of mesh pad in the direction of gas flow, cm

η = collection efficiency of cylindrical wire

The collection efficiency of cylindrical wire "η" can be obtained from Figure 8-4. The factor of 2/3 in the exponential was introduced by Carpenter and Othmer (1955) to correct for the fact that all the wires in the knitted mesh are not perpendicular to the flow. That factor is the ratio of the projected area of wires perpendicular to the flow to the cross-sectional area of wires along the wire length.

$$a_{\ell} = \frac{4(1-\varepsilon)}{d_c} \qquad (8\text{-}18)$$

Pressure Drop - York and Poppele (1963) have suggested that the total pressure drop in the knitted mesh is the sum of the pressure drop in the dry knitted mesh and the pressure drop due to the presence of liquid:

$$\Delta P = \Delta P_{dry} + \Delta P_L \qquad (8\text{-}19)$$

where:

ΔP_{dry} = pressure drop in absence of liquid, cm W.C.

ΔP_L = pressure drop due to presence of liquid, cm W.C.

York and Poppele considered the mesh to be equivalent to numerous small circular channels and used the D'Arcy formula for pressure drop in a pipe to correlate the dry pressure drop through the mesh. York and Poppele's data for knitted mesh with crimps in alternated and in same direction are plotted in Figure 8-5. Their data are close to those obtained by Stasangee (1948) and Shuring (1946). Similar curves obtained by Bradie and Dickson (1969) for spiral-wound and layered mesh are also plotted in Figure 8-5. Figure 8-5 should be used in determining dry pressure drop, which is calculated from the expression:

$$\Delta P_{dry} = \frac{f\, s_1 a_2\, \rho_G\, u_G^2}{\varepsilon^3} \qquad (8\text{-}20)$$

The unit of "ΔP_{dry}" is in dynes/cm². It can be converted to cm W.C. by dividing it by 981.

Pressure drop data due to presence of liquid are not available for all operating conditions or for mesh of different styles. Values of "ΔP_L" obtained by York and Poppele are presented in Figures 8-6 and 8-7, with liquid velocity as the parameter. Liquid velocity is defined as $\frac{\text{"L"}}{A}$ where "L" is the volumetric flow rate of liquid and "A" is the cross-sectional of the mesh in liquid flow direction. The specifications of the knitted mesh used are shown in the two figures.

Maximum Allowable Gas Velocity - Several factors govern the allowable gas velocity through wire mesh for a given set of conditions:

1. ρ_L and ρ_G
2. Liquid viscosity
3. Specific surface
4. Liquid entrainment loading
5. Suspended solid content

Application of the Souders-Brown equation for the calculation of allowable vapor velocity for wire mesh mist eliminator based on gas and liquid densities has been suggested by York (1954).

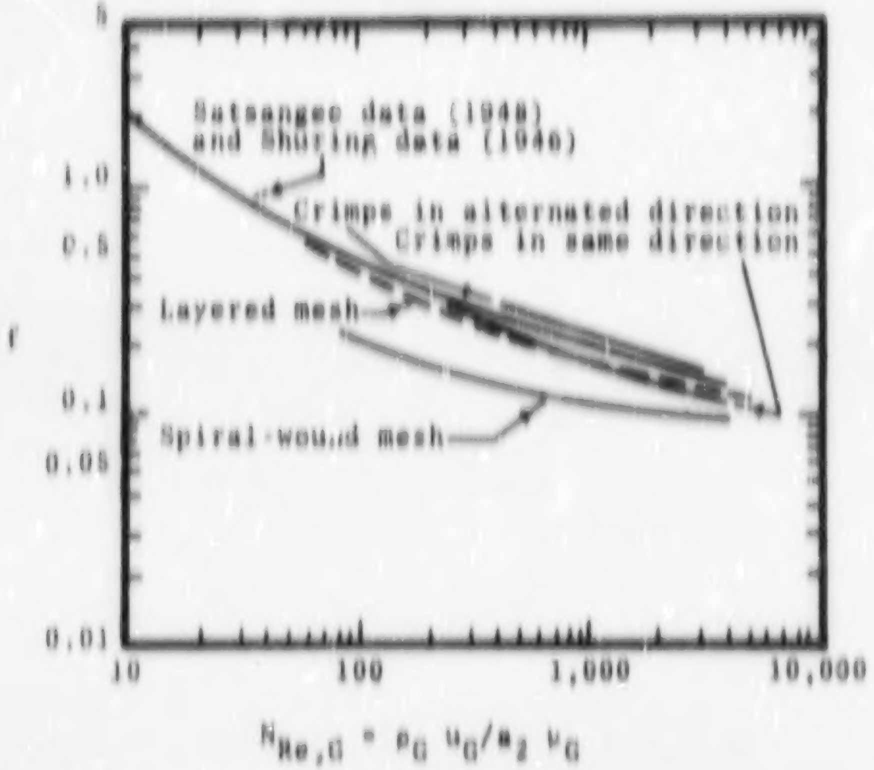

Figure 8-5. Friction Factor, f, versus Reynolds number, $N_{Re,G}$ for wire mesh entrainment separator with entrainment load.

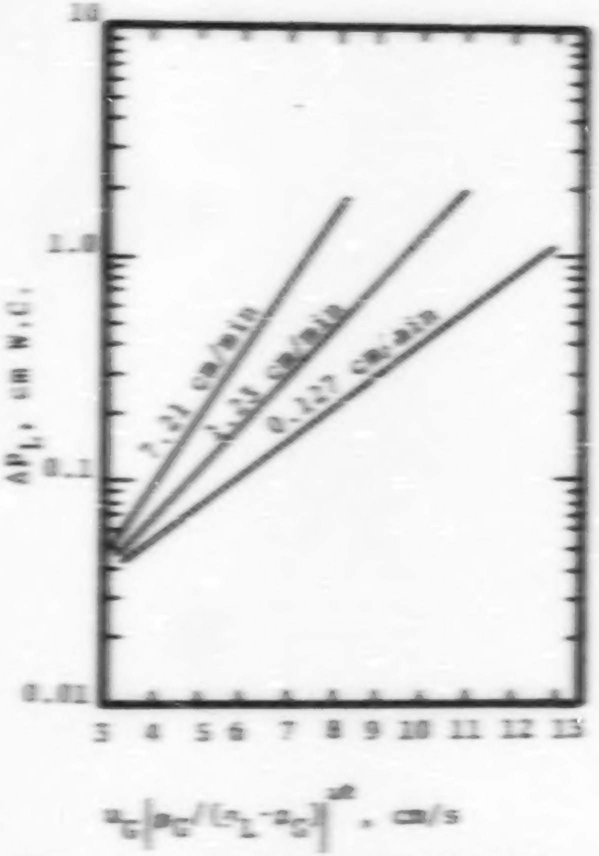

Fig. 8-6. Pressure drop due to presence of liquid in the knitted mesh with the crimps in the same direction.

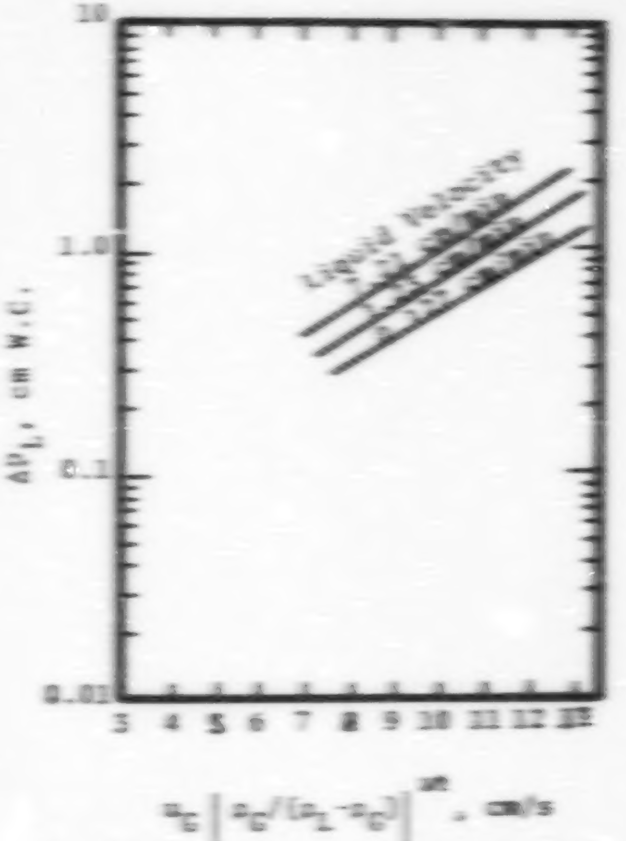

Fig. 8-7. Pressure drop due to presence of liquid in the knitted mesh with the crimps in the alternate direction.

$$u_{G\,max} = 30.5 \; a_3 \left(\frac{\rho_L - \rho_G}{\rho_G} \right)^{0.5} \qquad (8\text{-}21)$$

where "a_3" varies with operating conditions and mesh design. For most cases, $a_3 = 0.35$.

Zigzag Baffles

Baffles can efficiently separate drops greater than 10 μm in diameter, while some of the better designed devices can separate drop diameters of 5-8 μm. Common gas velocities are 2.0-3.5 m/sec, and the pressure drop for a 6-pass separator is about 2-2.5 cm W.C.

The most common baffle shape is zigzag with 3 to 6 passes. These can be fabricated from a continuous wavy plate or each pass is separated, in which case the separation distance is normally smaller than the width of the baffles. Cross-flow baffles are claimed to have higher drainage capacity than countercurrent flow baffles.

Primary Collection Efficiency - A model to predict primary efficiency was developed, based on turbulent mixing. The primary collection efficiency of a continuous zigzag baffle section is:

$$\eta = 1 - \exp\left[- \frac{u_{tc} \; n w \theta}{57.3 \; u_G \; b \; \tan\theta} \right] \qquad (8\text{-}22)$$

where:

η = primary collection efficiency, fraction

u_{tc} = drop terminal centrifugal velocity, in the normal direction, cm/sec

u_G = superficial gas velocity, cm/sec

n = number of bends or rows

θ = angle of inclination of the baffle to the flow path, degrees

w = width of baffle, cm
h = spacing between two consecutive baffles in same row, cm

The drop terminal centrifugal velocity can be determined by performing a force balance on the drop. The result is:

$$u_{tc} = \left[\frac{4}{3} \frac{d_d \rho_d a}{C_D \rho_G} \right]^{0.5} \qquad (8\text{-}23)$$

where:

d_d = drop diameter, cm
ρ_d = drop density, g/cm³
a = acceleration due to centrifugal force, cm/sec²
C_D = drag coefficient
ρ_G = gas density, g/cm³

If the drop Reynolds number is low ($N_{Re,D} < 0.1$), Stokes' law applies. For this condition, the drag coefficient is given by:

$$C_D = \frac{24}{N_{Re,D}} \qquad (8\text{-}24)$$

where $N_{Re,D}$ = drop Reynolds number

$$= \frac{d_d \, u_{tc} \, \rho_G}{\mu_G}$$

By combining equations 8-23 and 8-24, we obtain:

$$u_{tc} = \frac{d_d^2 \, \rho_d \, a}{18 \, \mu_G} \qquad (8\text{-}25)$$

The acceleration due to centrifugal force is defined by the following equation:

$$a = \frac{2\,(u_G')^2}{w \cot\theta} = \frac{2\,u_G^2 \sin\theta}{w \cos^2\theta} \qquad (8\text{-}26)$$

where:

u_G' = actual velocity between baffles, cm/sec
u_G = superficial gas velocity, cm/sec

If $N_{Re,D} > 0.1$, another appropriate drag coefficient should be used in equation 8-23. Foust, et al. (1959) gave a plot of drag coefficient as a function of Reynolds number in Figure 8-8, which can be used to determine "u_{tc}". The effect of surrounding drops on the motion of any individual drop is neglected.

Pressure Drop Determination of the pressure drop is based on the drag coefficient, "f_D", for a single plate held at an angle "θ" to the flow as presented in Figure 8-9 (Page and Johanson, 1927). Neglecting the effect of neighboring plates, pressure drop may be expressed as:

$$\Delta P = \sum_{i=1}^{n} 1.02 \times 10^{-3}\, f_D\, \rho_G\, \frac{u_G'^2}{2}\, \frac{A_p}{A_t} \qquad (8\text{-}27)$$

where:

ΔP = pressure drop, cm W.C.
A_p = total projected area of baffles per row in the direction of inlet air flow, cm²
A_t = duct cross-sectional area, cm²

The summation is made over the number of rows of baffles.

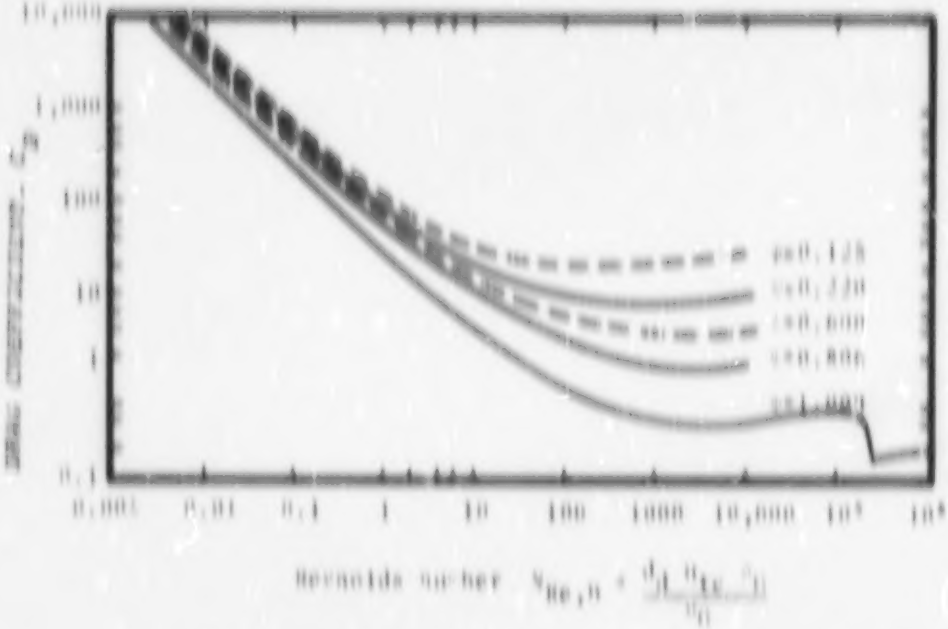

Figure 8-8. Drag coefficient versus Reynolds number after Foust et al (1950), with sphericity ψ as the parameter.

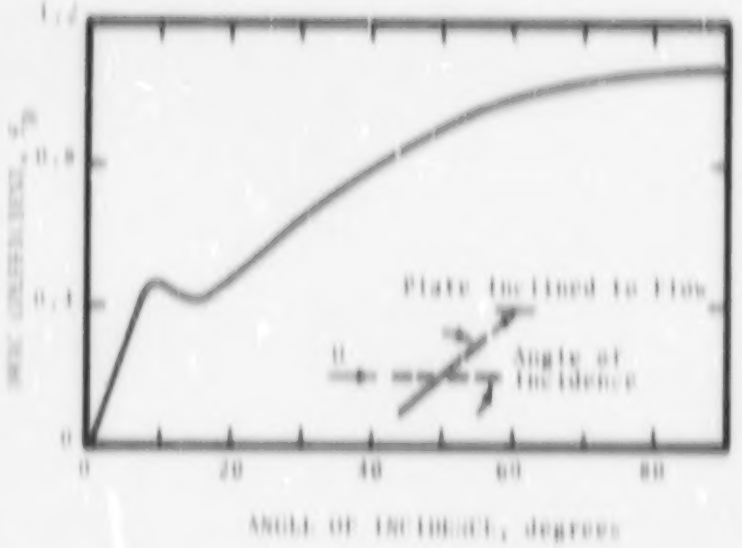

Figure 8-9. Drag coefficients for flow past inclined flat plates (data from A. Fage & F.C. Johansen, (1927).

The actual gas velocity, "u_G'", in the baffle section should be used in Equation (8-27). The actual gas velocity is related to superficial velocity by:

$$u_G' = u_G/\cos\theta \qquad (8\text{-}28)$$

Note that the angle of incidence for the second and subsequent rows of baffles will be twice the angle of incidence for the baffles in the first row.

Tray Towers

Tray towers are vertical channels in which the liquid and gas are contacted in stepwise fashion on trays or plates. The liquid enters at the top and flows downward by gravity. On the way, it flows across each tray and through a downspout to the tray below. The gas passes through openings in the tray, then bubbles through the liquid to form a froth, disengages from the froth, and passes onto the next tray above. There are various tray geometries. The sieve tray and bubble cap are the two most common types.

Sieve Plates - Primary efficiency - Taheri and Calvert (1968) derived an equation for sieve plate primary collection efficiency:

$$E = 1 - \exp(-40 F_g^2 K_p) \qquad (8\text{-}29)$$

where $0.30 < F_g < 0.65$,

$$K_p = \frac{\rho_d d_d^2 v_h}{9 \mu_G d_h} \qquad (8\text{-}30)$$

where:

F_g = foam density, ratio of clear liquid height to total foam height

v_h = velocity of gas through hole, cm/sec

d_h = hole diameter, cm

Pressure Drop - Perry (1963) has suggested that the pressure drop in sieve plates can be calculated according to:

$$\Delta P = h_w + h_{ow} + h_{dp} + h_r \qquad (8\text{-}31)$$

where:

h_w = weir height = 4-9 cm, assume 5 cm, if unknown

h_{ow} = head over the weir = $0.143\ F_w \frac{Q_L}{w_l}$

h_{dp} = dry plate head loss = $\frac{1}{c^2} \frac{\rho_G}{\rho_L} \frac{v_h}{2g}$

h_r = residual pressure drop = $0.013 \frac{\rho_{water}}{\rho_L}$

$$\frac{1}{c^2} = 1.14 \left| 0.4\ (1.25 - f_h) + (1 - f_h)^2 \right| \qquad (8\text{-}32)$$

where:

F_w = column wall curvature correction factor - 1.1
Q_L = liquid flow rate, here in m^3/hr
w_l = weir length, m
f_h = fraction of the perforated open area in the plate

Bubble-cap Trays - Equations used to predict primary collection efficiency and pressure drop of sieve plates can also be applied to bubble-cap trays.

DESIGN PROCEDURES

The general steps in designing an entrainment separator are as follows:

1. Based on process condition and separator configuration, construct the grade efficiency curve for the separation. Equations for primary efficiency can be used for this purpose. In case the gas velocity is higher than the reentrainment onset velocity, reentrainment should be subtracted from the primary efficiency.
2. Compute the collection efficiency for the whole population of the drops. This can be done either graphically or mathematically. For graphical solution, plot Pt_i versus fraction smaller than d_{di} (where Pt_i is penetration for drop size d_{di}). The area under the curve is the overall penetration. Outlet loading is equal to inlet loading times overall penetration.
3. Compute expected pressure drop.

In the process of designing an entrainment separator, the steps should be repeated for different proposed separator configurations. The final configuration can then be selected after optimization analysis.

REFERENCES

Akselrud, G., Zh. Fiz. Khim. 27, 1445, 1953.

Behie, S.W. and J.M. Beeckmans, "On the Efficiency of a Venturi Scrubber", Canadian Journal of Chemical Engineering, 51, 430, 1973.

Boll, R.H., "Particle Collection and Pressure Drop in Venturi Scrubber", Ind. Eng. Chem. Fundam. Vol. 12, No. 1, pp 40-50, 1973

Boll, R.H., L.R. Flais, P.W. Maurer, and W.L. Thompson, "Mean Drop Size in A Full Scale Venturi Scrubber via Transmissometer", EPA-A.P.T. Fine Particle Scrubber Symposium, San Diego, May 28-30, 1974.

Bradie, J.K. and A.N. Dickson. Removal of Entrained Liquid Droplets by Wire Mesh Demisters. Paper 24 in Fluid Mechanics and Measurements in Two-Phase Flow Systems. (A joint symposium of the Inst. of Mech. Engr. and the Yorkshire Branch of the Inst. of Chem. Engr.) 24-25, London. September 1969.

Brink, J.A. and C.E. Contant, "Experiments on an Industrial Venturi Scrubber", Ind. Eng. Chem. 50, 1157, 1958.

Calvert, S. "Source Control by Liquid Scrubbing" Chapter 46 in Air Pollution, Arthur Stern ed., 1968.

Calvert, S. "Venturi and Ohter Atomizing Scrubbers Efficiency and Pressure Drop" A.I.Ch.E. Journal, Vol. 16, No. 3, pp 392-396, 1970.

Calvert, S. Engineering Design of Fine Particle Scrubbers. APCA Journal, 24, 929-934, 1974.

Calvert, S., J.Goldshmid, D. Leith, and D. Mehta "Scrubber Handbook". A.P.T., Inc. Riverside, California. NTIS No. PB-213-016. August 1972.

Calvert, S. and D. Lundgren. Particle Collection in Closed Packed Arrays. Presented at AIHA. 1970.

Calvert, S., N.C. Jhaveri, and S. Yung, "Fine Particle Scrubber Performance Tests" EPA-650/2-74-093, NTIS No. PB-240-325.

Calvert, S., S. Yung, and J. Leung, "Entrainment Separator for Scrubbers - Final Report", EPA-650/2-74-119b, NTIS No. PB-248-050.

Carpenter, C.L. and D.F. Othmer. Investigation of Wire Mesh as an Entrainment Separator. AIChE Journal, p 549, 1955.

Crowe, C.T., Ph.D. thesis, University of Michigan, Ann Arbor, Michigan, 1961.

Dickinson, D.R. and W.R. Marshall, AIChE Journal, 14, 541-552, 1968.

Dropp, L.T. and A.J. Akbrut, "Working Processes and Calculation of the Efficiency of an Ash Trap with a Venturi Tube", Tepoloenergetika, No. 7, 63-68, 1972.

Ekman, F.O. and H.F. Johnstone, "Collection of Aerosols in a Venturi Scrubber" Ind. Engr. Chem. Vol. 43, No. 6, pp 1358-1363, 1951.

Fuchs, N.A. The Mechanics of Aerosols. The Macmillan Company. 1964.

Garuer, F. and R. Suckling, AIChE Journal, 4, 114, 1958.

Garner, F. and R. Keey, Chem. Eng. Sci., 9, 119, 1958.

Gieseki, J.A., Ph.D. Dissertation, University of Washington, Seattle, Washington, 1963.

Gleason, R.J. and J.D. McKenna, paper presented at the 69th National Meeting of AIChE, Cincinnati, Ohio, 1971. Final report of Pilot Scale Investigation of a Venturi-type Contactor for Removal of SO_2 by the Limestone Wet-scrubbing Process, Cottrell Environmental Systems, Inc., 1971.

Gretsinger, J. and W.R. Marshall, Jr., AIChE Journal, 1 312, 1961.

Güntheroth, H., Fortschr. Ber. VDI Z. Ser. 3 No. 13, 1966.

Herne, H. Internal Journal of Air Pollution, Vol. 3, No. 1-3, 26-34, 1960.

Hesketh, J.E. "Atomization and Cloud Behavior in Wet Scrubbers", US-USSR Symposium on Control of Fine Particulate Emission, Jan. 15-18, 1974.

Hesketh, J.E., A.J. Engel, and S. Calvert, "Atomization A New Type for Better Gas Scrubbing", Atmospheric Environment, Vol. 4, pp 639-650, 1970.

Hidy, G.M. and J.R. Brock, "The Dynamics of Aerocolloidal Systems", Pergamon Press, New York, 1970.

Hollands, K.G.T. and K.C. Goel, "A General Method for Predicting Pressure Loss in Venturi Scrubber", Ind. Eng. Chem. Fundam. 14, pp 16-22, 1975

Houghton, J.G. and W.H. Radford. Trans. A. Inst. of ChE, 35, 427, 1939

Hughes, R.R., Chem. Engr. Prog. 48, 497, 1952.

Ingebo, R.D. NACA TN3762, September, 1955.

Jackson, S. and S. Calvert. AIChE Journal, 12, 1075, 1966.

Johnstone, H.F. and M.H. Roberts, Ind. Eng. Chem., 41, 2417, 1949.

Kim, D.Y. and W.R. Marshall, Jr., AIChE Journal, 17, 575, 1971.

Langmuir, I. and K.B. Blodgett, Army Air Forces Technical Report 5418, 1946.

Leith, D. and W. Licht. The Collection Efficiency of Cyclone Type Particle Collectors - A New Theoretical Approach. Paper presented at San Francisco meeting of AIChE. December 1971.

Levich, V., "Physiochemical Hydrodynamics", Prentice-Hall, Englewood Cliffs, New Jersey, 1962.

Matrozov, V.I., O. Soobscheniya, Nauchno-Tekhnicheskikh Rabotakh NIVIF, Nos. 6/7, 152, 1953.

Morishima, N., T. Yoshida "Dust Collection on Atomized Droplets Calculation of Collection Efficiency with Consideration given to Droplet Size Distribution" Kagaku Kogaku, pp 1114-1119, 1967.

Morishima, N., T. Yoshida, Y. Kosoka, and Y. Nonaka "An Examination of Venturi Scrubber Design" Funtai Kogaku Kenkyu Kaishi (J. Res. Assoc. Powder Technol.) Vol. 9, No. 6, pp 357-362, 1972.

Mugele, R.A., AIChE Journal, 6, 3, 1960.

Nukiyama, S. and Y. Tanasawa, Trans. Soc. Mech. Engrs. (Japan), 4 (14), 86, 1938; 4 (15), 138, 1938; 5 (18), 68, 1939; 6 (22), II-7, 1940.

Perry, J.H. Chemical Engineering Handbook. 4th Edition. McGraw-Hill. New York. 1963

Perry, J.H. Chemical Engineering Handbook. 5th Edition. McGraw-Hill. New York. 1963.

Satsangee, P.D. Master's Thesis. Polytechnic Institute of Brooklyn, 1948.

Schurig, W.F. D.Ch.E. Dissertation. Polytechnic Institute of Brooklyn. 1946.

Shepherd, C.B. and C.E. Lapple. IEC Chem. 31, 1246, 1940.

Taheri, M. and C.M. Sheih, AIChE Journal, 12, 153-157, 1975.

Tohata, H., T. Nakoda, and I. Sekiguchi, "Pressure Losses on Venturi-Mixers", Kagaku Kogaku, 28, 64, 1964.

Torobin, L.B., W.H. Gauvin, Canad. J. of Chem. Eng. 38, 142, 1960.

Volgin, B.P., T.F. Efimova, and M.S.Gofman, Int'l. Chem. Eng., 8, 113, 1968.

Walton, W.H. and A. Woolcock, in "Aerodynamic Capture of Particles", ed. E.G. Richardson, Pergamon Press, Oxford, 129-153, 1960.

Wen, C.Y. and S. Uchida, "Simulation of SO_2 Absorption in a Venturi Scrubber by Alkaline Solution", Proceedings of Second International Lime/Limestone Wet-Scrubbing Symposium, New Orleans, Louisiana, 1972.

Yamauchi, J., T. Wada, and H. Kamei, "Pressure Drop Across the Venturi Scrubbers, "Kagaku Kogaku, 27, 974, 1963.

York, O.H. Performance of Wire Mesh Demisters. Chem. Engr. Prog. Vol. 50, No. 8, 421, 1954.

York, O.H. and E.W. Poppelle. CEP. 59, 45, 1963

Yoshida, T., N. Morishima, and M. Hayashi, "Pressure Loss in Gas Flow Through Venturi Tubes", Kagaku Kogaku, 24, 20-27 20-27, 1960.

Yoshida, T., N. Morishima, M. Suzuki, and N. Hukutome, " "Pressure Loss for the Acceleration of Atomized Droplets", Kagaku Kogaku, 29, 308-315, 1965

APPENDIX A. DERIVATION OF SCALING FACTOR

In solving equation 5-25 we assumed $u_{do}^{*} = 0$. In order to find $Pt(d_p)$ for other values of u_{do}^{*}, we make use of the following artifice. Imagine the given duct to be projected in the upstream direction until a distance l_H is reached such that at $z = -l_H$, the liquid velocity is zero. That is, the distance l_H is that length of a hypothetical duct having zero initial liquid velocity with established liquid velocity u_{do} at its exit. In this Appendix, we will distinguish quantities referring to the hypothetical duct from those referring to the given duct by using a prime (') with the former. Then from the geometry of the duct, we get

$$r_o' = r_o - l_H \tan\theta \tag{A-1}$$

and $$A_o' = A_o \left(1 - \frac{l_H \tan\theta}{r_o}\right)^{j} \tag{A-2}$$

From continuity of gas flow, we have

$$u_{Go}' = \frac{m_G}{\rho_G A_o'} = \frac{m_G}{\rho_G A_o \left(1 - \frac{l_H \tan\theta}{r_o}\right)^{j}}$$

$$= u_{Go} \left(1 - \frac{l_H \tan\theta}{r_o}\right)^{-j} \tag{A-3}$$

From the definition of C_{Do}, we have

$$C_{Do} = C_{Do}' \left[\frac{u_{Go}'}{|u_{Go} - u_{do}|}\right]^{0.5}$$

$$C_{Do}' = \frac{C_{Do}}{\left[\frac{u_{Go}'}{|u_{Go} - u_{do}|}\right]^{0.5}}$$

$$= C_{Do} \left[\frac{|u_{Go} - u_{do}|}{u_{Go}}\right]^{0.5} \left[1 - \frac{l_H \tan\theta}{r_o}\right]^{j/2} \tag{A-4}$$

Using equations A-1 through A-4 and the definitions of the various dimensionless parameters, the following relations are obtained:

$$L' = \left(L + l_H\right)\left(1 - S\, l_H\right)^{3/2} \qquad \text{(A-5)}$$

$$S' = S\left(1 - S\, l_H\right)^{-3/2-1} \qquad \text{(A-6)}$$

$$u_d' = u_d\left(1 - S\, l_H\right)^{3} \qquad \text{(A-7)}$$

$$B' = \left(\frac{Q_L}{Q_G}\right)\frac{\rho_L}{\rho_G}\;\frac{1}{C_{Do}'}\left(\frac{u_{Go}'}{u_{Go}' - u_{do}'}\right)^{0.8}$$

$$= \left(\frac{Q_L}{Q_G}\right)\left(\frac{\rho_L}{\rho_G}\right)\frac{1}{C_{Do}\left(\frac{u_{Go} - u_{do}}{u_{Go}}\right)^{0.8}\left(1 - \frac{l_H}{r_o}\tan\theta\right)^{3/2}}$$

$$= B\left(1 - S\, l_H\right)^{-3/2} \qquad \text{(A-8)}$$

which give the desired scaling factors.